The Effect of Mass Transport Limitation on Nitrification in the Activated Sludge Process

by

Michael K. Stenstrom, Ph.D., P.E.
Professor and Principal Investigator

and

Stephen Song, Ph.D.
Postgraduate Engineer

Civil Engineering Department
School of Engineering and Applied Science
Los Angeles, California 90024-1593

Report Number UCLA-ENG 87-28

August 1987

TABLE OF CONTENTS

LIST OF FIGURES

Page

LIST OF TABLES

Page

ACKNOWLEDGMENT

This project was supported in part by the National Science Foundation Grant No. CME-7911792. The authors are also very grateful to Debby Haines whose careful attention to detail improved this report.

ABSTRACT

The Effect of Mass Transport Limitation on
Nitrification in the Activated Sludge Process

A pseudo-homogeneous model of the nitrifying activated sludge process was developed to investigate the effects of mass transport resistance and heterotrophic/nitrifier competition on the apparent relationship between DO concentration and nitrification. The kinetics of both heterotrophic carbon oxidation and autotrophic NH_4^+–N oxidation within activated sludge flocs were described by interactive-type multiple-substrate limiting models.

The values for the model's parameters were estimated from a series of experiments that were conducted in a laboratory-scale nitrifying activated sludge reactor system. The experimental results indicated that the intrinsic relationship between DO concentration and nitrification should be modeled with the exponential saturation function rather than the Monod function.

Using the estimated parameter values, the model was then used to simulate steady state nitrification over a range of typical mean cell retention times (MCRT's), DO concentrations, and levels of mass

transport resistance. The effect of mass transport resistance on nitrification following an organic shock load was also simulated.

It was found that while the nitrifiers' intrinsic half-saturation coefficient for DO is about 0.5 mg/L or less, varying mass transport effects, MCRT's, and heterotrophic/autotrophic competition for DO can combine to give apparent limited DO concentrations that range from 0.5 mg/L to as high as 4.0 mg/L.

I. INTRODUCTION

Since the U.S. Environmental Protection Agency promulgated secondary effluent standards pursuant to the Clean Water Act of 1972, the activated sludge process has become the preferred method for the treatment of domestic wastewaters. Because of its ability to consistently meet secondary standards in a wide variety of situations, activated sludge has been employed in nearly 90% of the secondary treatment facilities constructed since 1973. Although this process is highly efficient for the removal of dissolved and colloidal organic pollutants, it is unreliable in removing ammonia. Ammonia is often discharged in the effluent of activated sludge plants not only as an unremoved constituent of the wastewater but also as a by-product of the treatment process itself. The typical activated sludge effluent may contain concentrations of this dissolved inorganic compound ranging from 10 to 50 milligrams per liter as nitrogen (mg-N/L).

The deleterious effects of ammonia on natural surface waters had been recognized and were well known by the mid-1960's. Now, public pressure for attaining "zero" pollutant discharge and increased emphasis on water reclamation are providing additional impetus for ammonia discharge abatement. The National Pollutant Discharge Elimination System (NPDES) permits for many activated sludge plants already include ammonia standards and it is likely that

as permits are updated more plants will be required to meet such standards. Where activated sludge plants cannot meet ammonia standards set by their NPDES permits, municipalities have either augmented these plants with tertiary processes or employed nitrification to remove ammonia. Although physio-chemical processes such as ammonia stripping, breakpoint chlorination, and ion exchange have been used, nitrification is often the most satisfactory alternative.

Nitrification is the sequential two-step autotrophic oxidation of ammonia. This process is affected primarily by two genera of chemoautotrophic bacteria--*Nitrosomonas* and *Nitrobacter*. The first oxidation step,

$$NH_4^+ + 1.5O_2 \longrightarrow NO_2^- + 2H^+ + H_2O \tag{1.1}$$

is affected by *Nitrosomonas* and the second oxidation step,

$$NO_2^- + 0.5O_2 \longrightarrow NO_3^- \tag{1.2}$$

is effected by *Nitrobacter*. A particularly economical implementation of nitrification, especially for upgrading existing activated sludge plants, accomplishes these reactions within the same reactor as that used for the heterotrophic oxidation of carbonaceous matter.

For simultaneous carbon oxidation and ammonia oxidation to occur, the reactor conditions must be conducive to the growth and activity of both heterotrophic and nitrifying bacteria. Factors that are normally considered to be

relevant to the growth and activity of heterotrophs are also relevant to nitrifiers. Such factors include: sludge age (MCRT), pH, temperature, dissolved oxygen (DO) concentration, electron donor substrate concentration, substrate composition, loading rate, and the presence of toxic substances. The effects of these factors on each of the two microbial populations, however, are generally different. The nitrifying population, being less robust than the heterotrophic population, usually requires greater minimal growth conditions. For the same reason, nitrifiers are sensitive to a larger number of factors. Such factors and their reported effects on nitrification in the activated sludge process have been compiled in the review papers of Painter (1977), Sharma and Ahlert (1977), and Focht and Chang (1975).

Of the many factors that are known to affect nitrifiers, the concentration of DO is one of the most important. Dissolved oxygen, being an obligate electron acceptor for nitrifiers, is a vital substrate and must be available in concentrations that will not limit the activity of the nitrifying population. Maintaining excessively high concentrations of DO to ensure that the nitrifiers are not oxygen limited, however, is not economically acceptable. This dichotomy between the requirement for high DO concentration to achieve maximum rates of nitrification and the requirement for low DO to achieve economical operation can only be resolved by operating at the minimum DO concentration at which the rate of nitrification is not oxygen limited. Such an "optimal" DO

concentration, however, has not yet been well established.

In their review of the literature, Stenstrom and Poduska (1980) found a wide variation in the reported effects of DO concentration on nitrification. The reported values of the limiting DO concentration ranged from 0.5 mg/L to 4 mg/L. Correspondingly, the reported values of the Monod half-saturation coefficient for DO ranged from 0.1 mg/L to 2 mg/L. Part of the large variability was attributed by the authors to differences in techniques that were used; determinations were made under pure culture conditions, activated sludge conditions, steady state conditions, and nonsteady state conditions. They also suggested that the variability could be the consequence of not recognizing the existence of synergistic factors. Mass transport limitation and multiple-substrate limiting kinetics were cited as factors that were likely to have acted in combination with DO concentration to produce the reported results.

To achieve efficient nitrification, a clearer quantification of the effects of DO concentration as well as the identification of other interdependent factors and their effects is needed. The objective of this research, therefore, is to resolve the incongruities in the literature and to develop a model of the nitrifying activated sludge process in terms of the relationships between DO concentration and other synergistic factors. Specifically, the synergism between the effects of mass transport limitation, multiple-substrate limiting conditions, and

heterotroph/nitrifier competition is investigated. A mathematical model describing the effects of this synergism on the relationship between the concentration of DO and nitrification is proposed.

The model was developed by adopting the pseudo-homogeneous approach that has been used in the modeling of heterogeneous catalytic reactors. In adopting this approach, microbial flocs were modeled as porous "catalytic" particles within which autotrophic and heterotrophic oxidation of substrates occur. In conjunction with the development of the model, a laboratory-scale nitrifying activated sludge system was constructed and used for a series of experiments in which data were collected for the estimation of the model parameters and the demonstration of the hypothesized effects. Using the values of the parameters estimated in this research, the model was then used to predict how the relationship between DO concentration and nitrification can be affected by other reactor conditions and process variables.

II. MATHEMATICAL MODELS OF NITRIFICATION

Current mathematical models of the activated sludge process have adopted the well developed techniques used in the modeling of homogeneous chemical reactors. This prevalent modeling approach envisions the mixed liquor as a homogeneous liquid in which homogeneous liquid phase reactions occur. Although the oxidation of soluble carbonaceous matter actually occurs in a flocculant microbial phase, this physical approximation has generally been intuitively acceptable because the microbial phase is very finely dispersed. The rate of substrate oxidation is usually modeled by the Monod function with the electron donor substrate (the carbon source) as the only limiting substrate.

Current models of the nitrifying activated sludge process have similarly adopted this homogeneous modeling approach. The nitrifying bacteria are assumed to be evenly dispersed along with the heterotrophic bacteria in the mixed liquor. It is further assumed that the activity of nitrifiers are not affected by the presence of heterotrophic bacteria and vice versa; that is, there is no interaction between the two populations. The rate of nitrification is modeled by the Monod function with ammonium-nitrogen as the only limiting substrate. The steady state model presented by Lawrence and McCarty (1970) is typical of this approach. Poduska (1973) extended this approach to describe nonsteady state nitrification.

ACTIVATED SLUDGE FLOCS

The suspended microbial cultures used in the nitrifying activated sludge process are usually found in concentrations ranging from 1500 mg/L to 4000 mg/L. At these concentrations, the heterotrophic and nitrifying microorganisms do not exist in the suspension as dispersed individuals but exist in flocs. Parker et al. (1970) and others have reported that the size of activated sludge flocs ranges from 50 to 1000 microns. The average floc size was reported to be in the range of about 200 to 500 microns. Figure 2.1 is adopted from Parker et al. (1970) and shows a typical size distribution of activated sludge flocs.

The size of activated sludge flocs as well as the size distribution are dependent on the turbulence in the mixed liquor. Parker et al. (1972) determined that the maximum stable floc size can be predicted by:

$$d_s = \frac{C}{G^n} \tag{2.1}$$

where

d_s = maximum stable floc size in microns

C = floc strength coefficient

G = average velocity gradient [1/sec]

n = stable floc size exponent.

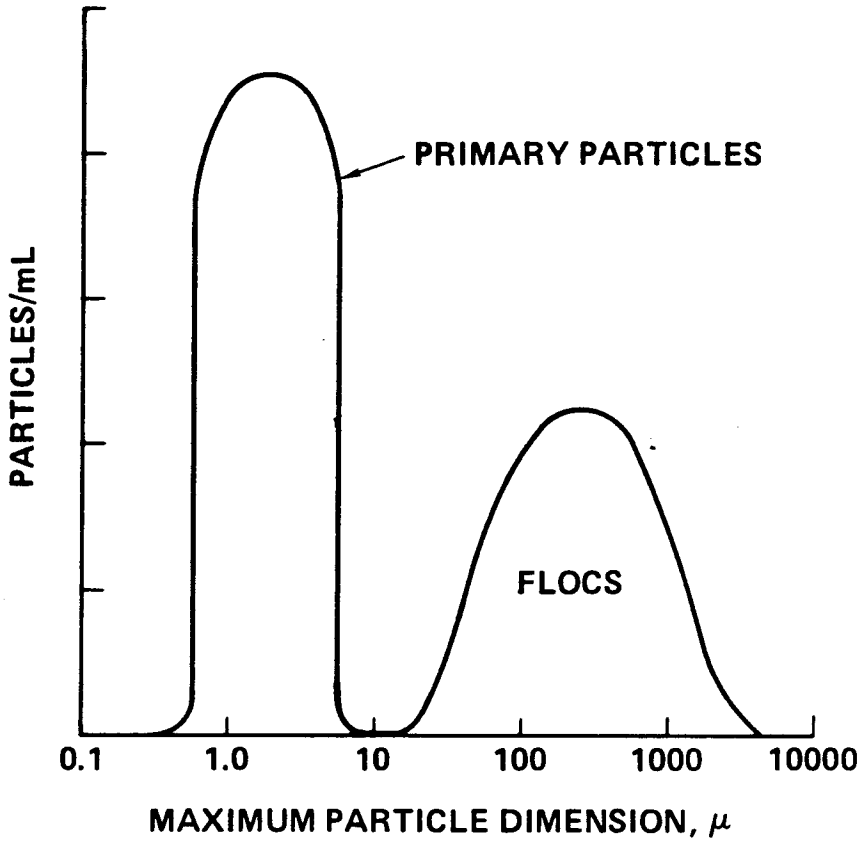

Fig. 2.1 Typical Floc Size Distribution in Activated Sludge

The authors reported experimental values of C for activated sludge in the range of 4500 to 6200 μ-sec.

For diffused aeration, the average velocity gradient, G, is given by

$$G = \left[\frac{Q\gamma h}{\mu}\right]^{1/2} \tag{2.2}$$

where

Q = unit air supply [ft^3/gal-hr]

γ = liquid specific weight

h = diffuser depth

μ = viscosity.

For impellers, G is proportional to the power dissipated by the impeller and is given by

$$G \propto (\rho N^3 D^5)^{1/2} \tag{2.3}$$

where

ρ = density of liquid

N = impeller speed

D = impeller diameter.

The velocity gradient in typical activated sludge plants ranges from 90 to

220 sec^{-1}.

Combining equation (2.3) with equation (2.1) gives the following relationship between stable floc size and impeller speed.

$$d_s \propto \frac{1}{(N^{3/2})^n} \tag{2.4}$$

The stable floc size exponent, n, is equal to 0.5 for filament fracture mode and is equal to either 1 or 2 for surface shearing mode. Parker et al. (1970) reported an experimental value of about 0.4 for activated sludge flocs.

MASS TRANSPORT LIMITATION

Though activated sludge flocs are relatively small, their size, per se, is insufficient to preclude the possibility of mass transport limitation. In the extensive literature on the modeling of heterogeneous chemical reactions, the extent of mass transport limitation in porous catalyst is often characterized by two dimensionless parameters - the Biot number and the Thiele modulus. The Biot number characterizes the influence of the external resistance (the resistance of the bulk liquid) and is given by

$$Bi = \frac{kL}{D_e} \tag{2.5}$$

where

Bi = Biot Number

k = the liquid phase mass transfer coefficient [L/T]

L = a characteristic dimension [L]

D_e = the effective diffusivity in the porous solid phase [L^2/T].

The Biot number is the ratio of the characteristic time for diffusion across the porous particle to the characteristic time for diffusion across the boundary between the fluid phase and the particle surface. Hence, transport limitation is dominated by external resistance when this ratio is small.

Petersen (1965) demonstrated, by using realistic values of mass transport parameters, that external mass transport limitation, cannot exist without the presence of internal mass transport limitation. The influence of internal resistance (the resistance of the particle matrix) is characterized by the Thiele modulus. The square of the Thiele modulus is often given by

$$\phi^2 = \frac{L^2 \bar{R}(C_B)}{D_e c_B} \tag{2.6}$$

where

ϕ = Thiele Modulus

$\bar{R}(C_B)$ = the intrinsic rate of reaction [M/L^3–T]

c_B = the concentration of the reactant in the bulk

fluid $[M/L^3]$

This modulus can be interpreted as being the ratio of the characteristic time for diffusion to the characteristic time for reaction. Alternately, it can be interpreted as the ratio of the intrinsic rate of reaction to the maximum rate of diffusion. Hence, the extent to which internal mass transport limitation is significant is dependent on the relative rates of reaction and diffusion.

In an analysis of oxygen transport and uptake in the activated sludge process, Kossen (1979) used the Thiele modulus concept. Using nominal literature values of oxygen uptake rates, effective diffusivities, floc sizes, and typical bulk DO concentrations, he showed that oxygen depletion can occur within flocs that are larger than about 500 microns. These results indicate that, for floc sizes that are commonly encountered in the activated sludge process, the transport of oxygen can be limited by diffusional resistance. His analysis also showed that external resistance can be significant in quiescent regions of a reactor.

In another theoretical analysis, Atkinson and Rahman (1979) attempted to predict the rate of carbonaceous uptake as a function of a Thiele type modulus. They concluded that there will be no internal limitation when the value of the modulus is less than 0.5 and that there will be no external limitation when the value of the modulus is less than 0.18. It should be noted that the

criteria for external limitation was determined by using the minimum possible Sherwood number. Their conclusion does not, therefore, necessarily contradict the empirical notion that the onset of internal limitation must occur before the onset of external limitation. The value of their modulus, computed from values of parameters that are within the range of typical activated sludge conditions, can be greater than ten.

Mueller et al. (1968) and Baillod and Boyle (1970) experimentally demonstrated that mass transport resistance can significantly affect the rate of carbonaceous substrate uptake in the activated sludge process. In each study, the influence of substrate transport limitation was assessed by measuring the rate of substrate uptake for a pure culture of floc forming bacteria in both flocculated and dispersed states. Mueller measured oxygen uptake rates and Baillod and Boyle measured both glucose and oxygen uptakes rates. Glucose was the only limiting substrate in these experiments. Both studies reported that the uptakes rates of the dispersed cultures were significantly higher than those of the flocculated cultures at low bulk glucose concentrations, while no differences in uptake rates were observed at high bulk glucose concentrations.

While both studies demonstrated the existence of diffusional resistance, neither could experimentally distinguish between contributions from external diffusional resistance and contributions from internal diffusional resistance. By

calculating rough estimates of mass transfer coefficients and specific surface areas of the flocs, Mueller et al. argued that external resistance was negligible in their experiments. Citing the same line of reasoning, although performing no calculations, Baillod and Boyle also made the same conclusion.

LaMotta and Shieh (1979) performed similar experiments using an enriched culture of nitrifying bacteria. In batch experiments, the initial rate of ammonia uptake was measured as a function of floc size. The initial concentration of ammonium-nitrogen was 1 mg-N/L and ammonium-nitrogen was selected as the only limiting substrate by maintaining a DO concentration of 15 mg/L. Since maximum initial uptake rates were obtained only for small flocs, they concluded that floc size can significantly affect the rate of nitrification. It should be noted that a floc size of 120 microns, which is the largest size found in this study, was already sufficiently large to induce mass transport limiting conditions. Citing the arguments presented by Mueller et al., transport limitation was again attributed solely to internal diffusional resistance.

MULTIPLE-SUBSTRATE LIMITING KINETICS

A number of empirical models have been developed to describe the kinetics of microbial growth under single-substrate limited conditions. The Monod model is the most popular of these and is given by

$$\mu = \frac{\mu_m S}{K_s + S} \tag{2.7}$$

where

μ	=	specific growth rate [1/T]
μ_m	=	maximum specific growth rate [1/T]
S	=	substrate concentration $[M/L^3]$
K_S	=	Monod constant, substrate concentration at which the uptake rate is half of the maximum $[M/L^3]$.

The major reason for the popularity of this model is probably because it allows linear analysis of kinetic data rather than because it fits data well. Much experimental evidence has shown that other empirical models often provide a better fit of experimental data. The principle deficiency of the Monod model is its inability to saturate rapidly enough. Dabes et al. (1973) used a number of different sets of experimental data to show that in many instances the Blackman model and the exponential model provides a much better fit of the data.

The Blackman model is defined by

$$\mu = \frac{\mu_m}{2} \frac{S}{K_S} \qquad S \leq 2K_S \tag{2.8}$$

$$\mu = \mu_m \quad S > 2K_S$$

This model does not allow for a gradual transition from zero-order to first-order kinetics; the rate is either zero-order or first-order. The exponential model is somewhat of a compromise between the Monod model and the Blackman model and is given by

$$\mu = \mu_m [1 - exp(-\ln \frac{2S}{K_s})] \qquad (2.9)$$

This model allows a continuous transition from zero-order to first-order, but this transition is much sharper than that allowed by the Monod model. Figure 2.2 is a comparison of these three models. From a review of the literature, Bader (1978) concluded that most of the published kinetic data fall somewhere between the curves for the Blackman model and the exponential model. Despite much evidence against the use of the Monod model, this model is incorporated into nearly all of the current models of the activated sludge process. Nitrification has nearly always been thought to follow Monod kinetics.

The specific rate of substrate utilization, q, is related to the growth rate by

$$q = \frac{\mu}{Y} \qquad (2.10)$$

where

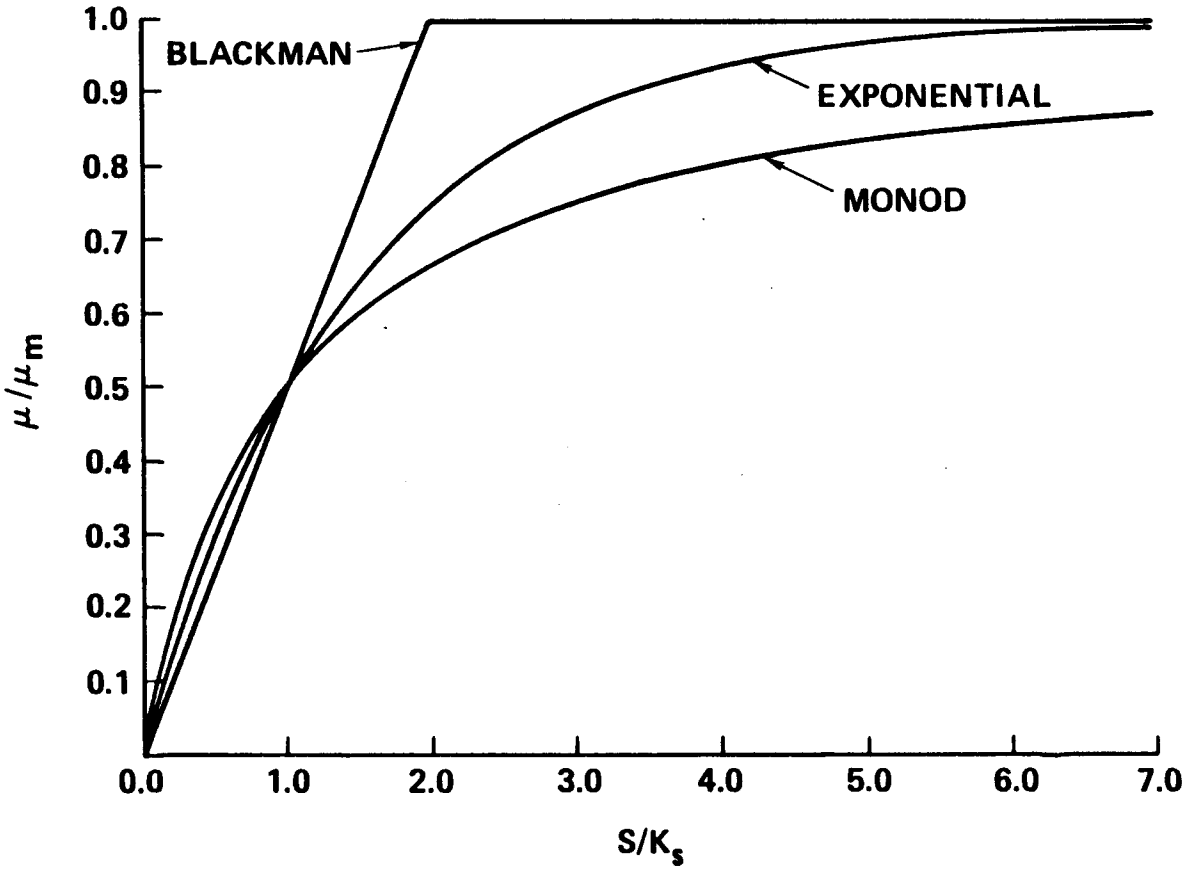

Fig. 2.2 Relationship Between Growth Rate and Substrate Concentration for Three Single-Substrate Limiting Models

Y = yield coefficient [mass of cells/mass of substrate].

When applied to the heterotrophic oxidation of organic carbonaceous matter (the electron donor substrate), the organic carbon source is assumed to be the only limiting substrate and its concentration is taken to be that in the bulk liquid. For the modeling of nitrification kinetics, ammonium-nitrogen (the electron donor substrate) is assumed to be the only limiting substrate and its concentration is also taken to be that in the bulk liquid.

While attention is usually focused on the electron donor, heterotrophic as well as autotrophic growth and activity require other substrates. Single-substrate limited growth conditions can usually be achieved only in laboratory environments where the feed to the system is carefully controlled by the experimenter. In the activated sludge process, where the availability of substrates is dependent on uncontrollable process variables such as influent substrate composition, single-substrate limiting conditions may not prevale. Oxygen, because it cannot be economically supplied in excess, can sometimes become a limiting substrate in full scale plants. In the treatment of some industrial wastewaters, dissolved inorganic nutrients such as nitrogen or phosphorus can be the limiting substrate.

Ryder and Sinclair (1972) developed a process model that allowed the limiting substrate for aerobic microbiological systems to switch between two substrates (carbon substrate and oxygen) depending on the dilution rate of the system. Bader et al. (1975) suggested that this model was not general enough; they proposed that there is a possibility of simultaneous double-substrate limiting conditions. Such conditions would occur in the transition from one limiting substrate to the other.

Models of multiple-substrate kinetics have been reviewed by Bader (1978) and more recently by Bader (1984). Such models were categorized as either noninteractive or interactive. The noninteractive model can be represented as

$$\mu = MIN\,[\mu(S),\mu(S),\ldots]. \tag{2.11}$$

The function MIN[ ] takes the minimum of the arguments, and μ is one of the single-substrate kinetics. Equation (2.11) allows more than one limiting substrate, but only one substrate can be limiting at a time; no substrate interactions are allowed. The interactive model, however, allows simultaneous substrate limitation and can be represented as

$$\mu = f\,[\mu(S),\mu(S),\ldots]. \tag{2.12}$$

The function f [ ] represents any arbitrary operator but multiplication and arithmetic averaging are the most common. The rational for both noninteractive and

interactive models was presented and it was concluded that the choice between the two types of models depends on the combination of substrates. He noted, however, that there is almost always some degree of substrate interaction and hence the interactive model may be preferable.

The same author, Bader (1978), developed an analysis for determining whether single-substrate limiting, double-substrate limiting, or simultaneous double-substrate limiting conditions will be encountered in continuous feed and batch cultures. It was shown that selection among the three possibilities is dependent on influent composition and sludge age. Using realistic values of kinetic parameters for glucose and ammonium-nitrogen uptake by heterotrophic bacteria, he (Bader, 1984) concluded that double-substrate limiting conditions are rare in real situations and are difficult to achieve even in laboratory conditions.

Stenstrom and Poduska (1980) performed a similar analysis for ammonium-nitrogen and oxygen uptake by nitrifying bacteria. They used the kinetic model proposed by Megee et al. (1972). This model is given by equation (2.12) with $f[\ ]$ being a multiplicative operator and μ being the Monod function. It was shown that nitrification can be alternately limited by either ammonium-nitrogen or DO, or be simultaneously limited by both depending on the growth rate of the nitrifiers (MCRT of the system) and the bulk concentra-

tions of the substrates. Although their analysis did not explicitly determine whether simultaneous substrate limiting conditions could possibly occur under typical activated sludge conditions, an inspection of their results, Stenstrom and Poduska, (Figures 1 and 2) indicate that a typical complete-mixed activated sludge reactor may operate at oxygen and ammonium-nitrogen concentrations that would lead to simultaneous substrate limitation.

Neither of the above analyses have considered the effects of mass transport limitation nor the effects of substrate utilization by symbiotic (though not necessarily commensalistic or mutualistic) microbial populations. When transport limitation exists, diffusional resistance in the liquid boundary layer and the resistance of the floc matrix reduce the availability of substrates. Because the effective diffusivities, D_e, of substrates can be different and because the rates of their consumption can also be different, transport limitation can have differing effects on different substrates.

In an analysis of glucose and oxygen transport into activated sludge flocs, Haas (1981) used a modulus that was described earlier by Weisz (1973). This modulus is conceptually similar to the more well known Thiele modulus but is a function of only "observable" variables. He demonstrated that when the value of the modulus was one, corresponding to the Weisz-Prater criterion for the onset of internal mass transport limitation, the depth of penetration of glu-

cose and oxygen was different. He concluded that "under various circumstances, ...there may be anoxic zones with excess nutrient or nutrient poor zones with excess oxygen." A corollary to his conclusion that multiple-substrate limiting conditions are possible is that, under certain conditions, there could also exists anoxic and nutrient poor zones; that is, simultaneous multiple-substrate limiting conditions are also possible.

The consumption of substrates by symbiotic populations may follow a more complex stoichiometric relationship than that considered in the analysis by Bader (1978). For example, in the nitrifying activated sludge process, heterotrophic and nitrifying bacteria both utilize, though at different rates, oxygen and nitrogen, while heterotrophic bacteria also utilize a carbon substrate. The observed stoichiometry for oxygen/carbon will not be the same as that expected when only heterotrophic activity is considered. Similarly, the observed stoichiometry for oxygen/nitrogen will not be the same as that expected when only nitrifier activity is considered. The observed stoichiometry will be dependent on the rates of substrate utilization by each population. These rates, in turn, are dependent on mass transport parameters as well as other process variables. Thus, bulk substrates concentrations that would not be expected to result in simultaneous substrate limitation may induce such limitations within flocs when transport resistance and complex reaction stoichiometries are considered.

MICROBIAL COMPETITION

Mass transport limitation can affect different segments of a heterogeneous microbial population differently. Bacteria that can tolerate low substrate concentrations will compete more effectively under mass transport limiting conditions than those that cannot. Lau et al. (1984) used the phenomenon of mass transport limitation and simultaneous double-substrate limiting kinetics to explain filamentous bulking in the activated sludge process in terms of competitive growth between floc forming bacteria and filamentous bacteria. Both groups of bacteria are aerobic microorganisms; but the filamentous group can tolerate much lower DO concentrations. Simulations showed that, depending on the bulk DO concentration and the size of the flocs, the growth of either of the two types of bacteria could be favored. Low bulk DO concentrations and large floc sizes, resulting in large anoxic regions within the flocs, favored the growth of the filamentous bacteria but high bulk DO concentrations and small floc sizes, resulting in small anoxic regions within the flocs, favored the growth of the floc forming bacteria.

A similar competitive relationship may exist between the heterotrophic and the nitrifying populations in the nitrifying activated sludge process. Both populations compete for oxygen but heterotrophs have a much lower limiting DO concentration. The Monod half-saturation coefficient for DO ranges from

0.014 to 0.073 mg/L for heterotrophs (Hao et al., 1983) while the coefficient ranges from 0.1 to 2 mg/L for nitrifiers.

ESTIMATION OF MODEL PARAMETERS

Since current models of the activated sludge process assume that no mass transport limitations can exist, the only model parameters that are not directly measurable are the kinetic parameters in the Monod equation. These parameters are typically determined by analyzing data obtained from a series of chemostat experiments. The chemostat (a continuous flow reactor without recycle) is operated over several values of MCRT's (MCRT is the mean cell retention time and is the inverse of the dilution rate of a chemostat) to obtain a range of steady state effluent concentrations. A plot of the data to a linearized form of the Monod function is constructed from which the values of the kinetic parameters are estimated by linear least squares analysis. The nonsteady state variation of this procedure, employing batch reactors instead, is also commonly used. Grady and Lim (1980) describes the differential and integral analysis of such experiments. In all cases, the values of the parameter estimates are obtained through linear transformation of the data and subsequent linear analysis. The authors also discussed the relative merits and shortcomings of these commonly used methods.

An inherent defect of all these methods is the introduction of bias, by the linear transformation of the data, into the estimates. The analysis of nitrification kinetics data in Charley et al. (1980) clearly demonstrates this problem. These authors used the Lineweaver-Burke transformation and linear least squares regression to determine Monod parameters for *Nitrosomonas*. They reported that "the significance of the results was always >95% with 6-10 degrees of freedom." They then used "the equation of this line...to generate the curve in Figure 6 [Charley, et al. 1982, page 1392] which is mathematically the best fit." Despite this claim, it is immediately obvious from an inspection of this figure that the generated curve is not the best fit. The mean of the residuals was obviously not minimized (the mean should be zero for the least squares criteria); in fact, all of the residuals were nonnegative. It was the residuals in the Lineweaver-Burke plot (Charley et al. 1980, Figure 4 on page 1391) that were minimized. The obvious solution, though seldom applied and was not in this case, is to perform nonlinear analysis. This is an example of a bias which occurs because of error transformation (Bard 1974).

A more serious problem with this methodology, however, is that the accuracy of the parameter estimates are susceptible to the effects of mass transport limitation. The effect of intrafloc diffusional resistance on the accuracy of parameter estimates obtained by this methodology has been investigated by Regan (1974), Gondo et al. (1975) and others. Shieh (1980) presented a

succinct analysis of this subject. Using the Thiele modulus concept, he showed that experimental data collected under mass transport limiting conditions cannot be linearized by any of the currently used transformations. Though such transformations should produce nonlinear results, the sparseness of typical experimental data cannot reveal the nonlinearities and linear analysis is, unbeknownst to the investigator, inappropriately applied. As a result, biased estimates of the parameters are obtained.

Nearly all of the values of the Monod half-saturation coefficients reported in the literature were obtained by the methodology described above. Since mass transport limitation was not explicitly eliminated from those experimental conditions, it is conceivable that varying degrees of transport limitation were present in those experiments. Accordingly, the wide range of values of the estimates can then be explained by the varying degrees of transport limitation under which the estimates were obtained.

III. MODEL DEVELOPMENT

Mass transport limitation is ignored or considered negligible in the homogeneous approach to the modeling of the nitrifying activated sludge process. The evidence and discussion presented in the previous section suggests, however, that mass transport limitation exists under typical process conditions and even under some experimental conditions. In the presence of this phenomenon, it appears that multiple-substrate limiting conditions may prevale and competition between heterotrophic and nitrifying bacteria may take place. The mathematical model developed herein proposes a possible mechanism by which the synergism amongst these factors is manifested in the relationship between DO concentration and the rate of nitrification.

The formulation of this model follows the pseudo-homogeneous approach of Froment (1972). In adopting this approach, the activated sludge flocs are modeled as porous catalytic particles through which substrates diffuse and within which autotrophic and heterotrophic competition for the substrates occur. The effect of this diffusion and reaction process on intrinsic substrate uptake rates is summarized in terms of global reaction rates. By envisioning that these global rates occur homogeneously throughout the reactor volume, homogeneous modeling techniques are then applied to the reactor.

FLOC MODEL

Diffusion and Reaction

As previously discussed, the degree of diffusional resistance is characterized by the Thiele modulus and the Biot number. Both dimensionless parameters account for particle geometry through the characteristic length parameter, L. The characteristic length is sometimes defined to be the ratio of the gross volume of the particle (solid plus void volume) to the external surface area of the particle. Application of this definition to activated sludge flocs has two advantages. The first advantage is that it avoids the difficulty of determining the meaning of "size" for the highly irregular shapes of activated sludge flocs. The second advantage is that the effect of floc shape on the relationship between the Thiele modulus and the effectiveness factor is minimized (Knudsen et al. (1966)).

The model of the diffusion and reaction process within activated sludge flocs is based on the use of an average characteristic length (L, as defined above) to account for distributions of floc size and shape. Although floc shape is not expected to be an important consideration, a specific geometry is needed to facilitate the derivation of the model equations. The following derivation begins with spherical geometry (Figure 3.1) and then generalizes to include cylindrical and slab geometries. The derived equation is a mathematical

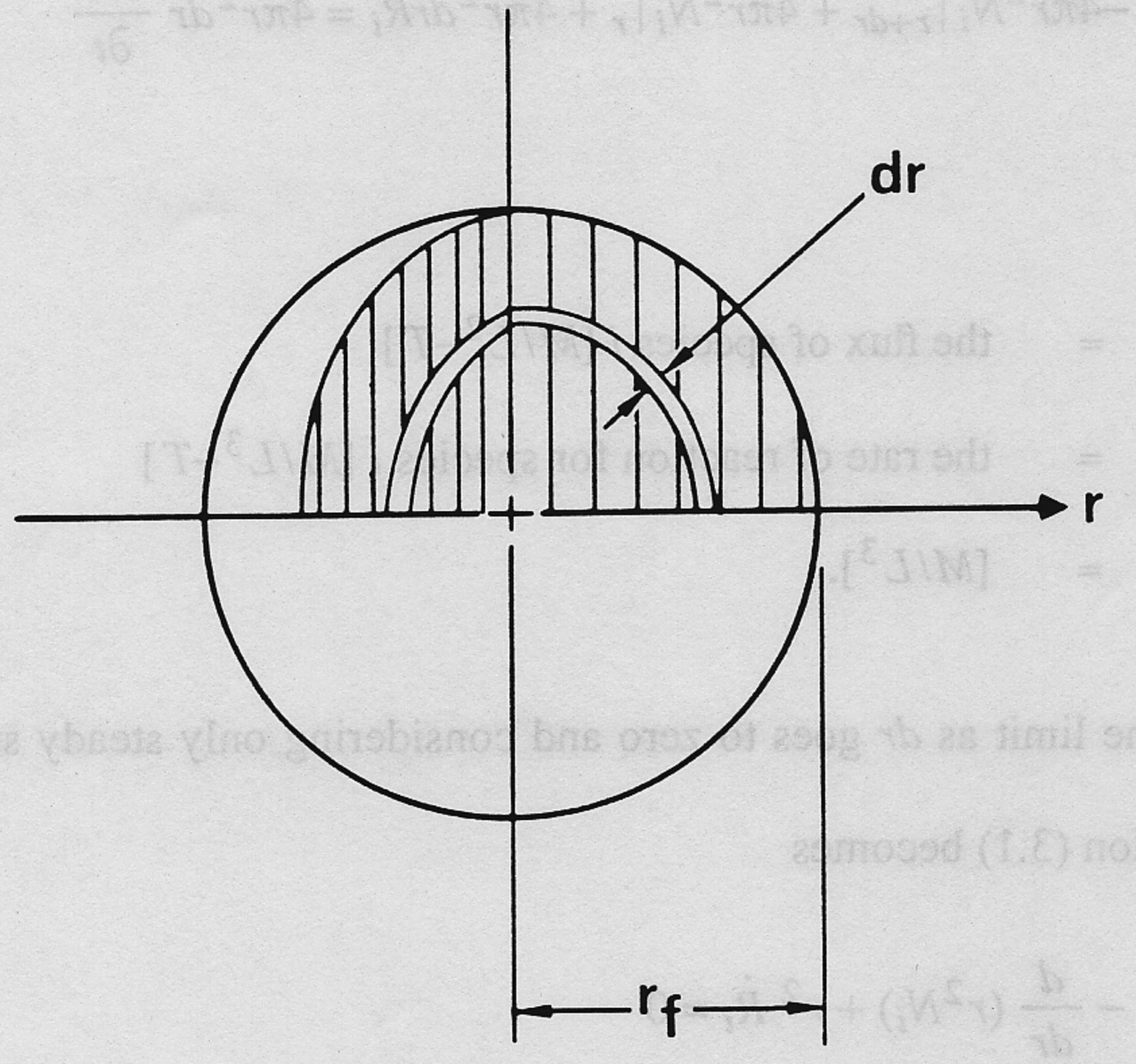

Fig. 3.1 Spherical Floc of Radius r_f

description of the concentration distribution of a reactant as it diffuses through a floc.

Applying the principle of conservation of mass to the spherical shell of thickness dr gives

$$-4\pi r^2 N_i|_{r+dr} + 4\pi r^2 N_i|_r + 4\pi r^2 dr\dot{R}_i = 4\pi r^2 dr \frac{\partial s_i}{\partial t} \tag{3.1}$$

where

N_i = the flux of species i $[M/L^2\text{–}T]$

$\dot{R}_i$ = the rate of reaction for species i $[M/L^3\text{–}T]$

s_i = $[M/L^3]$.

By taking the limit as dr goes to zero and considering only steady state conditions, equation (3.1) becomes

$$-\frac{d}{dr}(r^2 N_i) + r^2 \dot{R}_i = 0 \tag{3.2}$$

Assuming that Fick's law is valid, the flux can be expressed as

$$N_i = -D_{e,\,i} \frac{ds_i}{dr} \tag{3.3}$$

where

$D_{e,\,i}$ = the effective diffusivity of species i $[L^2/T]$

Substitution of equation (3.3) into equation (3.2) and assuming that effective diffusivities are constant throughout the floc gives

$$D_{e,\,i}\left[\frac{d^2 s_i}{dr^2}+\frac{2}{r}\frac{ds_i}{dr}\right]+\dot{R}_i=0 \tag{3.4}$$

The boundary condition at the center of the floc is

$$\frac{ds_i}{dr}\,|_{r=0}=0 \tag{3.5}$$

The boundary condition at the surface of the floc is

$$D_{e,\,i}\frac{ds_i}{dr}\,|_{r=r_f}=k_i(S_{B,\,i}-s_{i,\,s}) \tag{3.6}$$

where

k_i = mass transfer coefficient of species i [L/T]

$S_{B,i}$ = concentration of species i in bulk liquid $[M/L^3]$

$s_{i,s}$ = concentration of species i at floc surface $[M/L^3]$

r_f = radius of floc [L]

The dimensionless form of equation (3.4) is

$$\frac{d^2 c_i}{dx^2}+\frac{a-1}{x}\frac{dc_i}{dx}+\frac{a^2L^2}{D_{e,\,i}S_{B,\,i}}\dot{R}_i=0 \tag{3.7}$$

where

x = r/r_f

c_i = $s_i/S_{B,i}$

a = geometry factor: 1 for slab;
2 for cylindrical; 3 for spherical

L = ratio of floc volume to floc surface area [L]

The dimensionless forms of the boundary conditions are

$$\frac{dc_i}{dx}|_{x=0} = 0 \tag{3.8}$$

$$\frac{dc_i}{dx}|_{x=1} = a\ Bi_i(1 - c_{i,s}) \tag{3.9}$$

where Bi_i = Biot number for species i

Reactions

The physical and biochemical reactions that occur in the nitrifying activated sludge process are numerous and complex. It is assumed here that only soluble substrates are involved and that the only major reactions are: 1) the oxidation of carbonaceous substrates by heterotrophic bacteria, 2) the oxidation of ammonium-nitrogen by nitrifying bacteria, and 3) the endogeneous decay of both heterotrophic and nitrifying bacteria.

With glucose as the carbonaceous substrate, the stoichiometry of the heterotrophic oxidation of carbon can be expressed as

$$C_6H_{12}O_6 + (6-7.96Y_{H3})O_2 + (1.59\,Y_{H3})NH_4^+ \longrightarrow (1.59\,Y_{H3})C_5H_7NO_2$$
$$+ (1.59\,Y_{H3})H^+ + (6-3.19\,Y_{H3})H_2O + (6-7.96\,Y_{H3})CO_2 \quad (3.10)$$

where

Y_{H3} = yield coefficient for heterotrophic bacteria [mass cells/mass substrate].

Throughout the remainder of this section, it is assumed that glucose is the primary source of organic carbon for the heterotrophs. The stoichiometry of the nitrification process is given by

$$NH_4^+ + (2-0.868\,Y_{N2})O_2 + (2-0.124\,Y_{N2})HCO_3^- \longrightarrow (0.124\,Y_{N2})C_5H_7NO_2$$
$$+ (1-0.124\,Y_{N2})NO_3^- + (1+0.248\,Y_{N2})H_2O + (2-0.744\,Y_{N2})H_2CO_3 \quad (3.11)$$

Y_{N2} = yield coefficient for nitrifying bacteria [mass cells/mass substrate].

Equation (3.11) assumes that the oxidation of ammonia in equation (1.1) is the rate limiting step and consequently does not allow for the accumulation of nitrite. Endogeneous decay is assumed to follow the stoichiometry given by

$$C_5H_7NO_2 + 5O_2 + H^+ \longrightarrow 5CO_2 + 2H_2O + NH_4^+ \tag{3.12}$$

The derivation of the above equations are presented in Appendix B.

Intrinsic Reaction Rate Expressions

The rates of the above reactions may be affected by a number of factors as discussed previously. Although factors such as temperature, pH, and the presence of toxic substances are important, the present model focuses only on the effects of substrate concentrations. This model proposes that the intrinsic rate of substrate utilization can be potentially limited by one or more necessary substrates and that an interactive-type kinetic model can be used to describe these situations. The exponential rate function, rather than the Monod function, is used in conjunction with the multiplicative form of equation (2.12).

Rate of Glucose Uptake

Assuming that oxygen and glucose are the only potential rate limiting substrates, the rate of heterotrophic oxidation of glucose is given by

$$\dot{R}_3 = -q_{H3}\rho U[\frac{c_1}{K_{1H}}]\cdot U[\frac{c_3}{K_{3H}}] \tag{3.13}$$

where

q_{H3} = maximum specific glucose uptake rate for heterotrophs [1/T]

[mass glucose/total sludge mass - T]

ρ = density of total sludge mass within floc $[M/L^3]$

U[x] = exponential rate function given by $1 - exp\,[(-ln\,2)x]$

c_i = concentrations of species i inside floc $[M/L^3]$

K_{iH} = half-saturation coefficient of species i for heterotrophs $[M/L^3]$

subscript 1 denotes oxygen and 3 denotes glucose.

From equation (3.10), the rate of glucose uptake appears to be dependent on the concentration of ammonia as well. While ammonia certainly can be assimilated by heterotrophic metabolism, it should be recognized that it is only one of the sources of nitrogen available to the heterotrophic bacteria. Organic nitrogen in the forms of amino acids and proteins as well as inorganic forms such as nitrite and nitrate can also be utilized (Painter, 1970). The rate versus concentration relationship for these different forms of nitrogen may be depicted in Figure 3.2. Each curve represents the rate/concentration relationship for the situation where only that source of nitrogen is available and where the rate is not limited by any other substrates. When several sources are simultaneously available, it is likely that the heterotrophic bacteria will utilize the most preferable form of nitrogen until it is depleted and then switch to the next most preferred form.

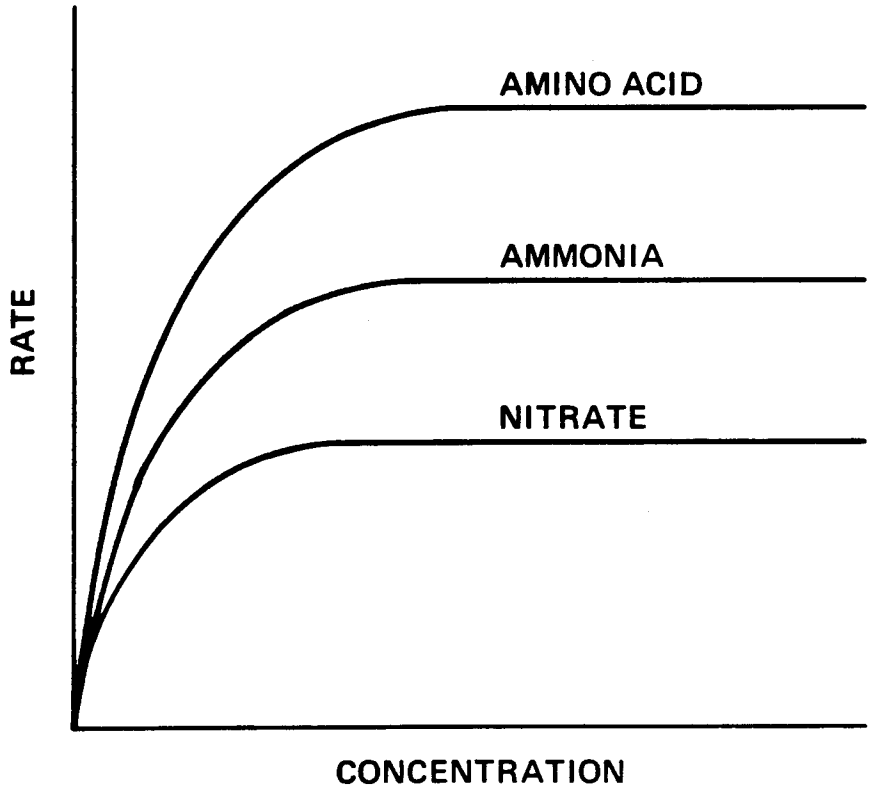

Fig. 3.2 Rate vs. Concentration Relationship for Three Forms of Nitrogen

In the nitrifying activated sludge process, several forms of nitrogen will be simultaneously available. If the process is fully nitrifying, the concentration of ammonia may be very low but the concentration of nitrate will be high. There may also be some organic nitrogen available from the influent as well as from endogeneous decay. It seems likely that a combination of nitrogen sources will be used and that the proportions of the different forms being used will vary depending on the relative abundance of the various forms under a given set of process conditions. Given these considerations, it is reasonable to expect that the rate of glucose oxidation will not be limited by ammonia. To be consistent with this discussion, however, the value of q_{H3} in equation (3.13) may be expected to vary as the dominant form of nitrogen available for heterotrophic uptake varied. This model, however, chooses to neglect this detail and assumes that q_{H3} is a constant.

Rate of Ammonia Uptake

The rate of reaction for ammonium-nitrogen is affected by the rate of uptake by heterotrophs, the rate of uptake by nitrifiers, and the rate of production resulting from endogeneous decay. The net rate of reaction is

$$\dot{R}_2 = -q_{H2}\rho U[\frac{c_1}{K_{1H}}]\cdot U[\frac{c_2}{K_{2H}}]\cdot U[\frac{c_3}{K_{3N}}]$$

$$- q_{N2}\rho U[\frac{c_1}{K_{1N}}]\cdot U[\frac{c_2}{K_{2N}}] + q_{D2}\rho U[\frac{c_1}{K_{1H}}] \qquad (3.14)$$

where

subscript 2 is for ammonium-nitrogen

q_{H2} = maximum specific ammonium-nitrogen uptake rate for heterotrophs [1/T] [mass NH_4^+–N/total sludge mass - T]

q_{N2} = maximum specific ammonium-nitrogen uptake rate for nitrifiers [1/T] [mass NH_4^+–N/total sludge mass - T]

q_{D2} = maximum specific ammonium-nitrogen production rate from endogeneous [mass NH_4^+–N/total sludge mass - T] decay [1/T]

K_{iN} = half-saturation coefficient of species i for nitrifiers [M/L^3].

The first term represents the uptake of ammonia by heterotrophic bacteria. Although this term includes an ammonia dependent term, it is not in contradiction with the previous discussion. Inclusion of an ammonia dependent term here simply ensures that the heterotrophs will not consume more ammonia than is available. The second term, representing the rate of ammonium-nitrogen uptake by the nitrifiers, assumes that inorganic carbon is not a potential rate limiting substrate. This assumption should always be valid since there should always be sufficient alkalinity in the mixed liquor to maintain proper pH for nitrification.

Rate of Oxygen Uptake

The rate of oxygen uptake is the sum of the rate due to heterotrophic activity, the rate due to nitrifier activity, and the rate due to endogeneous respiration. The net rate is given by

$$\dot{R}_1 = -q_{H1}\rho U[\frac{c_1}{K_{1H}}] \cdot U[\frac{c_3}{K_{3H}}] \cdot U[\frac{c_2}{K_{2N}}] - q_{N1}\rho U[\frac{c_1}{K_{1N}}] \cdot U[\frac{c_2}{K_{2N}}]$$

$$- q_{D1}\rho U[\frac{c_1}{K_{1H}}] \tag{3.15}$$

where

q_{H1} = maximum specific oxygen uptake rate for heterotrophs [1/T] [mass NH_4^+–N/total sludge mass - T]

q_{N1} = maximum specific oxygen uptake rate for nitrifiers [1/T] [mass NH_4^+–N/total sludge mass - T]

q_{D1} = maximum specific oxygen uptake rate for endogeneous respiration [1/T] [mass NH_4^+–N/total sludge mass - T]

Rate of Nitrate Production

The rate of nitrate production is given by

$$\dot{R}_4 = q_{N4}\rho U[\frac{c_1}{K_{1N}}]\cdot U[\frac{c_2}{K_{2N}}] \tag{3.16}$$

where

subscript 4 is for nitrate-nitrogen

q_{N4} = maximum specific nitrate production rate [1/T] [mass $NO_3^- - N$/total sludge mass - T]

All maximum specific rates in equations (3.13) through (3.16) are based on total cell mass and the floc density is the total cell mass of a floc divided by the gross volume of the floc.

Floc Model Summary

The potential rate limiting substrates in the nitrifying activated sludge process have been identified as oxygen, ammonia, and glucose. The mathematical description of the concentration distributions for each of these reactants within a floc is given by substituting the appropriate intrinsic reaction rate expression into equation (3.7). The floc model, thus, consists of three coupled, nonlinear, ordinary differential equations. For a fixed set of bulk reactant con-

centrations, this boundary-value problem can be solved to obtain the concentration distribution for each reactant. (The concentration distribution for nitrate can be calculated directly from the concentration distribution of the reactants). From these distributions, uptake rate distributions and microorganism growth rate distributions can be calculated. Global rates are then obtained by averaging these distributions over the volume of the floc.

REACTOR MODEL

The following derivation of the reactor model is for a continuous flow stirred tank reactor (CFSTR). Figure 3.3 is a schematic diagram of the reactor system. A substrate mass balance gives

$$(S_{IN,i} - S_i)F + X_T\bar{R}_i V = V\frac{dS_i}{dt} \quad \text{for } i=2,3,4 \tag{3.17}$$

$$K_L a(S_1^* - S_1) + X_T\bar{R}_1 V = V\frac{dS_i}{dt} \tag{3.18}$$

where

F = influent flow rate [L^3/T]

$S_{IN,i}$ = influent concentration of substrate i [M/L^3]

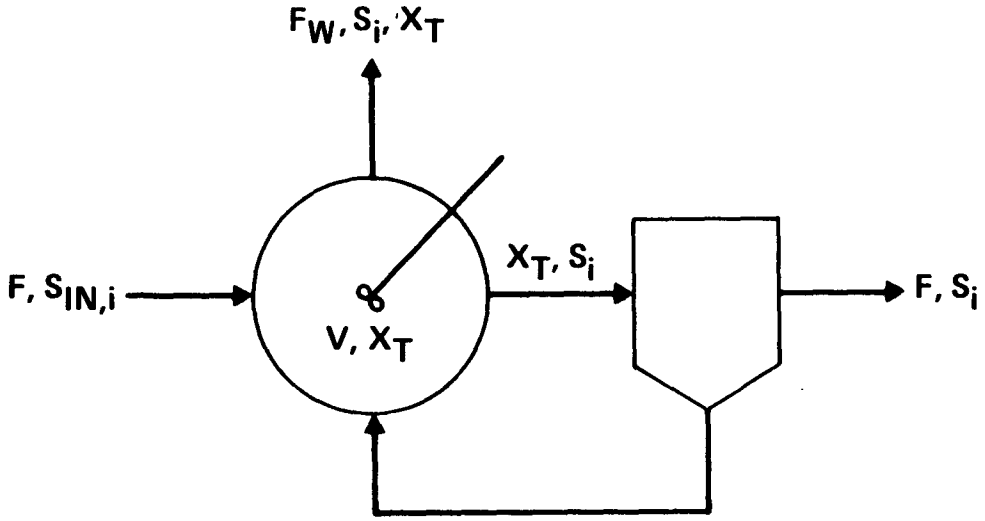

Fig. 3.3 Schematic Diagram of Complete-Mixed Activated Sludge Process

S_i = effluent concentration of substrate i $[M/L^3]$

$\bar{R}_i$ = global specific reaction rate of substrate i [mass of substrate/mass of total sludge - T]

X_T = mixed liquor concentration $[M/L^3\text{–}T]$

V = volume of aeration basin $[L^3]$

$K_L a$ = oxygen transfer coefficient [1/T]

S_i^* = saturation concentration of DO $[M/L^3]$.

Assuming that the microorganism concentration in the influent and effluent are negligible, the mass balance for the nitrifiers and the heterotrophs, respectively, are:

$$\frac{-1}{\theta_c} X_N + X_T(\bar{R}_N + f_N \bar{R}_D) = \frac{dX_N}{dt} \tag{3.19}$$

$$\frac{-1}{\theta_c} X_H + X_T(\bar{R}_H + f_H \bar{R}_D) = \frac{dX_H}{dt} \tag{3.20}$$

where

θ_c = MCRT [T]
or F_w/V where F_w is waste flow rate

X_N = concentration of nitrifiers $[M/L^3\text{–}T]$

X_H = concentration of heterotrophs $[M/L^3\text{–}T]$
note that $X_N + X_H = X_T$

$\bar{R}_N$ = global specific growth rate for nitrifier

[mass of nitrifiers/mass of total sludge -T]

$\bar{R}_H$ = global specific growth rate for heterotrophs
[mass of heterotrophs/mass of total sludge -T]

f_N = nitrifier fraction, X_N/X_T

$\bar{R}_D$ = global specific decay rate [1/T]

The reactor model, thus, consists of equations (3.17) through (3.20). If the concentration of DO in the reactor is controlled, then equation (3.18) is unnecessary.

The global specific rates in the reactor model are obtained from the simultaneous solution of the floc model (equation (3.7) for i = 1,2,3). The two models are linked by the boundary conditions given by equations (3.8) and (3.9) and by the following relationships

$$q_{N2} = q'_{N2} \cdot f_N \tag{3.21}$$

$$q_{H3} = q'_{H3} \cdot f_H \tag{3.22}$$

where

q'_{N2} = maximum specific ammonium-nitrogen
uptake rate for nitrifiers
[mass NH_4^+–N/mass of nitrifiers -T]

q'_{H3} = maximum specific glucose uptake rate for heterotrophs
[mass glucose/mass of heterotrophs -T]

These equations simply state that the maximum specific rates that are based on

total sludge mass, q_{N2} and q_{H3}, can vary as the relative sizes of the nitrifying and heterotrophic populations shift. It is assumed that the maximum specific rates based on specific populations, q'_{N2} and q'_{H3}, are intrinsic properties of those populations and are therefore constant.

IV. EXPERIMENTAL INVESTIGATION

The objective of the experimental investigation is twofold. The first objective is to qualitatively demonstrate that mass transport limiting conditions can affect the relationship between DO concentration and nitrification. The second objective is to determine whether the mathematical model proposed in the previous section can adequately describe the observed effects. The latter objective is accomplished by solving a parameter estimation problem. A series of experiments were conducted to satisfy both objectives. The experimental data was collected from a laboratory-scale activated sludge system that was designed and constructed for this investigation.

PARAMETER ESTIMATION

Of the large number of kinetic and physical parameters contained in the model, only the physical parameters of the reactor model can be easily determined by direct measurements. The values of the kinetic and physical parameters of the floc model remain to be determined by parameter estimation.

Not all of the kinetic parameters in the reaction rate expressions (3.13-3.16) are independent. Assuming that equations (3.10-3.12) are adequate models of the stoichiometry of substrate uptake in the nitrifying activated sludge process, the following relationships can be used to reduce the number of

kinetic parameters.

$$q_{H1} = 0.178(6–7.97\ Y_{H3})q_{H3}$$

$$q_{N1} = 2.29(2–0.868\ Y_{N2})q_{N2}$$

$$q_{H2} = 0.124\ Y_{H3}q_{H3}$$

$$q_{N4} = (0.124\ Y_{N2}–1)q_{N2}$$

$$q_{D2} = –0.09\ q_{D1}$$

Direct measurements of some of the physical parameters of the floc model have been attempted by a number of previous investigators. These attempts invariably required the removal of a floc sample from actual reactor conditions before applying the measurement procedure. Dick (1966) pointed out that physical characteristics of activated sludge flocs are not fundamental properties of the sludge. The size, shape, and density of a floc is dependent on a number of factors that are not intrinsic to the sludge itself. These factors include the degree of turbulence experienced by the floc, the recent history of turbulence experienced by the floc, and the concentration of the mixed liquor. In addition, the effect of these factors on the physical characteristics of a floc may depend on properties of the sludge that are controlled by process variables such as sludge age and feed composition. It is not surprising then that the values of various floc parameters from the literature span wide ranges. For example, the reported values of the diffusivity of oxygen in activated sludge flocs range from 8% to 100% of its value in pure water. The range of values for

the effective diffusivity of glucose is similar.

Although direct measurements of floc parameters can potentially be quite useful, such measurements must be made under *in situ* conditions. No satisfactory *in situ* procedures, however, have yet been shown to be reliable. Fortunately, it is not necessary to have explicit estimates of all the physical parameters in the floc model. From an inspection of equations (3.7) to (3.9), it can be seen that the dimensionless model only requires a small number of parameter groups. The number of groups can be further reduced by the use of the following relationships.

The effective diffusivity of a reactant in a porous catalytic particle is often related to its diffusivity in the bulk liquid by

$$D_e = \frac{\varepsilon}{\tau} D_L \tag{4.1}$$

where

ε = porosity of particle

= porosity/tortuosity

τ = tortuosity of particle.

The term $\frac{\varepsilon}{\tau}$ is purely a property of the particle. The liquid diffusivities of

nonelectrolytes in dilute solutions can be estimated with the use of the empirical equation developed by Wilke and Chang (1955). The liquid diffusivities of electrolytes in dilute solutions can be estimated from the equation suggested by Nerst (1888). Calculations of the liquid diffusivities of oxygen, glucose, ammonium-nitrogen (NH_4^+–N), and nitrate-nitrogen (NO_3^-–N) are presented in Appendix B. Substitution of equation (4.1) into equations (3.7) and factoring the floc density, ρ out of the reaction rate expression gives

$$\frac{d^2c_i}{dx^2} + \frac{a-1}{x}\frac{dc_i}{dx} + \frac{a^2L^2\rho\tau}{\varepsilon D_{L_i}S_{B,i}}\dot{R}' = 0 \tag{4.2}$$

The number of parameters in the boundary conditions given by equations (3.9) can also be reduced. The Biot number is related to the Sherwood number by

$$Bi = Sh\left[\frac{D_L}{D_e}\right] \tag{4.3}$$

where

Sh = Sherwood number

The Sherwood number correlation for convective mass transfer over spheres is given by

$$Sh = 2.0 + 0.6\,\mathrm{Re}^{0.5} Sc^{0.33} \tag{4.4}$$

where

Re = Reynold's number

Sc = Schmidt number

With these relationships, the Biot numbers in equations (3.9) can then be expressed in terms of only the Reynolds number and $\frac{\varepsilon}{\tau}$. The kinetic parameters and physical parameters needed for the floc model are summarized in Table 4.1

The parameter estimation problem requires a set of experimental observations from which values of the model parameters are selected to "best fit" the observations. The solution of this problem would be difficult if all of the parameters in Table 4.1 were to be estimated from one set of observations. One reason is that not all of the parameters may be active over a given set of observations. For example, under experimental conditions in which the concentration of DO is limiting, the concentration of NH_4^+–N probably will not be limiting. In this situation, K_{1N} is an active parameter but K_{2N} is not. If the concentration of DO is not limiting, then K_{2N} may be active while K_{1N} may be inactive. Even if a set of observations for which all the model parameters are active is available, the solution of the estimation problem can still be hampered by any correlation between the model parameters.

Table 4.1 Nitrification Kinetic and Stoichiometric Parameters

Half-Saturation Coefficients:

K_{1N}, K_{1H}, K_{2N}, K_{3H}

Specific Rates:

q_{H3}, q_{N2}, q_{D1}, q_{D2}

Yields:

Y_{H3}, Y_{N2}

Mass Transport Parameters:

$L^2\rho$, ε/τ, Re

SUBPROBLEMS

The approach to the solution of the parameter estimation problem taken in this investigation was to divide the problem into four subproblems. In each subproblem, experimental conditions were chosen to isolate only a few of the model parameters. Because the focus of this investigation emphasizes certain features of the model, the grouping of parameters into the subproblems as well as the method of solutions of the subproblems reflect the relative importance of each subset of parameters.

Subproblem 1

The formulation of the mathematical model assumed that there is an intrinsic effect of DO concentration on the rate of nitrification and that this effect can be affected by mass transport resistance. It was also proposed that the exponential rate function, rather than the Monod function, is an appropriate model of the intrinsic rate. The objective of this subproblem is to determine whether the exponential rate function is indeed more appropriate than the Monod function. The parameter to be estimated is K_{1N}.

Four sets of experiments were performed for this problem. The experimental conditions were chosen to isolate the intrinsic rate relationship and to eliminate all other model parameters. The most important condition to be

satisfied is the minimization of mass transport resistance. Complete isolation of the rate relationship and the elimination of the remaining parameters was accomplished by conducting relatively short term batch experiments in which nitrification was the only reaction of significance and DO was the only rate limiting substrate.

The first set of experiments was used to determine the reactor conditions necessary to ensure the elimination of transport resistance. The next three sets, using the information obtained from the first set, were conducted to obtain data on the relationship between nitrification rate and DO concentration. The resulting data was fitted with both the exponential and Monod model. The value of K_{1N} that gave the best fit for each function was determined.

Subproblem 2

The objective of this subproblem is to determine whether the stoichiometric relationships given by equations (3.10)-(3.12) adequately describe the stoichiometry of the reactions occurring in the laboratory-scale activated sludge system. The parameters to be estimated are: q_{H3}, Y_{H3}, q_{N2}, Y_{N2}, q_{D1}, and q_{D2}. The parameter estimation problem was simplified by eliminating mass transport resistance and running batch experiments.

Two sets of experimental runs (each consisting of two replication runs) were used to estimate the kinetic parameters. In the first set, the nitrification reaction and endogeneous reaction were the only reactions of significance. The parameters q_{N2}, Y_{N2}, q_{D1}, and q_{D2} were estimated from this set. With the estimated values for these parameters, q_{H3} and Y_{H3} were then estimated in the second set. In this set, all three reactions were allowed to proceed at their maximum rates.

Subproblem 3

The remaining kinetic parameters to be determined are K_{1H}, K_{2N}, and K_{3H}. Though the role of these parameters are analogous to that of K_{1N}, estimation of their values by conducting experiments similar to those in Subproblem 1 was not feasible. Estimation of these parameters would require accurate measurements of concentrations that are on the same order of magnitude as the true values of the parameters. The reported values of K_{1H}, as noted previously, are on the order of 0.01 mg/L (Dalton et al. (1979)). The reported values of K_{2N} are on the order of 0.1 mg/L (Hao et al. (1983)) and the reported values of K_{3H} are on the order of 1.0 mg/L (Lee et al. (1984)). The experimental apparatus and instrumentation that was used in this investigation is not capable of such low level measurements.

Another approach was used. It was recognized that the concentration of NH_4^+–N and glucose in the effluent of a properly a operated activated sludge process must be low. Because the steady state concentration of NH_4^+–N and glucose will probably be on same order of magnitude as their respective half-saturation coefficients, the parameters K_{2N} and K_{3H} will be active. With the values of the parameters estimated in Subproblems 1 and 2, and assuming that mass transport resistance was minimal, it was possible to select reasonable values for K_{2N}, and K_{3H} so that the steady state solution of the model matched observed effluent concentrations from steady state experiments. It was also possible to select a value for K_{1H} by matching solutions of the model with the observed effluent concentrations from steady state experiments that were conducted under mass transport limiting conditions.

Subproblem 4

The objective of this subproblem is to demonstrate that mass transport resistance can affect the intrinsic relationship between DO concentration and nitrification. The extent of the mass transport resistance is estimated in terms of the parameters $L^2\rho$, $\frac{\varepsilon}{\tau}$ and Re.

Three experimental runs were simultaneously conducted. In two of the runs, the experimental conditions were identical with the exception of the mix-

ing intensity. In these runs, continuous feed activated sludge reactors were operated at "low" DO concentrations for about 24 hours. The response of the nitrifiers and the heterotrophs were measured in terms of effluent substrate concentrations. Estimates of the mass transport parameters were obtained by selecting values of the parameters for which the solution of the mathematical model best fitted the effluent data. In the third run, a control reactor was operated at a "high" DO concentration and high mixing intensity during the same experimental period.

REACTOR SYSTEM

The laboratory-scale activated sludge reactor system that was designed and constructed for the experimental work comprises of three separate, but identical, activated sludge reactor subsystems. A schematic diagram of a subsystem is shown in Figure 4.1.

Reactors and Temperature Control

Each cylindrical reactor has a maximum volume of 18 liters and a working volume of 14.5 liters. The jacketed reactors were constructed from 15 inch long sections of concentric 10 inch diameter and 12 inch diameter plexiglass tubing. Water from a Haake KT33 Circulating Water Bath can circulate through each jacket at a rate of up to 20 gallons per hour. The temperature in

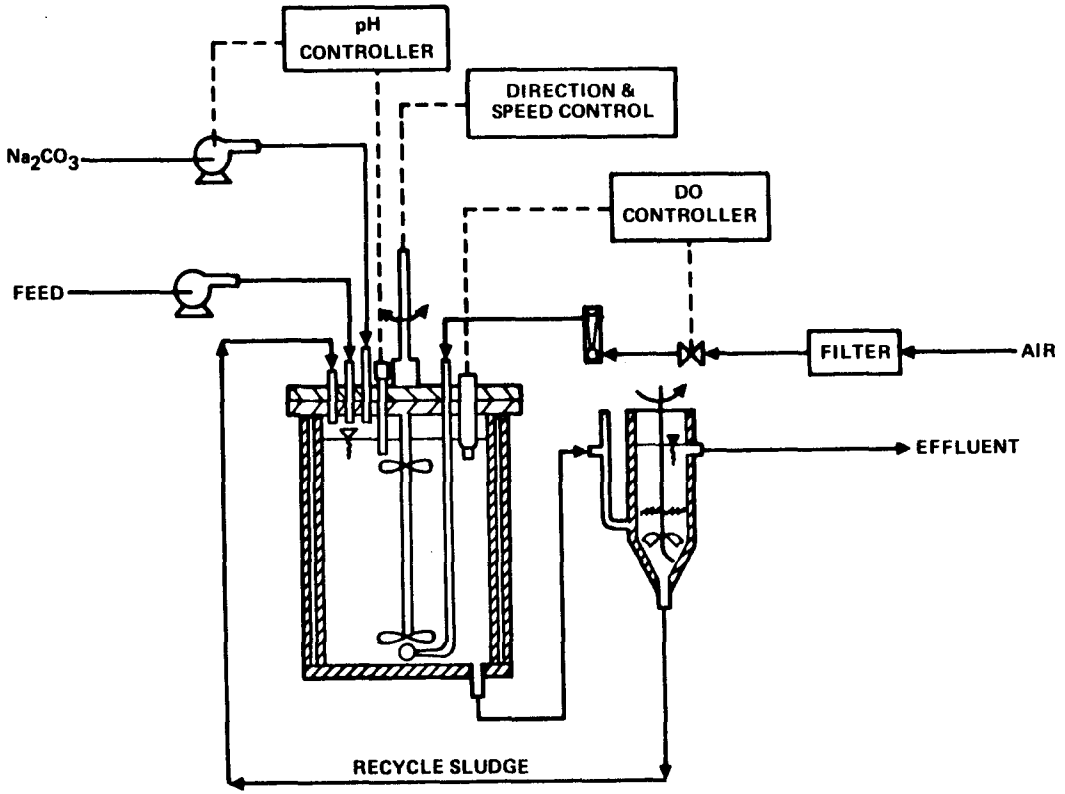

Figure 4.1 Laboratory Scale Reactor

each reactor could thus be maintained to within about 1°C of a temperature set point.

The large ratio of wall surface area to reactor volume in these reactors are not typical of full-scale activated sludge reactors. Attached-growth in a laboratory-scale reactor may have a significant effect on the observed kinetics of substrate uptake. To prevent the accumulation of wall growth, each reactor is equipped with a motorized scrapper assembly. This assembly is essentially a set of rotating baffles with Teflon squeegee blades that scrape the wall and the bottom of the reactor. The frame of the assembly was constructed from 316 stainless steel and the width of the baffles (including the width of the squeegee) is 7/8 inch.

Mixing and DO Control

Because the main purpose of this experimental work is to investigate the synergism between mass transport limitation and DO concentration, the reactor system had to allow for the independent control of the level of turbulence and DO concentration in the mixed liquor. This was accomplished to a large degree by using impellers for mixing and a fine bubble diffuser to provide DO.

Mixing for each reactor is provided by two 5 inch axial flow impellers. The marine-type impellers are mounted on a common shaft and are located at 3

inches and 11 inches from the bottom of the reactor. The upper impeller is about 2.5 inches below the surface of the mixed liquor. The impeller rotational speed could be varied from zero to 1725 rpm and the direction of flow is also reversible.

At low rotational speeds (less than about 100 rpm), it was necessary to have the flow directed downwards to keep the mixed liquor in complete suspension. At high rotational speeds (greater than about 300 rpm), it was also necessary to have the flow directed downwards to minimized surface aeration. For these reasons and to maintain consistency throughout the experiments, the flow was always directed downwards.

Aeration is provided by a 1 inch spherical fine bubble diffuser located directly below the bottom impeller. Air flow rates of up to 5.0 SCFH are possible, but to minimize the mixing effects from diffused aeration, the flow rates were usually kept below 2.0 SCFH during experiments. Because the impellers direct the flow downwards, aeration efficiency largely depends on the rotational speed of the impellers. In the experiments in which the same DO concentration had to be maintained under different turbulence conditions (impeller speeds), a mixture of air and pure oxygen was used in the reactor with the lower oxygen transfer efficiency. By using this air/oxygen mixture, it was possible to use the same air flow rates with different impeller speeds and still maintain the same

DO concentration.

The DO concentration in each reactor was continuously measured by a YSI 5739 DO probe and a YSI Model 57 Oxygen Meter. The probe was inserted through the 3/4 inch plexiglass reactor top to a depth of about 2.5 inches below the surface of the mixed liquor. The tip of the probe was at the same level as the top impeller and within an inch of the impeller tip. This location insured adequate agitation over the membrane of the probe even under low turbulence conditions and prevented bubbles from being trapped on the membrane.

Since the effect of DO concentration is one of the main concerns of this investigation, precise control of DO concentration was necessary. A differential gap controller was designed and constructed for this purpose. Whenever the DO concentration dropped below the set point, a solenoid valve was activated to add extra air flow to the mixed liquor. This controller was able to maintain the DO concentration within about 0.1 mg/L of the set point.

pH Control

Nitrification is highly sensitive to pH. Although this investigation was not concerned with the effect of pH, it was necessary to maintain a constant, though not necessarily optimal pH. Each reactor has a Horizon Model 599-20

pH Controller. The pH in the reactor was continuously measured with a Orion GX series pH electrode (Model 91500). The electrode was inserted through the reactor top and located in a manner similar to the DO probe. Whenever the pH of the mixed liquor dropped below the desired pH set point, the Controller activated a pump to deliver a 2N soda ash (Na_2CO_3) solution until the set point was reached. During the entire experimental investigation, the pH was maintained between 7.4 and 7.6.

Feed System

Feed to the reactors were prepared by an automatic feed dilution system. A diagram of the system is shown in Figure 4.2. Concentrated feed ingredients were pumped into a reservoir and mixed with tap water to give the desired concentration. The system was kept refrigerated to minimize growth in the feed reservoir. The feed was distributed to the reactors through Tygon tubing.

Clarifiers

Each clarifier was constructed from a 12 inch section of 4 inch diameter Schedule 40 PVC pipe. A polypropylene funnel with a 60° cone formed the bottom. The volume of the clarifier is about 2.2 liters. Mixed liquor flows to the side arm of the clarifier from the bottom of the reactor by gravity. The level of the mixed liquor in the reactor is controlled by the elevation of the clarifier.

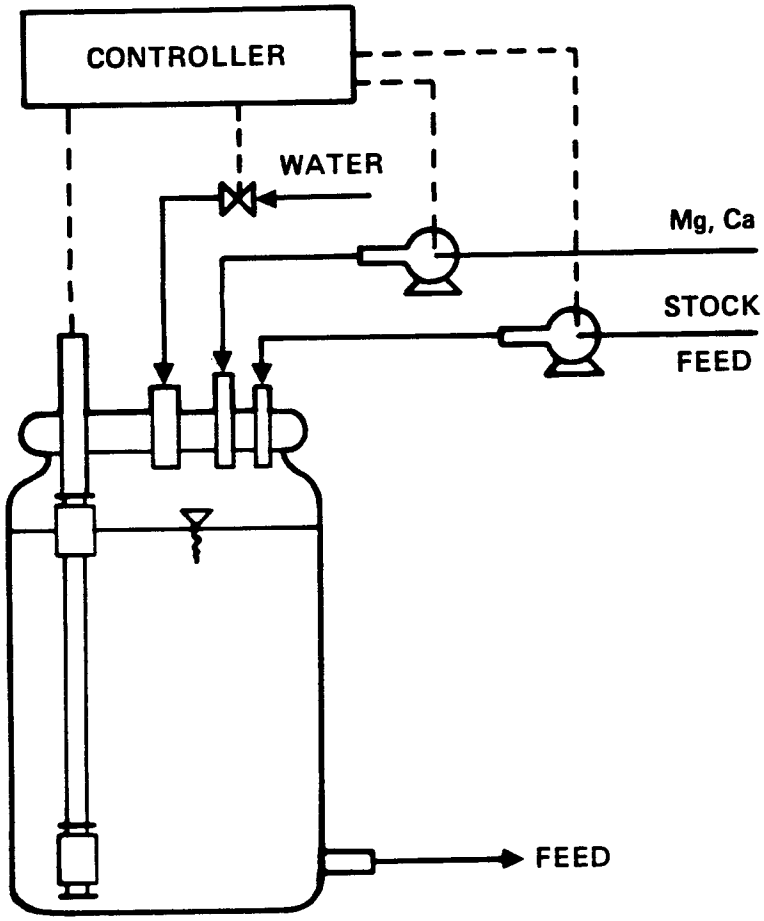

Fig. 4.2 Schematic Diagram of Automatic Feed Dilution System

The side arm promotes flocculation before the mixed liquor enters the clarifier and the rake assembly prevents bridging by breaking sludge blanket on the stationary spikes protruding from the wall of the funnel.

Operation

The reactors were seeded with activated sludge from the City of Los Angeles' Hyperion wastewater treatment plant. The sludge was then fed the synthetic substrate shown in Table 4.2 made from stock solutions shown in Table 4.3. This formula is a slight modification of that used by Poduska (1975). Feed was pumped into each reactor at the rate of about 2.2 L/hr. This corresponds to an organic loading rate of 6.2 g TOC/day and a nitrogen loading rate of about 3.1 g NH_4^+-N/day.

Return sludge was pumped from the bottom of the clarifier at the rate of 13.5 L/hr for 40 seconds at intervals of six minutes. This was equivalent to a recycle ratio of about 0.69. Sludge was wasted daily from the mixed liquor to maintain a target concentration. The MLSS concentration was maintained at about 1500 to 2500 mg/L. Normal operating conditions and the range of typical operating data are summarized in Table 4.4.

A number of difficulties were encountered during the operation of the reactor system. The most serious problems were associated with the flocculat-

Table 4.2 Influent Feed Composition to Reactors

Constituent	Concentration*
$C_6H_{12}0_6$	300*
NH_4Cl	230
$K_2HPO_4 \cdot 3H_20$	88
Na_2SO_4	28
Yeast extract	28
$MgCl_2 \cdot 6H_20$	12
$CaCl_2 \cdot 2H_20$	7

* concentration in mg/L

Table 4.3 Stock Solution Composition

Constituent	Concentration*
$C_6H_{12}0_6$	105.3
NH_4Cl	80.8
$K_2HPO_4 \cdot 3H_20$	31.0
Na_2SO_4	10.0
yeast extract	10.0
trace mineral solution	3 mL/L
$MgCl_2 \cdot 6H_20$	17.5
$CaCl_2 \cdot 2H_20$	9.6
Trace Mineral Solution	
$FeCl_3 \cdot 6H_20$	19.4
$MnCl_2 \cdot 4H_20$	4.7
$ZnCl_2$	3.3
$CuCl_2 \cdot 2H_20$	2.1
$CoCl_2 \cdot 2H_20$	2.9
$(NH_4)Mo_70_{24} \cdot 4H_20$	2.1
$Na_3C_6H_50_7 \cdot 2H_20$	176.5
$Na_2B_40_7 \cdot 10H_20$	1.1

*concentration in g/L unless otherwise noted

Table 4.4 Range of Normal Operation

Range of Normal Steady State Operating Conditions

pH:	7.5 - 7.6
temperature:	22^oC–25^oC
impeller speed:	170 rpm - 200 rpm
DO concentration:	5 mg/L - 6 mg/L
sludge age:	4 days - 8 days

Range of Normal Steady State Operational Data

MLSS:	1500 mg/L - 2500 mg/L
% MLVSS:	89 - 97
SVI:	70 - 150
SOUR:	18 mg/g-hr - 25 mg/g-hr
Effluent	
SS:	5 mg/L - 40 mg/L
TOC:	4 mg/L - 10 mg/L
NH_4^+–N:	0.1 mg/L - 0.5 mg/L
NO_2^-–N:	0.05 mg/L - 0.2 mg/L
NO_3^-–N:	45 mg/L - 60 mg/L

ing and settling characteristics of the sludge. Filamentous bulking was a frequent problem. During the onset of bulking, the performance of the reactors in terms of the effluent composition was not affected. Nitrification was not affected. When the bulking problem became severe, the reactors were operated as sequencing-batch reactors in an attempt to remedy the problem. This operational change was sometimes successful but required several MCRT's before the settling characteristics improved.

Filamentous bulking is usually attributed to persistent low DO conditions or low nutrient (nitrogen and/or phosphorus) conditions (Lau, et al. (1984) The reactors, however, were normally operated at DO concentrations of about 5 mg/L to 6 mg/L and the feed composition was not nutrient poor. In searching for the cause of the bulking, it was found that bulking appeared to be related to the amount of biological growth that accumulated in the feed lines.

A less frequent, but no less severe, problem was characterized by a gradual increase in effluent turbidity. After about two or three days of increasing effluent turbidity, the color of the sludge changed from its normally light tan color to a dark greyish brown color. During this period, it appeared that nitrification was affected. The effluent concentration of NH_4^+-N would increase from its normal concentration of about 0.2 mg/L to as much as 1 or 2 mg/L. the effluent concentration of NO_3^--N would decrease from its normal concentration

of about 50 mg/L to as low as 35 mg/L. It was not determined whether the loss of nitrification was due to a loss of solids, an inhibition effect, or a combination of both. A possible source of this problem was again thought to be associated with growth in the feed preparation system. Although regular cleaning of the feed distribution system did not entirely eliminate this problem, the severity of this problem was reduced.

All of the data described in the following sections were collected during periods in which the reactors appeared to be operating normally. The reactors were always operated for about two MCRT's at normal operating conditions following the recovery from any major process upset. The reactors were judged to be normal when the effluent characteristics and sludge characteristics remained stable within the normal range for a period of about one MCRT.

ANALYTICAL METHODS

Mixed liquor suspended solids (MLSS) and mixed liquor volatile suspended solids (MLVSS) were determined according to Method 209C and 209D of Standard Methods (1985). Gooch crucibles of 25 mL capacity and Whatman 934-AH filters were used. Sample sizes from 5 mL to 10 mL were used and each determination was averaged from duplicate samples.

Ammonium-nitrogen measurements were maded with the Orion 95-10 Ammonia Selective Electrode. Nitrate-nitrogen measurements were made with the Orion 93-07 Nitrate Ion Electrode. Both electrodes were used with a Orion Model 407A Specific Ion Meter. The procedure in the Instruction Manual for each electrode was followed. A sample size of 30 mL was used and the samples were filtered through a Whatman 934-AH filter. All determinations were averaged from duplicate samples.

Nitrite-nitrogen concentrations were determined according to Method 419 of Standard Methods (1985). A Bausch & Lomb Spectronic 20 spectrophotometer was used at a wavelength of 543 nm. Each determination was averaged from duplicate samples.

Total organic carbon (TOC) determinations were made with an Ionics Model 1270 Total Oxygen Demand and Total Organic Carbon Analyzer. Samples were filtered through a Whatman 934-AH filter. Inorganic carbon interference was removed by adding 0.7 mL of 2N HCl to 10 mL sample volumes and sparging with nitrogen at a flow rate of about 100 cc/min for 10 minutes. Triplicate samples were used and determinations were averaged from the last two samples.

V. RESULTS AND DISCUSSION

Subproblem 1

All of the experiments for this subproblem were conducted in the activated sludge reactors that were previously described. Prior to the start of each set of experiments, the reactors were operated at the steady state conditions described in Table 4.4. The sludge age during this experimental period was about four to five days and the system was fully nitrifying. In preparation for each set of experiments the sludge from the reactors were collected, mixed and redistributed. This was done to ensure that the sludge in each reactor had the same characteristics.

About a half hour prior to the start of a set of experiments, the feed to all three of the reactors was shut off and the mixed liquor in each reactor was allowed to aerate at a DO concentration of at least 4 mg/L. Immediately prior to the start of the experiments, the DO concentrations (and/or impeller speeds) were set to the desired levels for the particular experiment. The mixed liquor in all the experiments were aerated by air only; pure oxygen was not used. Once the DO concentrations stablized to their desired levels, a small volume (about 20 mL) of concentrated NH_4Cl solution was added to each of the reactors to bring the NH_4^+–N concentration to about 80 mg/L. During the course of each experimental run, the concentration of NH_4^+–N and the concentration of

$NO_3^- - N$

was measured at hourly intervals. A sample volume of about 50 mL was withdrawn from each reactor at each sampling period. The samples were immediately filtered analyzed. The DO concentration during all runs was always within about 0.1 mg/L of the set point. The pH of each reactor was automatically maintained at 7.5 by addition of a 2N Na_2CO_3 solution.

Since only three reactors were available, only three runs could be conducted simultaneously for each set of experiments. Between sets of experiments the reactors were operated at steady state for a period of about five to 10 days. The experimental conditions for the four sets of experiments are summarized in Table 5.1. The three runs conducted in Set I were used to determine the minimum impeller rotational speed at which mass transport resistance is eliminated.

The results for Set I are shown in Table A.1 and Figures A.1-A.3 in Appendix A. As expected, the rate of nitrification for each of the three runs was zero order with respect to $NH_4^+ - N$. Linear regression could, therefore, be applied to determine the rate of nitrification. The regression equations and the associated r values (square root of the coefficient of determination) are included in Table A.1. The regression lines are included in Figures A.1-A.3.

Table 5.1 Summary of Experimental Conditions

Run	DO = 0.7 mg/L		RPM = 170	
No.	SET I	SET II**	SET III**	SET IV**
1	100*	0.25**	0.5	0.7
2	170	1.0	2.0	2.0
3	400	4.0-7.0	4.0-7.0	4.0-7.0

* impeller speeds in (rpm)

**DO concentrations in (mg/L)

Figure 5.1 is a summary of the Set I results. It appears that impeller speeds of at least 170 rpm reduce the floc size sufficiently to remove mass transport resistance. The difference between the specific rates of NH_4^+-N uptake and NO_3^--N production was probably due to an accumulation of NO_2^-N. Although NO_2^-N concentrations were not measured in this set of experiments, the accumulation of NO_2^-N can be inferred from the steady drop in the $(NH_4^+-N + NO_3^-N)$ concentration during the experiment. This hypothesis is supported by measurements of significant concentrations of NO_2^-N in similar experiments that were conducted for Subproblem 2.

An impeller speed of 170 rpm was used for the remaining three sets of experiments. The results for these experiments are presented in Tables A.2-A.4 and Figures A.4-A.12. The specific rates were again estimated from linear regression, and are summarized in Table 5.2. From the $(NH_4^+-N + NO_3^-N)$ concentration profiles, it appears that there was accumulation of NO_2^-N in at least the first two hours of each experimental run. The accumulation of NO_2^-N will be discussed in the next section (Subproblem 2). For the purposes of this section, it is only necessary to recognize that any NO_2^-N accumulation will affect only the observed NO_3^-N production rate and should not have any affect on the observed NH_4^+-N uptake rate. The following analyses are, therefore, based on only the observed NH_4^+-N uptake rates.

Table 5.2 Specific NH_4^+–N Uptake Rate vs. DO Concentration

	(Specific NH_4^+–N Uptake Rates)		
DO (mg/L)	*SET II*	*SET III*	*SET IV*
0.25	0.55*	-	-
0.50	-	3.11	-
0.70	-		-3.77
1.0	3.61	-	-
2.0	-	6.22	6.29
4.0-7.0	5.28	7.09	6.59

* specific rates in (*mg* NH_4^+–*N*/*g*–*hr*)

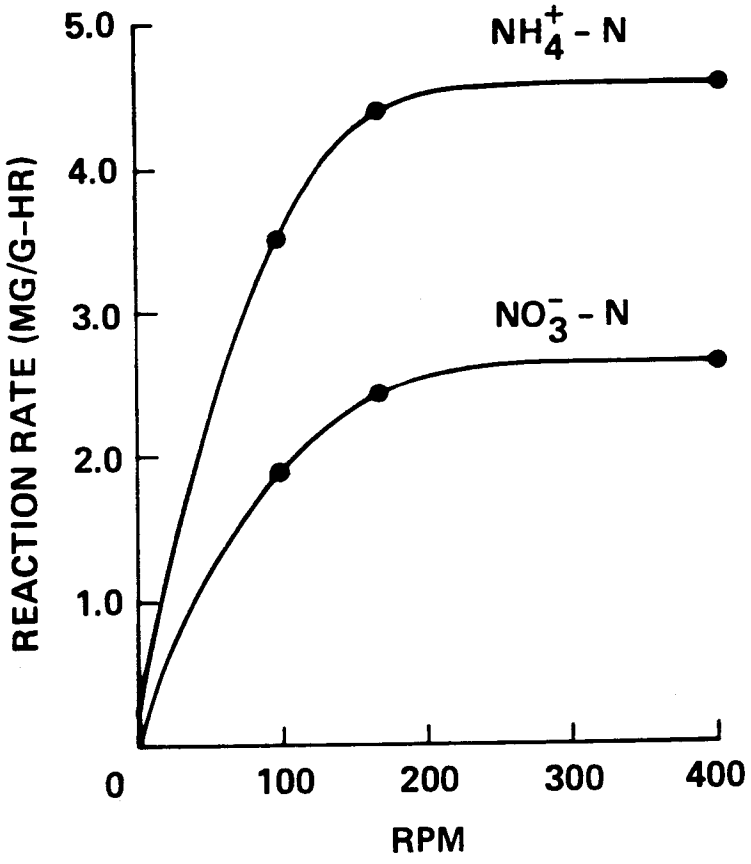

Fig. 5.1 Set I: NH_4^+–N Specific Uptake Rate and NO_3^-–N Specific Production Rate vs. Impeller Speed in RPM

For each set of experiments, both the exponential model, equation (2.9), and the Monod model, equation (2.7), were used to describe the relationship between the specific NH_4^+–N uptake rate and DO concentration. The models were fitted to the data by nonlinear least squares regression and the estimated values for q_{N2}, and K_{1N} are shown in Table 5.3. For each set of experiments, the correlation index (R^2) for the exponential model is higher than that for the Monod model. With the lowest R^2 at 0.93, the Monod model appears to fit the data adequately, though not as well as the exponential model. The parameter values estimated with the Monod model are, however, consistently and significantly higher than those estimated with the exponential model. In fact the estimates for q_{N2} that were generated by using the Monod model are objectionably high. It is obvious from the experimental data that the specific NH_4^+–N uptake rate is not likely to increase significantly with increasing DO concentrations beyond about 4 mg/L. Yet the Monod estimates predict that it can increase by 14% to 21% at DO concentrations above 7 mg/L. It appears that the Monod model was not able to estimate realistic values for q_{N2} from what appears to be reasonable data.

Since the primary objective is to estimate K_{1N}, it was decided that estimates of K_{1N} could be more accurately determined by eliminating q_{N2} from the models. Because K_{1N} represents an intrinsic characteristic of nitrifying bacteria, the elimination of q_{N2} would isolate the estimation of K_{1N} from the effect

Table 5.3 Nonlinear Least Squares Estimates of K_{1N} and q_{N2}

	SET II	*SET III*	*SET IV*
Monod Model			
K_{1N}	1.01*	0.732	0.589
q_{N2}	6.37**	8.16	7.49
R^2	0.94	0.98	0.93
Exponential Model			
K_{1N}	0.727*	0.622	0.560
q_{N2}	5.38**	7.10	6.67
R^2	0.96	1.0	0.99

* concentrations in (mg/L)

** maximum specific rates in ($mg\ NH_4^+–N/g–hr$)

of variation in gross sludge characteristics (that is, the mass fraction of active nitrifiers in the sludge) between sets of experiments. Elimination of q_{N2} was accomplished by normalizing the specific uptake rates in each set of experiment with respect to the value of q_{N2} estimated with the exponential model for that set. The normalized data is shown in Table 5.4. The normalized exponential model is

$$\frac{\mu}{\mu_m} = 1 - \exp\left[-ln\,2\left[\frac{s_1}{K_{1N}}\right]\right] \tag{5.1}$$

and the normalized Monod model is

$$\frac{\mu}{\mu_m} = \frac{s_1}{s_1 + K_{1N}} \tag{5.2}$$

The least squares fit of these models to the normalized data is shown in Figure 5.2. The R^2 for the exponential model was 0.984 and the R^2 for the Monod model was 0.913. The deficiency of the Monod model in describing the relationship between the concentration of DO and the rate of nitrification is clearly demonstrated in Figure 5.2. Although these results are specific to DO and nitrifiers and do not necessarily generalize to other substrates, Dabes et al. (1973) have demonstrated this same deficiency of the Monod model with kinetic data on glucose uptake, oxygen uptake, and phosphate uptake.

Table 5.4 Normalized Specific NH_4^+–N Uptake Rates vs. DO Concentration

DO (mg/L)	Normalized Specific NH_4^+–N Uptake Rates ($mg\ NH_4^+$–N/g–hr) SET II	SET III	SET IV
0.25	0.104	-	-
0.50	-	0.438	-
0.70	-	-	0.571
1.0	0.681	-	-
2.0	-	0.876	0.953
4.0	0.996	0.999	0.999
7.0	1.0	1.0	1.0

Monod: $$\frac{\mu}{\mu_m} = \frac{DO}{DO + 0.48}$$

$R^2 = 0.913$

Exponential: $$\frac{\mu}{\mu_m} = 1 - exp(-ln2\ \frac{DO}{0.62})$$

$R^2 = 0.984$

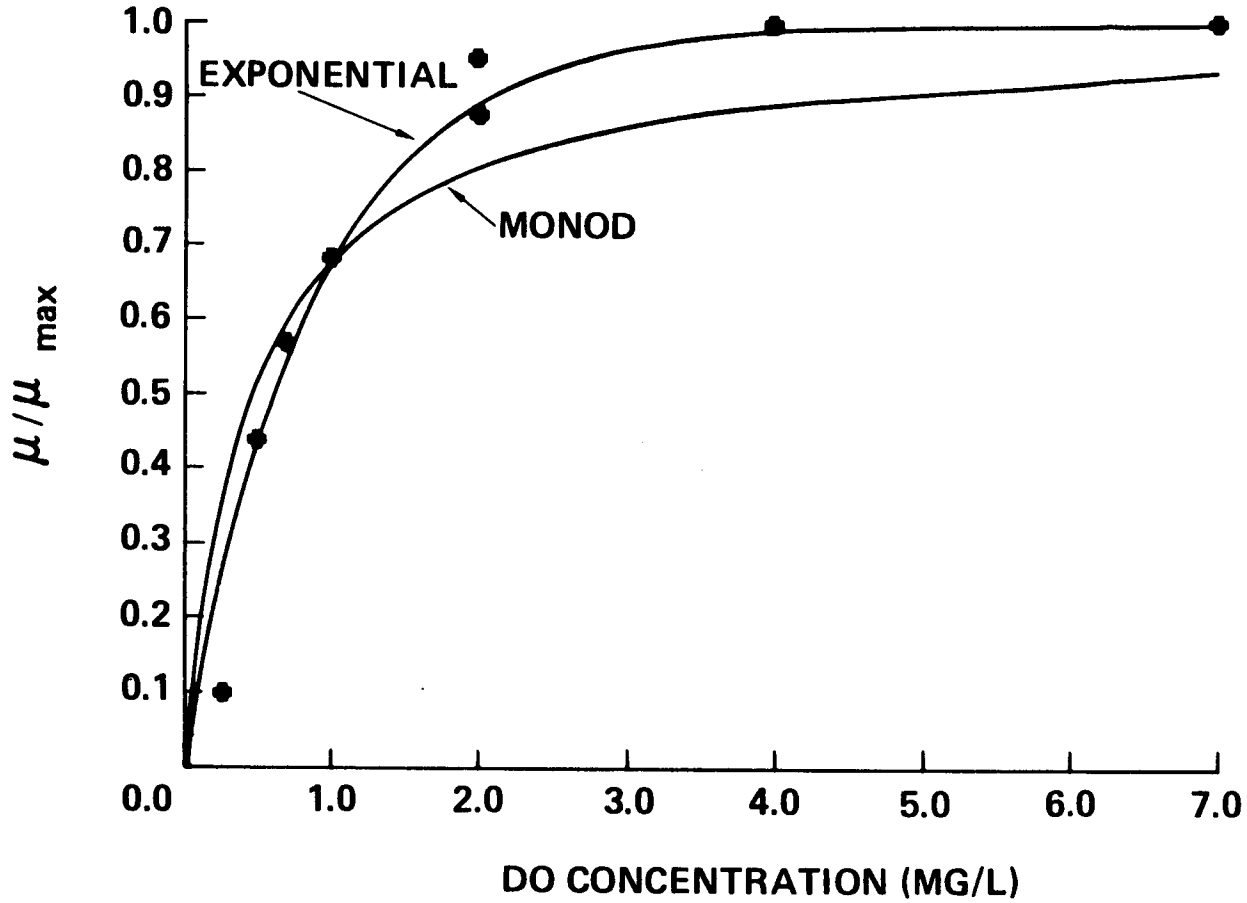

Fig. 5.2 Exponential and Monod Fit of Normalized NH_4^+–N Uptake Rate vs. DO Concentration Data at 170 RPM.

Subproblem 2

All of the experiments for this subproblem were conducted in a miniature analogue of the laboratory-scale reactors - a specially equipped one-liter Pyrex beaker. The beaker was equipped with a set of baffles and a water jacket that was formed by coiling a length of Tygon tubing around the bottom and wall of the beaker. Water from the Haake water bath was circulated through the tubing to maintain a constant temperature. Mixing was accomplished by a 1.5 inch Teflon-coated magnetic stirring bar. The stirring bar rotated at about 450 rpm in all the experiments. Two fine bubble diffusers and pure oxygen ~~was~~ were used to provide aeration. The concentration of DO was monitored by placing a DO probe in the beaker. The pH was monitored by placing a pH probe in the beaker and the pH was automatically controlled with addition of a 2N Na_2CO_3 solution.

The mixed liquor used in these experiments ~~were~~ was taken from the sludge that was wasted from the laboratory-scale reactors. During these experiments the reactors were operated at a sludge age of about eight days. All other operating conditions were the same as those described previously. Waste sludge from all three reactors was mixed and settled for about a half hour and concentrated by a factor of two (to MLSS concentrations of about 4000 mg/L). The concentrated mixed liquor was then transferred to the one liter batch reactor and

aerated for about a half hour before starting an experiment. The concentration of DO throughout all experiments was between 6 mg/L and 8 mg/L.

In the first set of experiments, about 20 mL of a concentrated solution of NH_4Cl was added to the batch reactor and the concentrations of NH_4^+-N, NO_2^--N, and NO_3^--N were measured during the course of the experiments. About 60 mL of sludge was withdrawn at each sampling period. The sample was immediately filtered and the NO_2^--N analysis was immediately performed. The other analyses were performed at the conclusion of each each run. The concentration of TOC and MLSS was measured at the start and end of the experiments.

The results from the first run is shown in Table A.5 and Figure 5.3. The second replication run was conducted three days after the first run and those results are shown in Table A.6 and Figure 5.4. The accumulation of NO_2^--N in both runs supports the supposition that was made in the previous section. Nitrite accumulation appears to have occurred at all concentrations of DO in the range from 0.25 mg/L to 8 mg/L. Since there was inadequate quantification of the amount of accumulation in the experiments for Subproblem 1, it is difficult to determine whether there is any relationship between DO concentration and NO_2^--N accumulation. It is clear, however, that NO_2^--N accumulation was never observed under normal steady state conditions. Nor was accumulation

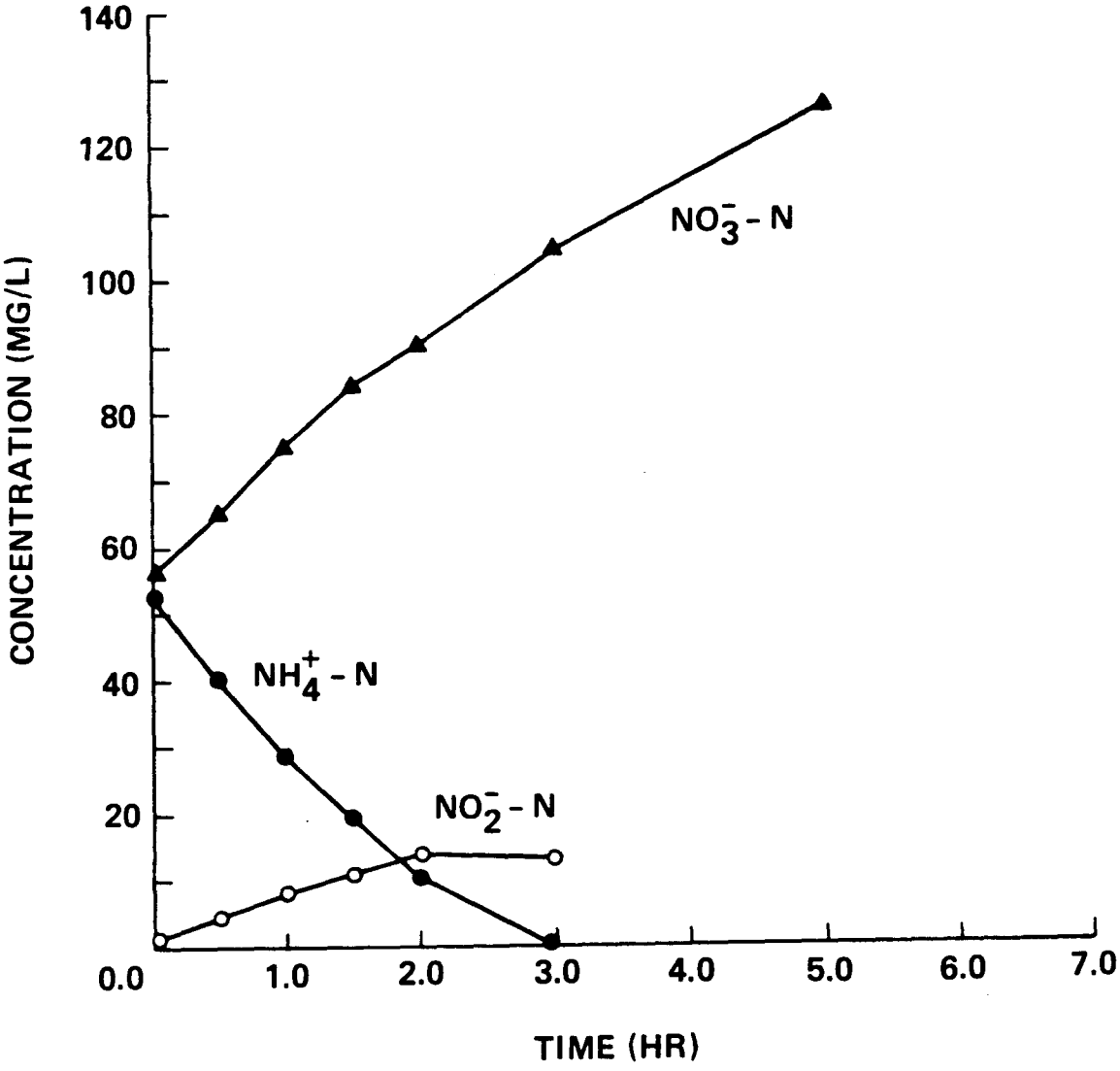

Fig. 5.3 Set I: NH_4^+–N, NO_2^-–N and NO_3^-–N Concentration versus Time

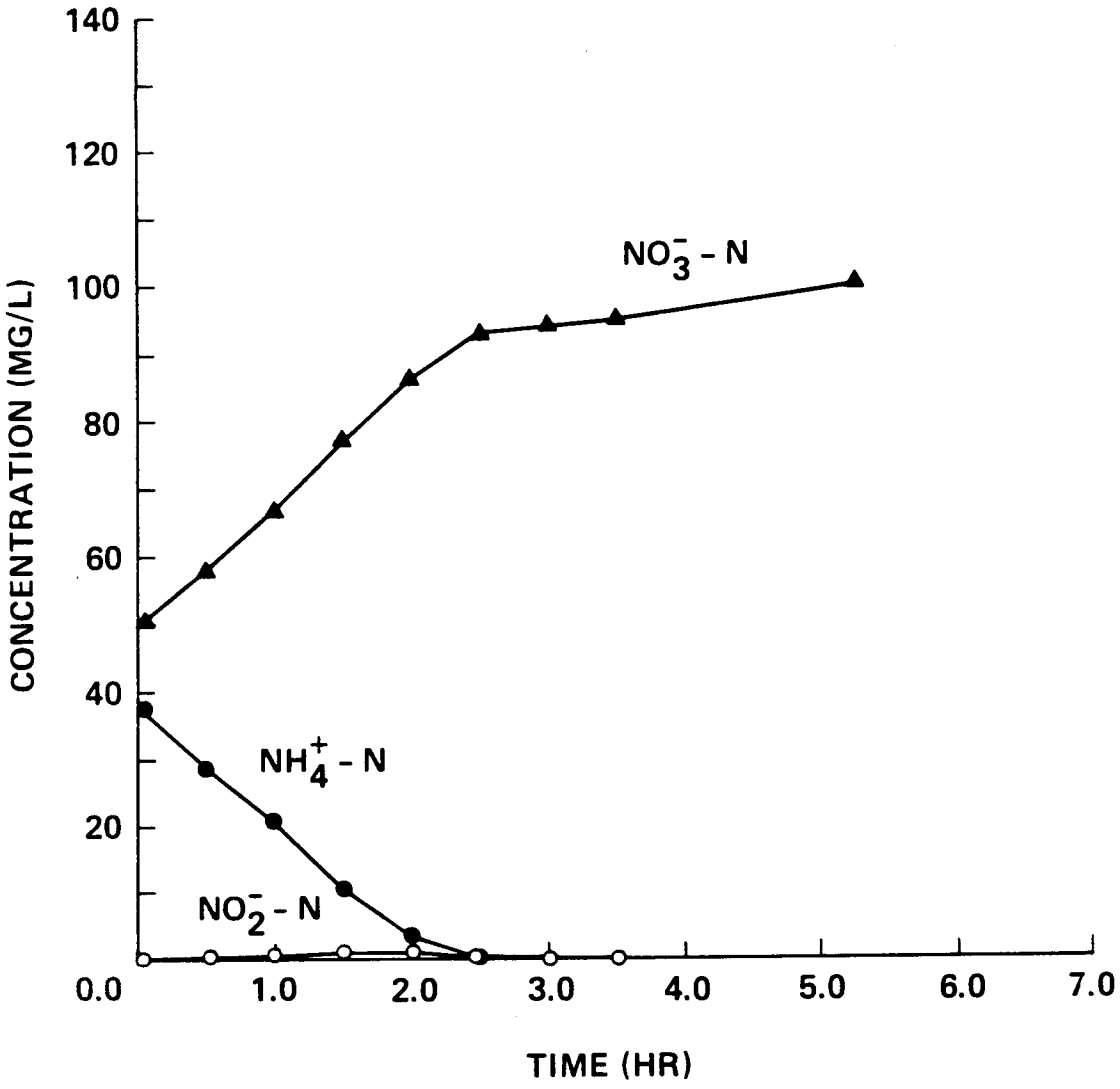

Fig. 5.4 Set I: NH_4^+–N, NO_2^-–N and NO_3^-–N Concentration versus Time

observed in much of the continuous feed experiments of Subproblem 3 and 4. It appears that $NO_2^- - N$ accumulation occurs only when the rate of $NO_2^- - N$ production becomes significantly greater than that which occurs under normal steady state conditions. A reasonable inference from these observations is that the maximum specific uptake rate for $NO_2^- - N$ is lower than that for $NH_4^+ - N$. The specific rate here is relative to the total sludge mass or total nitrifying population and not relative to a specific group of nitrifiers (that is, *Nitrosomonas* or *Nitrobacter).*

Because the mathematical model does not allow for the accumulation of $NO_2^- - N$, it cannot be directly used to estimate the kinetics parameters. It was to assume that the accumulation of $NO_2^- - N$ does not affect the rate of $NH_4^+ - H$ oxidation by *Nitrosomonas*. The model, without modifications, would then still be valid for predicting nitrification performance in terms of $NH_4^+ - N$ uptake but may not be valid for predicting $NO_3^- - N$ production in situations where significant accumulations of $NO_2^- - N$ occur.

The kinetic parameters q_{N2}, Y_{N2}, and q_{D2}, however, cannot be estimated from only $NH_4^+ - N$ uptake data. The following ad hoc analysis, based on the rate expressions in equations (3.13)-(3.15), was used. The first step of the analysis is to check the integrity of the nitrogen data. This can be done by using the following nitrogen balance

$$R_2 = -R_4 - R_{NO_2} + R_{TIN} \tag{5.3}$$

where

R_4 = observed specific $NO_3^- - N$ production rate [1/T]

R_{NO_2} = observed specific $NO_2^- - N$ production rate [1/T]

R_{TIN} = specific rate of change of total inorganic nitrogen [1/T]

The various rates are taken from the linear portion of the data (the first two hours). The nitrogen data for the first run balances to within about 2% and the data for the second run balances to within about 8%. The parameters q_{N2} and Y_{N2} are calculated from the following equations

$$R_4 = q_{N2}\,(0.124\,Y_{N2} - 1) \tag{5.4}$$

$$R_1 = 2.29(2 - 0.868\,Y_{N2})q_{N2} + 3.43\,R_{NO_2} + q_{D1} \tag{5.5}$$

where

R_1 = observed specific oxygen uptake rate [1/T]

The first term on the right hand side of equation (5.5) is the specific rate of oxygen uptake resulting from the production of $NO_3^- - N$. The second term is the specific rate of oxygen uptake resulting from the production of $NO_2^- - N$. The coefficient 3.43 represents the number of grams of oxygen that is required to

oxidized one gram of NH_4^+–H to NO_2^-–N (see equation (1.1)). The specific rate of endogeneous respiration is obtained directly from the oxygen uptake rate measurements taken towards the end of each run. Having calculated values for q_{N2}, q_{D2} can be calculated from

$$R_2 = q_{N2} + q_{D2} \tag{5.6}$$

The estimates calculated from each run are as follows.

	Run 1	*Run 2*
q_{N2}	4.92	4.76
Y_{N2}	0.11	0.07
q_{D2}	0.68	0.64

The units of q_{N2} and q_{D2} are in mg/g-hr.

The q_{N2} estimates obtained here are about 70% of the values estimated from Subproblem 1.

The values of Y_{N2} appear to be consistent with those generally reported in the literature. It should be noted however, that the calculations that were used to estimate Y_{N2} are extremely sensitive to errors in the measurement of the various specific uptake rates. Because of the small relative magnitude of Y_{N2}, a small relative error in R_1, for example, is reflected as a large absolute error in Y_{N2}. This sensitivity analysis, however, can be conversely interpreted as being

advantageous. Since, for the purposes of this investigation, it is of more interest in obtaining an estimate of Y_{N2} that will allow the model to make predictions of reaction stoichiometry rather than to obtain the true value of Y_{N2}, it can be argued that an accurate value of Y_{N2} is unnecessary since a large change in its value will have only a small effect on the observed stoichiometry.

In the second set of experiments, about 3.6 mL of the concentrated stock feed solution, Table 4.2 was added at the start of the experiments. The concentrations of TOC, NH_4^+-H, NO_2^-N, and NO_3^-N were measured during the course of the experiments. The concentration of TOC was used as an indirect measure of glucose concentration. The relationship between the two is

$$(mg\ glucose/L) = 2.5\ (mg\ TOC/L) \tag{5.7}$$

The MLSS concentration was measured at the start and end of each experiment.

Table A.7 and Figure 5.5 shows the results from the first run and Table A.8 and Figure 5.6 shows the results from the replication run. The first run was conducted on the day following the the first run of the first set of experiments (nitrifiers only) and the second run was conducted on the day following the first run.

It was suspected that the rate of glucose uptake may involve other mechanisms in addition to that described by equation (3.10). In a review paper

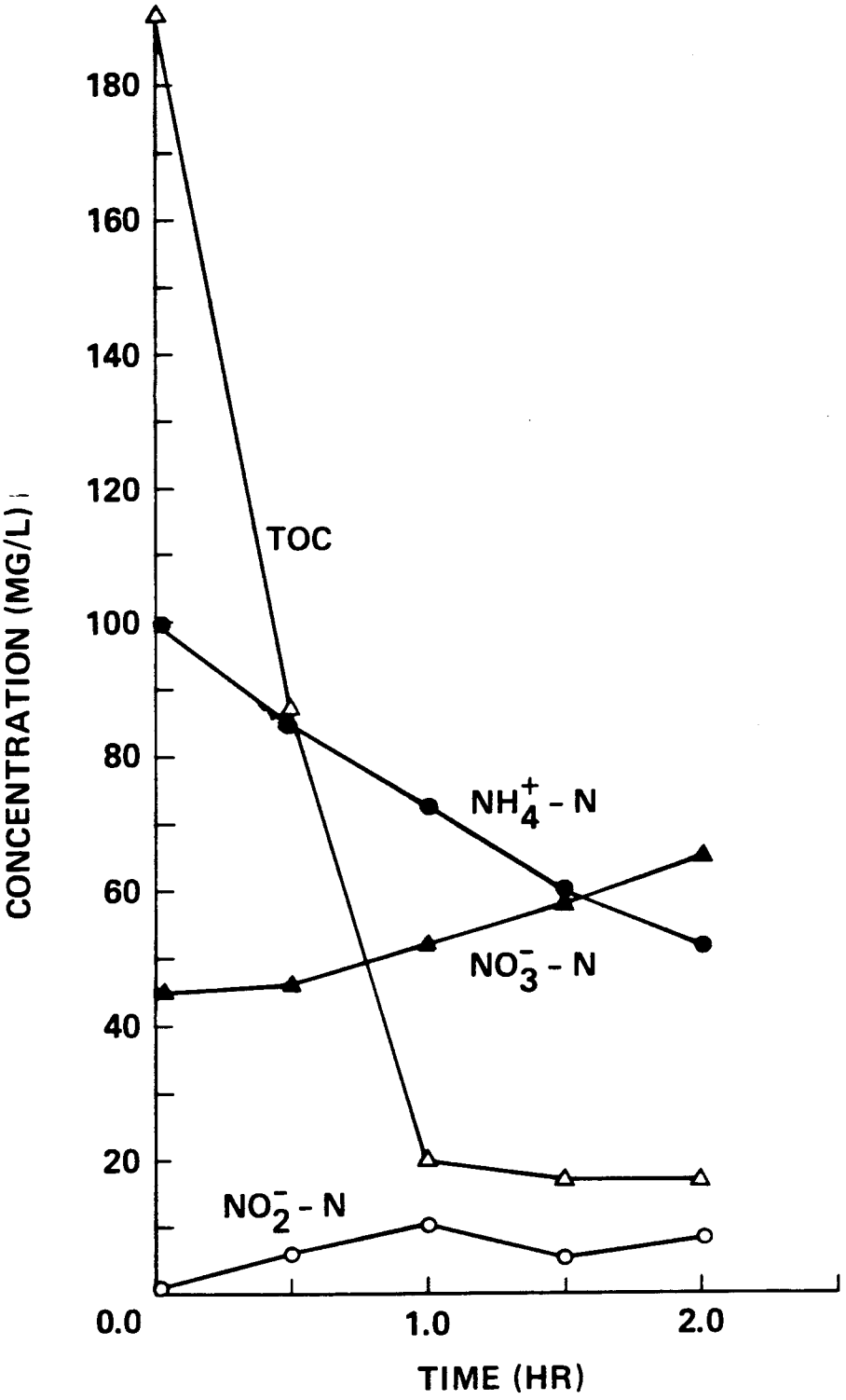

Fig. 5.5 Set II: TOC, NH_4^+–N, NO_2^-–N and NO_3^-–N Concentration versus Time

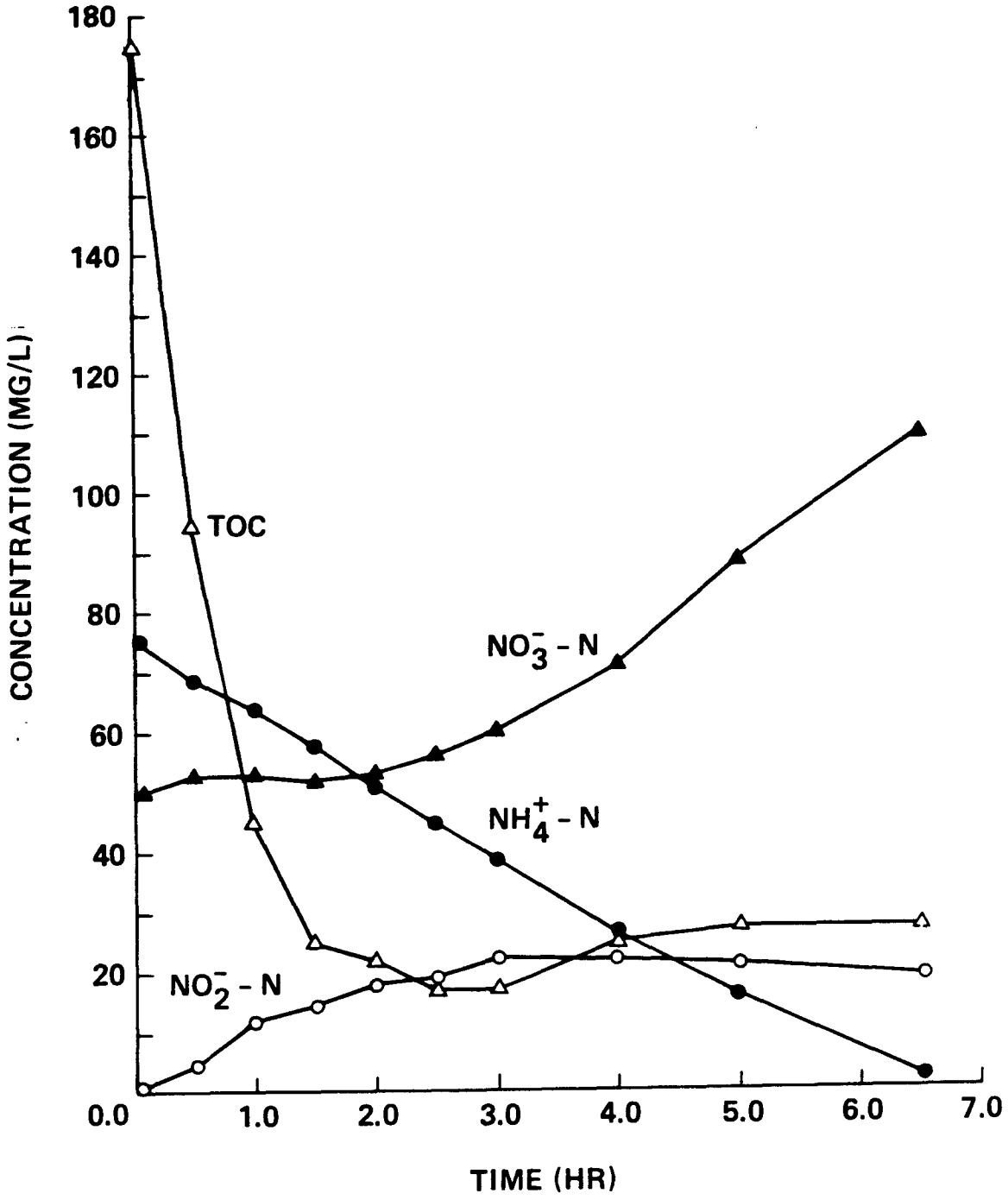

Fig. 5.6 Set II: TOC, NH_4^+–N, NO_2^-–N and NO_3^-–N Concentration versus Time

on the dynamics of microbial growth on soluble substrates, Daigger and Grady (1982) presented much evidence of a storage response in cultures that have been just subjected to a large and suddenly increase in the concentration of their carbon-source substrate. This storage response involves the transport of of extracellular substrates into cells, the oxidation of a small portion, and the synthesis of storage polymers (carbohydrate and/or lipid). The portion that is oxidized is significantly smaller than that oxidized to obtain energy for cell growth and the stoichiometry of this response would, therefore, be quite different than that predicted by equation (3.10); the ratio of the observed rate of carbon uptake to the observed rate of oxygen uptake would be much greater. Evidence was also presented to suggest that the storage rate and capacity may be related to the degradability of the substrate; substrates that are easier to degrade are more likely to trigger this response. It was noted that the highest storage rates and capacities were observed for glucose.

Though it was expected that equation (3.10) is an inadequate description of glucose uptake for the conditions of these experiments, modifications of the reaction stoichiometry to included storage response was unnecessary for the purposes of this investigation. The only relevant aspect of the heterotrophic uptake of carbon is the effect of this reaction on the nitrifiers. It was assumed that this effect is manifested through the potential competition between the heterotrophs and the nitrifiers for oxygen and nitrogen. For this reason it was

decided that q_{H3} and Y_{H3} should be estimated from oxygen uptake and nitrogen uptake data. The calculated value of q_{H3} can then be compared with the observed glucose uptake rate to assess whether other uptake mechanisms were active. If the observed rate of glucose uptake is significantly greater than the estimated value of q_{H3}, then it may be inferred that some mechanism such as a storage response was active. In this case q_{H3} can be interpreted to represent the maximum specific rate of glucose oxidation via equation (3.10).

The values of q_{H3} and Y_{H3} are calculated from

$$R_{TIN} = 0.124\,(Y_{H3}\,q_{H3} - Y_{N2}\,R_{NO_2}) + q_{D2} \tag{5.8}$$

$$R_1 = 0.178(6 - 7.96\,Y_{H3})\,q_{H3} + OUR_N + q_{D1} \tag{5.9}$$

where

R_1	=	observed specific oxygen uptake rate [1/T]
R_{NO_2}	=	observed specific nitrite/nitrate production rate [1/T]
OUR_N	=	specific oxygen uptake rate for nitrifiers [1/T]

The first equation expresses that total nitrogen is conserved. The specific endogeneous respiration rate, q_{D1}, is directly obtained from the oxygen uptake measurement at the end of the experiment. The value of Y_{N2}, and q_{D2} are assumed to be 0.09 and 0.662, respectively. The resulting estimates and the

observed specific glucose uptake rates are

	Run 1	*Run 2*	
q_{H3}	71.1	34.4	$\bar{x} = 105.5/2 = 52.7$
R_3	123	98	
Y_{H3}	0.44	0.29	$\bar{x} = 73/2 = .37$

The estimate of q_{H3} from Run 1 was about 58% of the observed specific glucose uptake rate and that from Run 2 was about 35% of the observed specific glucose uptake rate R_3. It appears that a large portion of the glucose uptake can be attributed to storage response.

The inconsistency in the estimates from Run 1 and Run 2 may be partially attributed to differences in sludge characteristics. The rate of glucose uptake, oxygen uptake, and nitrite/nitrate production in Run 2 were all about 80% of that in Run 1. A possible source of error that would result in such an uniform difference in specific rates is an error in the determination of the MLSS concentration. A 20% error in one MLSS determination is not likely since the typical experimental error is usually only about 5% to 10%, but if the MLSS determination for Run 1 was 10% low and the one for Run 2 was 10% high, the 20% error could be accounted for.

The behavior of the nitrifiers in these two runs were significantly different than that encountered in the first set of experiments. The concentration of $NO_2^- - N$ accumulated to a much higher level and at a much faster rate than that in the first set of experiments. The rate of nitrite/nitrate production in Run 1 was only about 63% of that estimated in the first set of experiments and the rate in Run 2 was less than 50%. The nitrate concentration in both runs exhibited a definite lag period before it increased at a constant rate. It is unlikely that this difference in behavior is attributable to differences in sludge characteristics since this behavior was not observed on the day prior to these experiments nor on the second day following these experiments (in Run 2 of Set I). It appears that the nitrifiers were affected by something associated with the rapid uptake of glucose by the heterotrophs and that *Nitrobacter* was more adversely affected.

Subproblem 3

The results from the Set I experiments in Subproblem 1 provided some evidence for the existence of mass transport limiting effects. Though the differences in the maximum specific $NH_4^+ - N$ uptake rates from those experiments appear to be significant, better assessment of the effects of mass transport limitation on nitrification can be achieved in longer term experiments; any differences in rates can be magnified, in terms of effluent concentrations, over a

longer period of time.

Four sets of experimental runs consisting of three runs per set (one run per reactor) were conducted to investigate the effects of different impeller speeds at different DO concentrations. For all four sets, the impeller speed for Reactor 1 was set at about 60 rpm and that for Reactor 2 was set at about 200 rpm. The impeller speeds were chosen to represent reasonable extremes of mixing intensities that may be encountered in full-scale activated sludge plants. It is reasonable to expect that even at the lowest mixing intensities the mixed liquor should still be completely suspended and that at the highest mixing the turbidity in the effluent should not be excessive. The low impeller speed (60 rpm) was the lowest speed that could be used and still maintain the mixed liquor in complete suspension. The high impeller speed was not high enough to significantly affect the turbidity of the effluent.

As discussed previously, it was necessary to use a pure oxygen/air mixture to aerate Reactor 1. Reactors 2 and 3 were aerated with air only. The other operating conditions for these reactors were the same as those in Table 4.4. The sludge age was about seven days. Reactor 3, serving as a control, was operated at all times under the normal operating conditions described in Table 4.4. Prior to the start of each set of experiments, the mixed liquor from the three reactors were collected, mixed, and then redistributed.

At the start of each experiment, the DO concentrations for Reactors 1 and Reactor 2 were set as follows.

SET:	*I*	*II*	*III*	*IV*
DO(mg/L)	4.0	1.5	1.0	0.75

About 20 hours (about 3 hydraulic retention times) after the start of an experiment, the effluent from each reactor was analyzed for TOC, NH_4^+–N, and NO_3^-–N. The MLSS concentration at the beginning and at the end of the 20 hour period for each reactor was also measured. No mixed liquor was wasted during an experiment. At the conclusion of each set, the DO concentration for Reactors 1 and 2 were returned to the normal operating conditions; the impeller speeds remained at 60 rpm and 200 rpm respectively. Sets of experiments were conducted about two days apart.

The results are shown in Table 5.5. Nitrification was significantly affected in only the experiment in which the impeller speed was 60 rpm and the DO concentration was 0.75 mg/L. The effluent concentrations of NH_4^+–H and NO_3^-–N in the other experiments fell within the typical range of concentrations measured under normal operating conditions. The activity of the heterotrophic population did not appear to have been significantly affected in any of the

Table 5.5 Results of Subproblem III

		Reactor 1 60 RPM			Reactor 2 200 RPM			Reactor 3 DO = 4.0 mg/L		
SET	DO*	NH_4^+–N*	NO_3^-–N*	TOC	NH_4^+–N	NO_3^-–N	TOC	NH_4^+–N	NO_3^-–N	TOC
I	4.0	0.22	45	7	0.28	42	7	0.15	47	7
II	1.5	0.16	47	7	0.14	46	7	0.12	48	7
III	1.0	0.20	45	7	0.18	47	7	0.10	48	7
IV	0.75	10	20	7	0.32	42	6	0.13	48	6

* concentrations in (mg/L)

experiments.

The results from Set IV clearly demonstrate that nitrification can be affected by the level of mixing intensity in the reactor. For the same concentration of DO (0.75 mg/L), a difference in the mixing intensity resulted in a vast difference in the rates of nitrification. The results also demonstrate that the heterotrophic population is more competitive than the nitrifying population under oxygen limiting and/or mass transport limiting conditions. In Reactor 1 of Set IV where nitrification was already significantly limited, the heterotrophic uptake of glucose was not at all affected. It should be noted that within one day (and probably much earlier) after being returned to a DO concentration of at least 4 mg/L, the concentrations of NH_4^+-H and NO_3^--N in the effluent of this reactor was again within the range of normal effluent concentrations. It can therefore be reasoned that the observed effect was not the result of any significant shifts in the composition of the microbial population and that the effect did not cause any such shifts over a 20 hour period.

Although the observed effect was only transient, long term consequences can be extrapolated. If the conditions of Reactor 1 of Set III were maintained over an extended period of time (a few MCRT's), the fraction of nitrifiers in the total microbial population will continue to decrease to new equilibrium level. The rate of this decrease and the level of this equilibrium will depend on the

MCRT; the lower the MCRT, the faster the rate and the lower the equilibrium level. In the extreme, wash-out of the nitrifying population may be possible. In contrast with the traditional notion of "wash-out" in which the washing-out of a microbial population is induced by increasing the sludge wasting rate (reducing the MCRT), the wash-out in this case is induced by low DO concentration and/or low mixing intensity.

With the results from Table 5.5 and the range of normal operating data of Table 4.4, the estimates of K_{2N}, K_{3H}, and K_{1H} were obtained by selecting values of these parameters so that the steady state solution of the mathematical model (in terms of steady state effluent concentrations and oxygen uptake rates) would fall within the range of the data. Since the role of these parameters in the mathematical model is not directly related to the effect of DO on nitrification, it was decided that precise estimates of these parameters are not necessary.

The value of K_{2N} was selected by requiring the model's prediction of steady state effluent NH_4^+–N concentration under high DO conditions to be within the observed range of normal effluent NH_4^+–N concentrations. The value of K_{3H} can be similarly selected if the range of normal effluent concentration of glucose was known. The concentration of glucose, however, was never directly measured; it was assumed that its concentration could be indirectly determined by TOC. TOC determinations, however, measures other dissolved organic car-

bon compounds in addition to glucose. TOC will, therefore, be an accurate measure of glucose only if the concentration of glucose was much larger than the total concentration of other organic carbon sources. In the glucose uptake experiments of the previous section, the rate of glucose uptake was probably accurately determined from TOC since the concentration of glucose was high (about 450 mg/l). The concentration of glucose in the effluent, however, is probably quite low and TOC is probably not a good measure of its concentration. It was decided that the concentration of glucose in the effluent should be on the same order of magnitude as K_{3H}; that is, it should be on the order of about 5 mg/l.

With this assumption and the observed data on effluent NH_4^+–N concentrations, the values of K_{3N} and K_{2N} were selected. The selection process simply began by trying the values of K_{3H} and K_{2N} that have been reported in the literature and then subjectively adjusting the values until the steady state effluent concentrations predicted by the model came within the range of the observed data. The resulting values are: $K_{2N} = 0.13\ mg/L$ and $K_{3N} = 3.0\ mg/L$.

The value of K_{1H} was selected by requiring that the steady state effluent glucose concentration remain relatively constant over the range of DO concentrations from 0.2 mg/L to 4.0 mg/L and at the range of mass transport condi-

tions associated with the range of impeller speeds used in this subproblem. Since the data indicate that heterotrophic activity was not affected over the range of DO concentrations used nor over the range of mass transport conditions used, any arbitrarily low value of K_{1H} should give the desired result. It was decided, however, that the value of K_{1H} should be reasonably consistent with the values that have been reported in the literature. The value of 0.01 mg/L was found to satisfy both criteria.

Although the procedure for estimating K_{2N}, K_{3H}, and K_{1H} was subjective, the values of the estimates appear to be justifiable. The values of the parameters are all consistent with values reported in the literature and the behavior of the model matches the observations.

Subproblem 4

The three experimental runs for this subproblem were conducted in the laboratory-scale reactors. These experiments were conducted three days after the conclusion of the experiments for Subproblem 2. In preparation for the experiments, the mixed liquor from all three reactors was collected, mixed together, and then redistributed to the reactors. The three reactors were then operated at the following impeller speeds and DO concentrations:

Reactor	Speed (rpm)	DO (mg/L)
1	60	4.0
2	200	4.0
3	150	4.0

All other operating conditions were identical for the three reactors and were the same as those described previously in Table 4.4. The reactors were operated at these conditions for about 48 hours prior to the start of the experiments.

The experimental conditions for the three runs are as follows.

Time (hr)	1	2	3
-48 - 0	4.0	4.0	4.0
0 - 9	0.20	0.20	4.0
9 - 24.5	0.75	0.75	4.0
24.5 - 27	4.0	4.0	4.0

As discussed in a previous section, Reactor 1 had to be aerated with an air/pure oxygen mixture to compensate for the lower oxygen transfer efficiency. Reactor 2 and 3 were aerated with air only.

During the experiments, the concentrations of TOC, NH_4^+-H, NO_2^--N, and NO_3^--N were measured. Samples volumes of about 120 mL were taken from the outlet of each reactor at each sampling period. The samples were immediately filtered and the NO_2^--N analysis was performed immediately. For the samples collected during the first nine hours, the other analyses were performed at time=10 hours. For the remaining sampling periods, all analyses were performed immediately. The MLSS concentration for each reactor was measured at the beginning and at the end of the experiment.

The results are shown in Table 5.6 and the results for Runs 1 and 2 are shown in Figure 5.7. Reaffirming the results of the experiments in the previous section, the relationship between DO concentration and nitrification was again affected by mass transport limitation. A notable feature of the results is that the rate of heterotrophic uptake of glucose did not appear to be at all affected even at a DO concentration of 0.20 mg/L.

The values of the parameters $L^2\rho$, K_{1N}, $\frac{\varepsilon}{\tau}$ and Re for Run 1 were estimated by fitting the model's solution with the NH_4^+-H and NO_3^--N data. The procedure was as follows:

1. The value of $L^2\rho$ was first estimated by assuming reasonable values for $\frac{\varepsilon}{\tau}$ and Re and using the value of K_{1N} estimated from subproblem 1. The

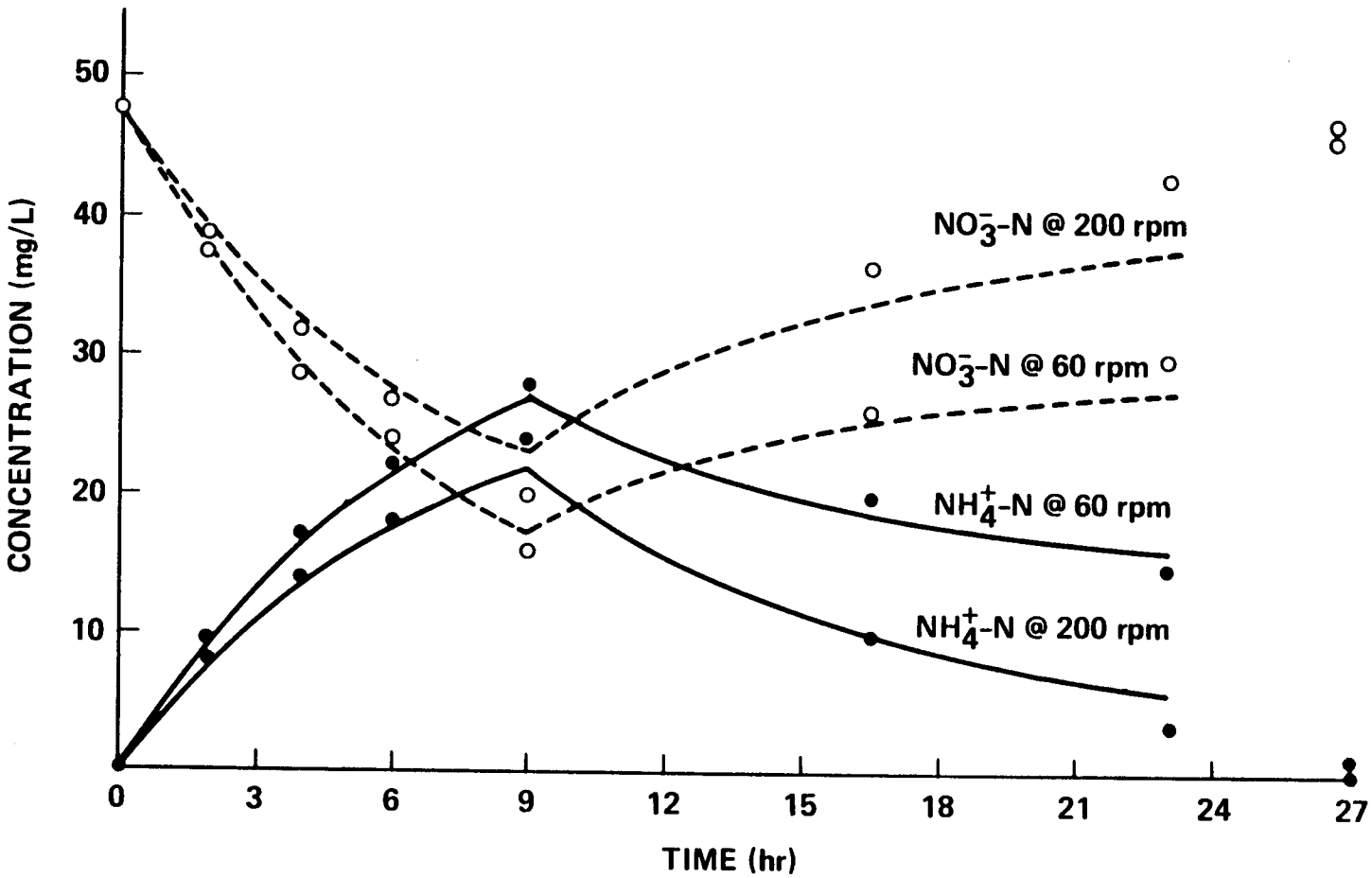

Fig. 5.7 Concentration vs. Time for Impeller Speeds at 60 rpm and 200 rpm and DO Concentrations at 0.20 mg/L and 0.75 mg/L

Table 5.6 Results of Subproblem IV

Time	DO	NH_4^+–N^{**}			NO_2^-–N^{**}			NO_3^-–N^{**}			TOC^{**}		
<0	4.0												
0	0.20	0.21	0.16	0.10	0.12	0.07	0.07	48	48	50	4	5	5
2	0.20	9.4	7.9	0.12	0.07	0.12	0.11	37.5	39	50	5	6	5
4	0.20	17	14	-	0.05	0.14	0.09	29	32	50	6	6	5
6	0.20	22	18	0.15	0.06	0.11	0.09	24	27	48	6	7	6
9	0.75	28	24	0.2	0.05	0.09	-	16	20	-	6	6	6
16	0.75	20	10	-	0.11	0.21	-	26	36.5	-	-	-	-
23	0.75	15	3.6	0.08	0.12	0.29	0.07	30	43	50	-	-	-
24.5	4.0	-	-	-	-	-	-	-	-	-	-	-	-
27	4.0	1.1	0.18	-	1.63	0.08	-	46	47	-	-	-	-

* time in (hr)
** concentration in (mg/L)
\+ reactor number

assumed value for $\frac{\varepsilon}{\tau}$ was 0.5 and the assumed value for Re was 100.

a. The value of $L^2\rho$ was estimated from the NH_4^+–N data with the least squares criteria.

b. The value of $L^2\rho$ was reestimated from the NH_4^+–H and NO_3^-–N data with a maximum likelihood criteria.

2. Using the value of $L^2\rho$ from step 1 and the estimated value of K_{1N} from subproblem 1 as initial estimates, the values of these parameters were reestimated from the NH_4^+–H data. A least squares criteria was used.

3. Using the values of $L^2\rho$ and K_{1N} estimated from step 2 as initial estimates, the values of these parameters were then reestimated along with $\frac{\varepsilon}{\tau}$ and Re. The estimates were obtained from the NH_4^+–H and NO_3^-–N data with a maximum likelihood criteria.

From preliminary simulations with the model, it was known that the behavior of the model solution under the conditions of these experiments was most strongly influence by the parameter group $L^2\rho$, or $L^2\rho/\frac{\varepsilon}{\tau}$. The stepwise procedure took advantage of this dominance by generating increasingly accurate estimates of $L^2\rho$ in a number of one or two dimensional problems before solving the four-dimensional problem in step 3. Because of the dominance of $L^2\rho$, scaling of

this parameter was necessary in the estimation problems of step 2 and 3.

The results from step 3 for Runs 1 are as follows.

Run	$L_2\rho$	K_{1N}	$\frac{\varepsilon}{\tau}$	Re
1	1×10^{-3}	0.56	0.5	100

The units of $L^2\rho$ are cm^2–g/L and the units of K_{1N} are mg/L. The optimization in step 3 did not change the values of $\frac{\varepsilon}{\tau}$ and Re. If the optimization routine was operating properly, these results would indicated that the behavior of the solution under these experimental conditions is not dependent on $\frac{\varepsilon}{\tau}$ and Re; that is, external diffusional resistance is negligible. To check whether the estimated values were at a local optimum, the starting values of $\frac{\varepsilon}{\tau}$ and Re were changed. The value of $\frac{\varepsilon}{\tau}$ was set to 1.0 and the value of Re was set to 1.0. Step 3 was repeated with these starting values and the values of $L^2\rho$ and K_{1N} from above. The following is a comparison of these results with the previous results.

Run	$L^2\rho$	K_{1N}	$\frac{\varepsilon}{\tau}$	Re
1	$1.0\,x\,10^{-3}$	0.56	0.5	100
1	$1.9\,x\,10^{-3}$	0.46	1.0	1.0

The values of $\frac{\varepsilon}{\tau}$ and Re again were not significantly changed in the optimization. The value of $L^2\rho$ doubled and the value of K_{1N} was reduced by about 18%. From these results, it can be seen that the behavior of the solution is dependent almost entirely on the group $L^2\rho/\frac{\varepsilon}{\tau}$; the estimated value of this group was essentially the same in both optimizations (about $2\,x\,10^{-3}$). By recognizing that this group is the "unknown" portion of the Thiele modulus, it can be concluded that, under the mass transport conditions of Run 1, transport limitation was due almost entirely to internal (intrafloc) resistance.

Because of the above conclusion, only step 1 of the estimation procedure was applied to the data from Run 2. The value of $L^2\rho/\frac{\varepsilon}{\tau}$ for Run 2 was found to be $1.5\,x\,10^{-4}$. The solution of the model using the estimated values of the parameters are shown in Figure 5.7 as solid lines.

The general behavior of the model appears to be consistent with the experimental results; that is, the observed rate of nitrification is lower when there is more mass transport limitation and, for a given level of transport limitation, the observed rate is lower when the concentration of DO is lower.

The model's adequacy in fitting the data can be assessed by determining whether the values of the estimates are physically realistic. The change in the "size" of the flocs as a result of the difference in impeller speeds in Reactors 1 and 2 can be checked against the change predicted by equation (2.4). The ratio of stable floc sizes to impeller speeds is given by

$$\frac{d_1}{d_2} = \left[\frac{n_2}{n_1}\right]^x \tag{5.10}$$

where

d_1 = floc size in Reactor 1

d_2 = floc size in Reactor 2

n_1 = impeller speed in Reactor 1

n_2 = impeller speed in Reactor 2

x = $\frac{3}{2}n$.

The ratio of the floc sizes for these experiments is 3.65 and the ratio of impeller speeds is 3.33. From equation (5.10), the value of n, the stable floc size

exponent, is calculated to be about 0.7. This value is within the range of theoretical values presented in the literature (0.5 for filamentous fracture and 1 to 2 for surface shearing).

An estimate of the "size" of the flocs can also be made if reasonable assumptions about the density of the flocs are made. In these experiments, the concentration of the MLSS was about 2.1 g/L. The SVI (sludge volume index) was about 100. From these two measurements, it can be inferred that the density of the flocs must be at least 21 g/L. It is also likely that the density will not be more than about 80 g/L. It is assumed that the flocs are spherical, then the diameters of the flocs in Run 1 are about 200 to 400 microns and the diameters of the flocs in Reactor 2 are about 60 to 100 microns. These estimated floc sizes are well within the typical range of sizes reported for activated sludge flocs.

VI. SIMULATION

The results of the previous section demonstrates the effects of mass transport limitation under steady state influent conditions at a MCRT of about seven days. It is known, however, that nitrification is also strongly influenced by other process conditions including organic shock loading and MCRT. The effects on nitrification from combining these two factors with mass transport limitation is simulated in this section with the model developed in Chapter 3 and with the values of the model's parameters estimated in Chapter 5. The floc model is solved by finite-difference and the reactor model is integrated with the IMSL subroutine DGEAR. The Fortran code of the model is listed in Appendix C.

MCRT

The primary importance of the MCRT as a process control variable for nitrification is in determining whether or not nitrification will occur. Nitrification will only occur if the rate of growth of nitrifiers exceeds the rate of removal of nitrifiers from the process. A MCRT of at least three days is usually needed to avoid wash-out of the nitrifiers. It was shown in the previous section that the rate of nitrification, and hence the rate of growth of the nitrifiers, can be affected by DO concentration and the mass transport characteristics of the system. This suggests that the minimum MCRT required for nitrification may be

affected by these two factors.

The mode from Chapter 3 is used to simulate the steady state behavior of a complete-mixed nitrifying activated sludge process at MCRT's of 3, 6, and 12 days. For each MCRT, two values of $\frac{L^2\rho\tau}{\varepsilon}$ are used to represent the two levels of mass transport limitation encountered in the experiments of the previous section. Each combination of MCRT and $\frac{L^2\rho\tau}{\varepsilon}$ is simulated over constant bulk DO concentrations ranging from 0.25 mg/L to 4.0 mg/L. The values of other model parameters are summarized in Table 6.1.

The results of these simulations, in terms of the steady state effluent concentrations, specific uptake rates, cell concentrations, and nitrifier fraction, are presented in Tables A.9-A.11. The distinct difference between the behavior of the heterotrophs and the nitrifiers under the various process conditions is apparent. The heterotrophs are primarily affected by only the MCRT, while the nitrifiers are sensitive to DO concentration and mass transport limitation as well. The steady state effluent NH_4^+-N and NO_3^-N concentrations are also shown in Figures 6.1-6.3.

It can be seen from these figures that the effects of both DO concentration and mass transport resistance on nitrification are dependent on the MCRT.

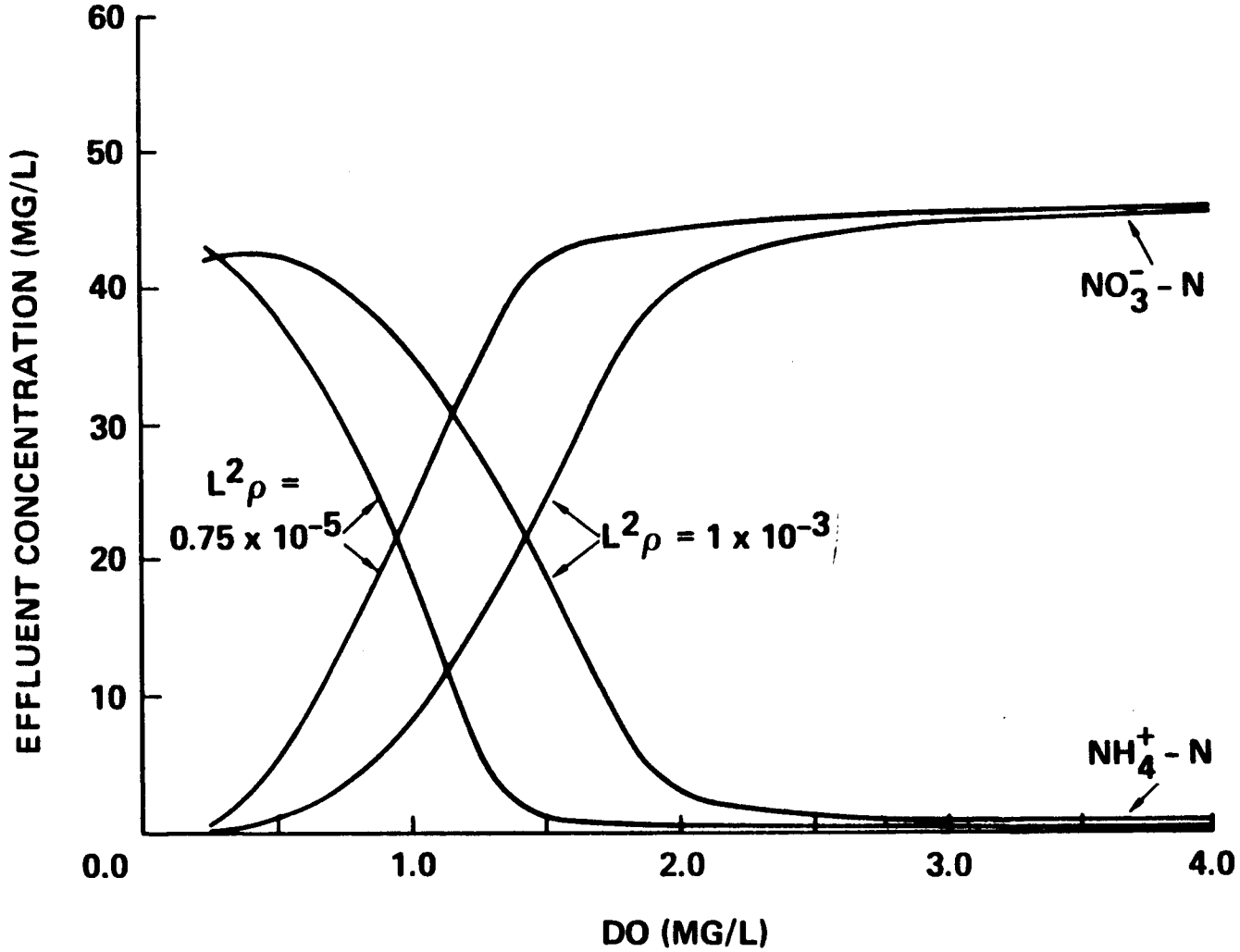

Fig. 6.1 Effluent Concentrations of NH_4^+–N and NO_3^-–N for $L^2\rho = 1 \times 10^{-3}$ cm^2-g/L and $L^2\rho = 0.75 \times 10^{-5}$ cm^2-g/L at MCRT = 3 days

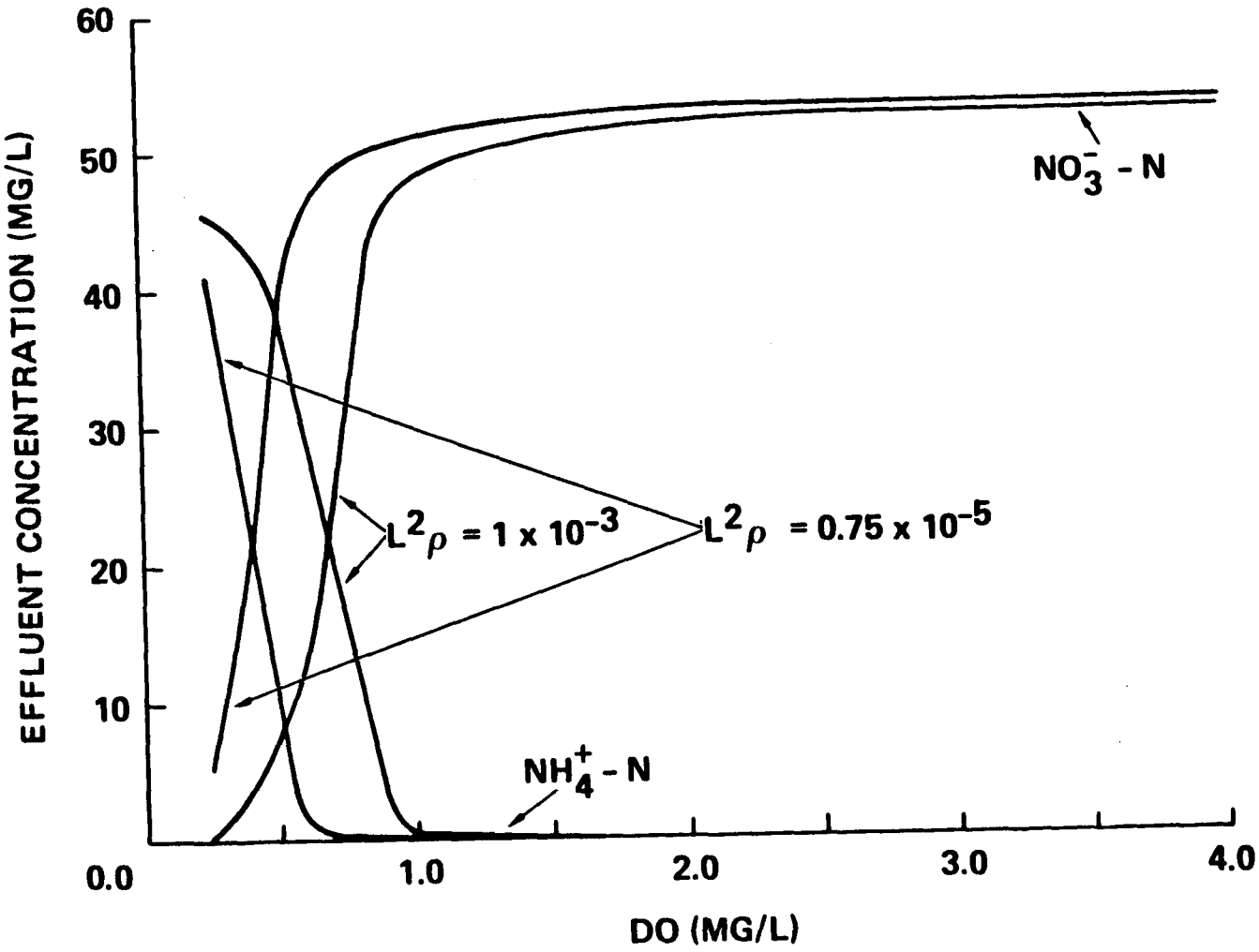

Fig. 6.2 Effluent Concentrations of NH_4^+–N and NO_3^-–N for $L^2\rho = 1 \times 10^{-3}$ cm^2-g/L and $L^2\rho = 0.75 \times 10^{-5}$ cm^2-g/L at MCRT = 6 days

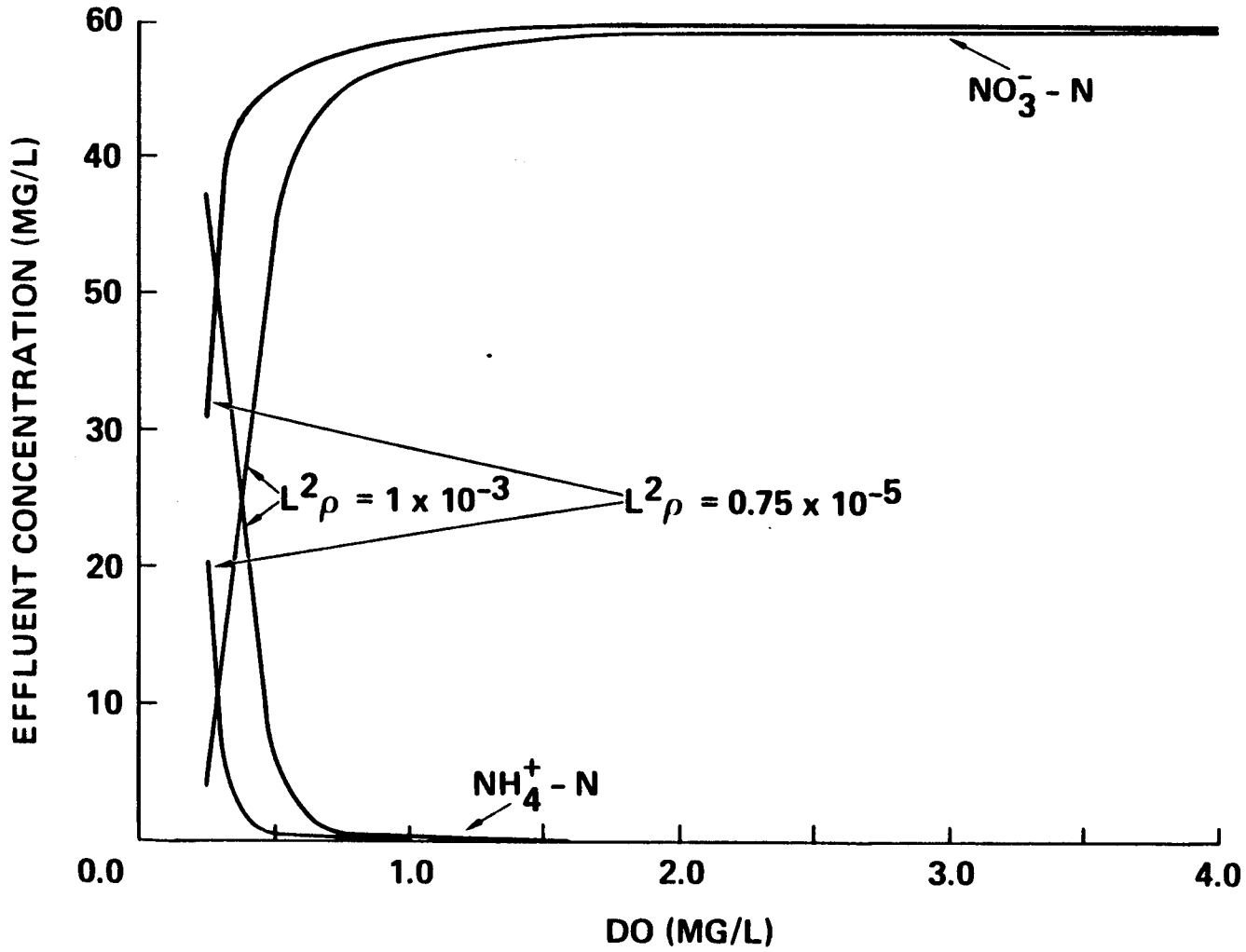

Fig. 6.3 Effluent Concentrations of NH_4^+–N and NO_3^-–N for $L^2\rho = 1 \times 10^{-3}$ cm^2-g/L and $L^2\rho = 0.75 \times 10^{-5}$ cm^2-g/L at MCRT = 12 days

Table 6.1 Model Parameters

Half-Saturation Coefficients:

K_{1N} = 0.56 mg/L
K_{1H} = 0.01 mg/L
K_{2N} = 0.13 mg/L
K_{3H} = 3 mg/L

Specific Rates:

q_{H3} = 70 mg/g-L
q_{N2} = 6.8 mg/g-L
q_{D1} = 3.2 mg/g-L
q_{D2} = 0.7 mg/g-L

Yields:

Y_{H3} = 0.44
Y_{N2} = 0.09

Mass Transport Parameters:

$\frac{\varepsilon}{\tau}$ = 0.5
Re = 100
$K_L A$ = 15.3 HR^{-1}

Reactor Parameters:

D = 0.143 HR^{-1}

influent NH_4^+–N = 55 mg/L

influent Glucose = 300 mg/L

influent NO_3^-–N = 0 mg/L

Or conversely, it can be said that the wash-out MCRT for nitrifiers is dependent on the DO concentration and mass transport resistance.

For the range of conditions covered by these simulations, the DO concentration at which nitrification (in terms of effluent NH_4^+–N and NO_3^-–N concentrations) becomes effective decreases with increasing MCRT, and for a given MCRT, increases with increasing mass transport resistance. The apparent limiting DO concentration for nitrification, therefore, is not determined by only K_{1N}, but is also determined by other characteristics of the process.

The apparent limiting DO concentrations for nitrification in the low mass transport resistance simulations vary from about 1.5 mg/L at a MCRT of three days to about 0.5 mg/L at a MCRT of twelve days. The limiting DO concentrations in the higher mass transport resistance simulations vary from about 2.5 mg/L at a MCRT of three days to about 0.7 mg/L at a MCRT of twelve days.

Organic Shock Loading

It is sometimes observed that nitrification in a nitrifying activated sludge process can be temporarily "inhibited" by organic shock loads. The role of mass transport limitation in determining the transient effects of this type of process upset is simulated with the model from Chapter 3. The behavior of the

system is again simulated for the two levels of mass transport limitation encountered in the previous experiments and the values of the model's other parameters are given in Table 6.1.

The steady state behavior of a complete-mixed nitrifying activated sludge process that is operating at a MCRT of six days and with a constant aeration rate that results in a bulk DO concentration of 4.0 mg/L is shown in Table A.10. The process is then subjected to a shock load that raises the concentration of glucose in the reactor to 250 mg/L. The ensuing transient behavior is shown in Figures 6.4 and 6.5.

The bulk DO concentration is lowered by the increased heterotrophic uptake of oxygen that accompanies the oxidation of glucose. The effect of this reduction on nitrification is seen to be dependent on the mass transport characteristics of the system. Although the concentration of DO in the simulation with low mass transport resistance (Figure 6.4) dropped at a slightly higher rate to a level that is about 0.5 mg/L lower than shown in Figure 6.5, nitrification was only slightly affected. The rate of nitrification in Figure 6.5 is significantly reduced.

Nitrification in Figure 6.5 appears to become "inhibited" immediately following the shock load. The rate of nitrification was immediatedly reduced by about 17% and remained at this rate until the concentration of glucose

dropped below about 10 mg/L. The apparent relationship between bulk DO concentration and nitrification is quite different than that predicted by the steady state results of Table A.10 and Figure 6.2. The steady state results indicated that even under high mass transport resistance, the limiting bulk DO concentration at a MCRT of 6 days is about 1.0 mg/L. The bulk DO concentration here, in Figure 6.5, never dropped below about 1.4 mg/L and nitrification was affected even when the bulk DO concentration was between 4.0 mg/L and 2.0 mg/L during the first quarter hour of the simulation.

This apparent discrepancy, is the result of mass transport limitation and heterotrophic/nitrifier competition. Figures 6.6 and 6.8 show the distribution of reactant concentrations within a floc before the shock load and one hour after, respectively, for the simulation with the higher mass transport resistance (Figure 6.5). Figures 6.7 and 6.9 show the corresponding rates of heterotrophic and nitrifier activity calculated from the concentration distributions.

The increase in oxygen uptake rate by the heterotrophs not only reduces the bulk concentration of DO, but also affects the concentration distribution of DO within the floc. Although the drop in bulk DO concentration from 4.0 mg/L to 1.4 mg/L does not affect the intrinsic rate of nitrification, the steep DO concentration gradient created by the high oxygen uptake rate of the heterotrophs does change the effective rate of nitrification. After one hour, the the intrinsic

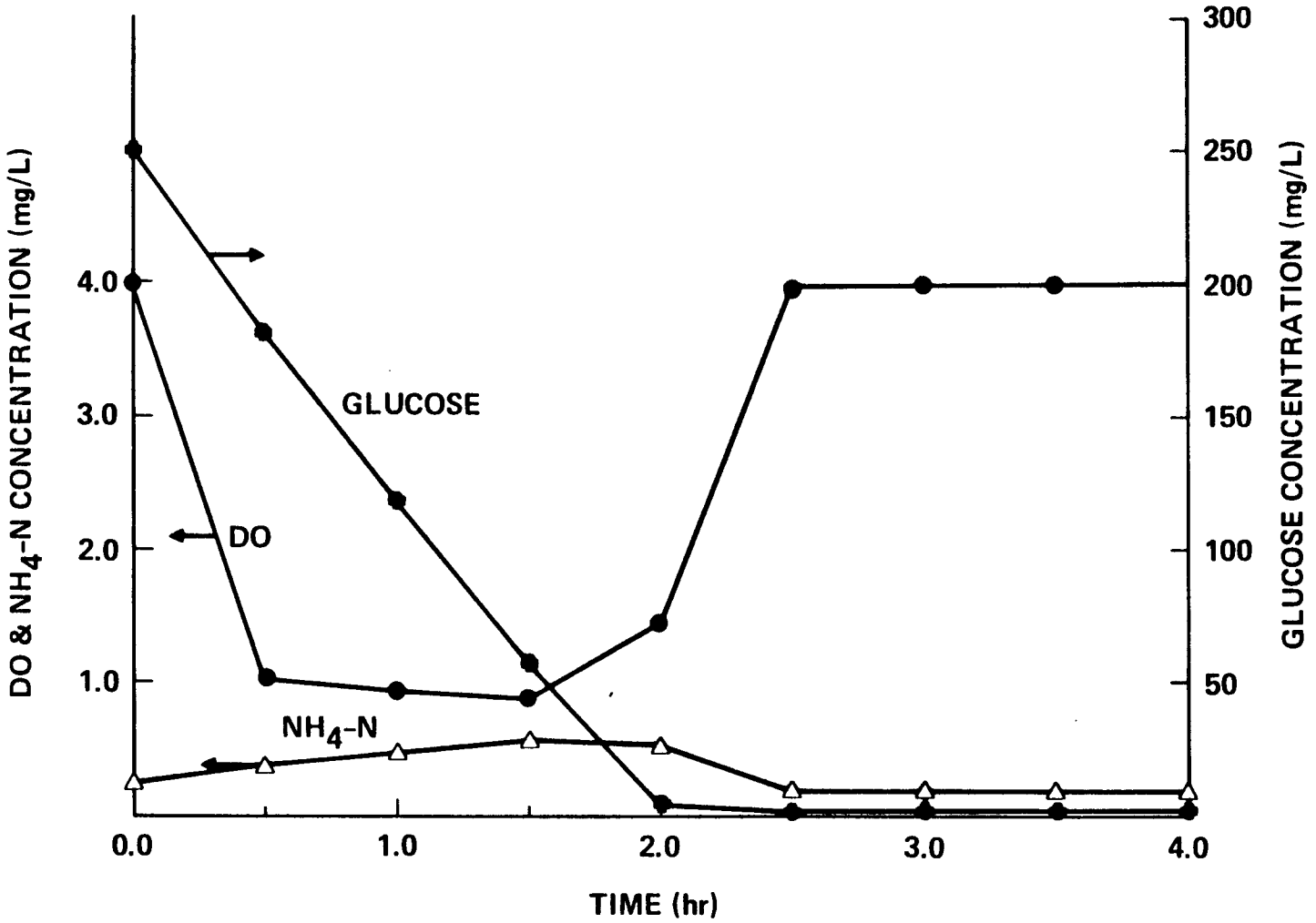

Fig. 6.4 Concentrations vs. Time Following Organic Shock Load with $L^2\rho = 0.75 \times 10^{-5}$ cm^2-g/L

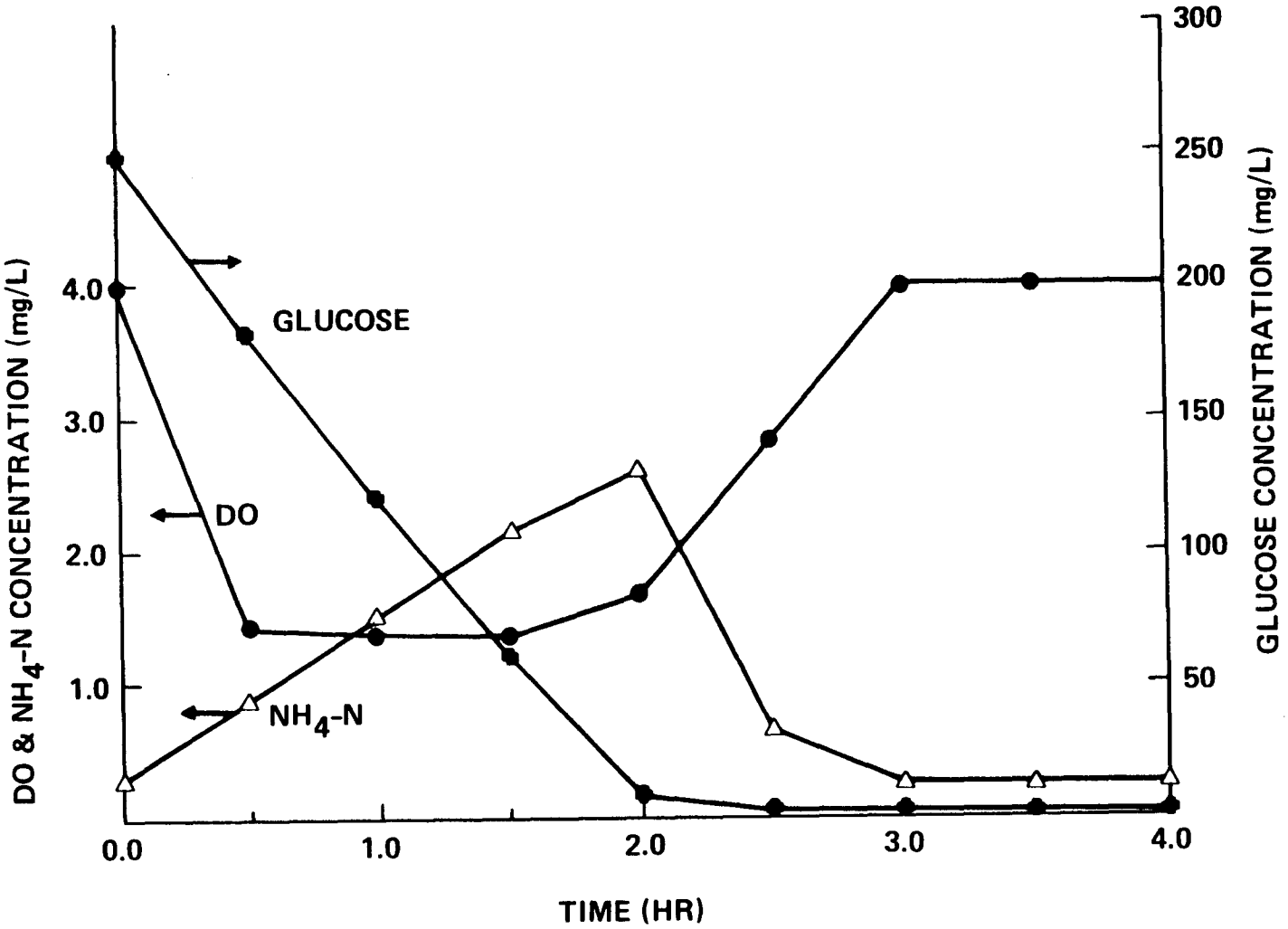

Fig. 6.5 Concentrations vs. Time Following Organic Shock Load with $L^2\rho = 1 \times 10^{-3}$ cm^2-g/L

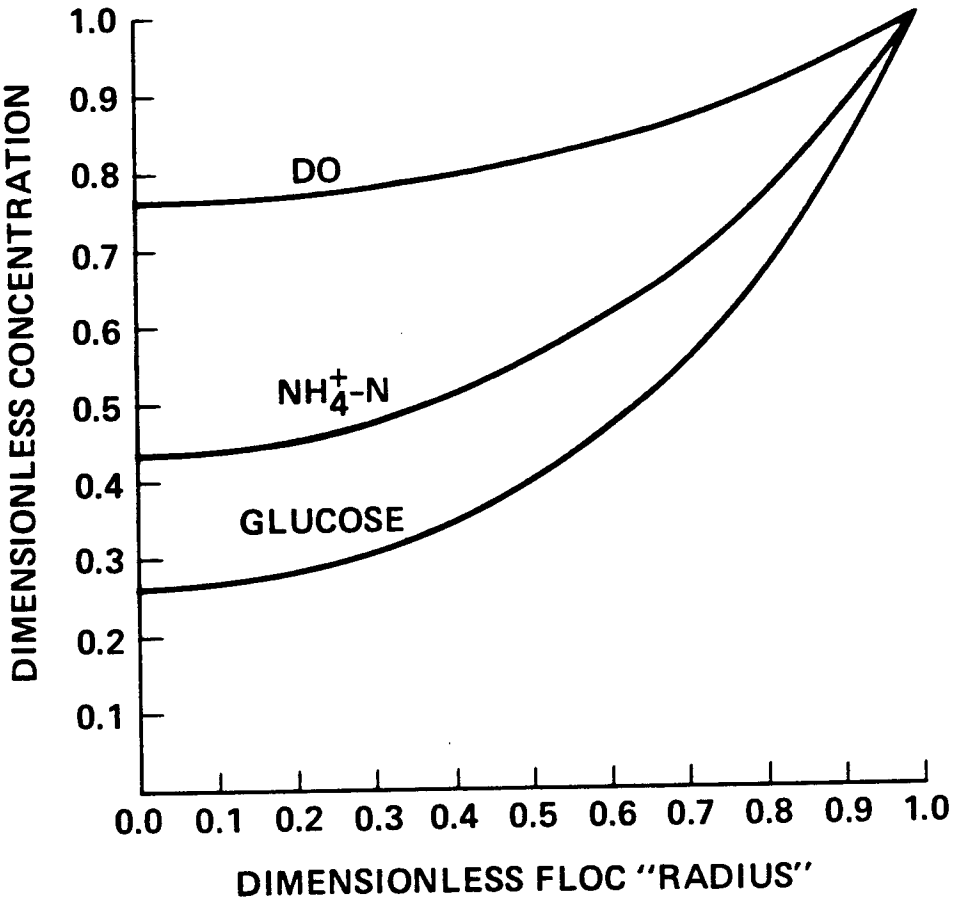

Fig. 6.6 Concentration Distributions for DO, NH_4^+–N, and Glucose with $L^2\rho\tau/\varepsilon = 2 \times 10^{-3}$ cm^2-g/L under Steady State Conditions.
Bulk Concentrations:
DO = 4.0 mg/L,
NH_4^+–N = 0.25 mg/L,
Glucose = 2.3 mg/L

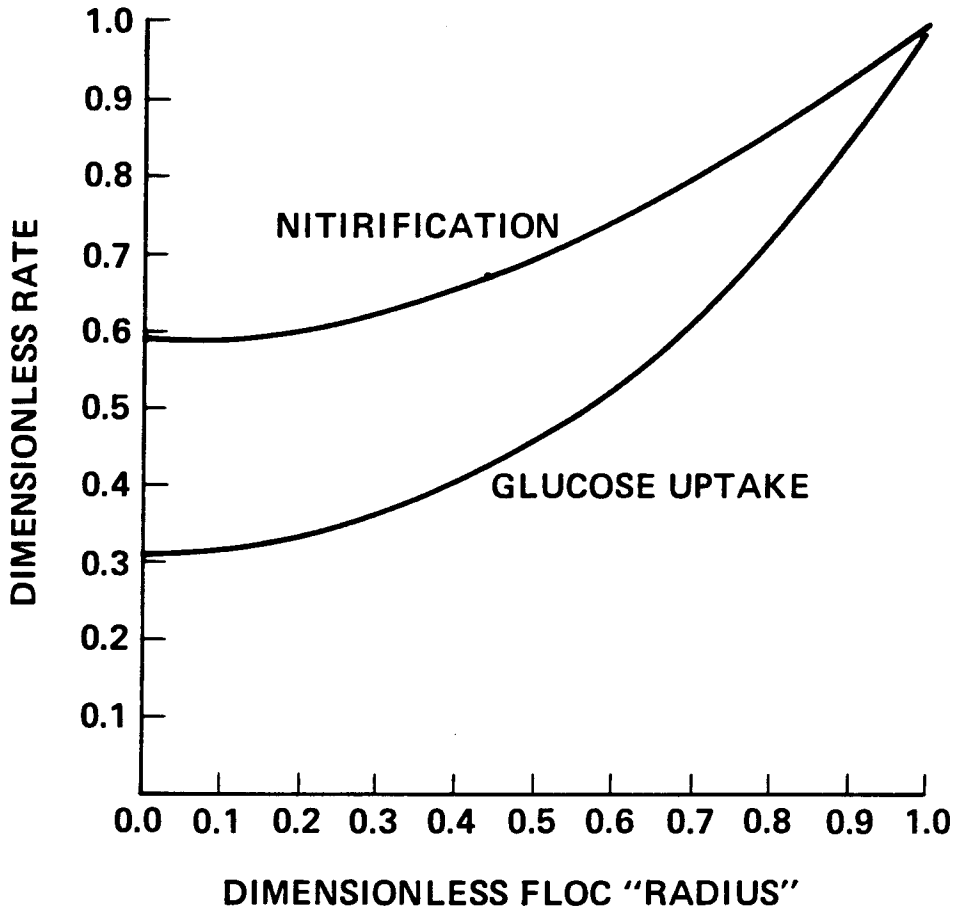

Fig. 6.7 Rate Distribution for Heterotrophs and Nitrifiers with $L^2\rho\tau/\varepsilon = 2 \times 10^{-3}$ cm^2-g/L under Steady State Conditions.
Intrinsic Rates:
Glucose Uptake = 29 mg/g-hr,
Nitrification = 4.8 mg/g-hr

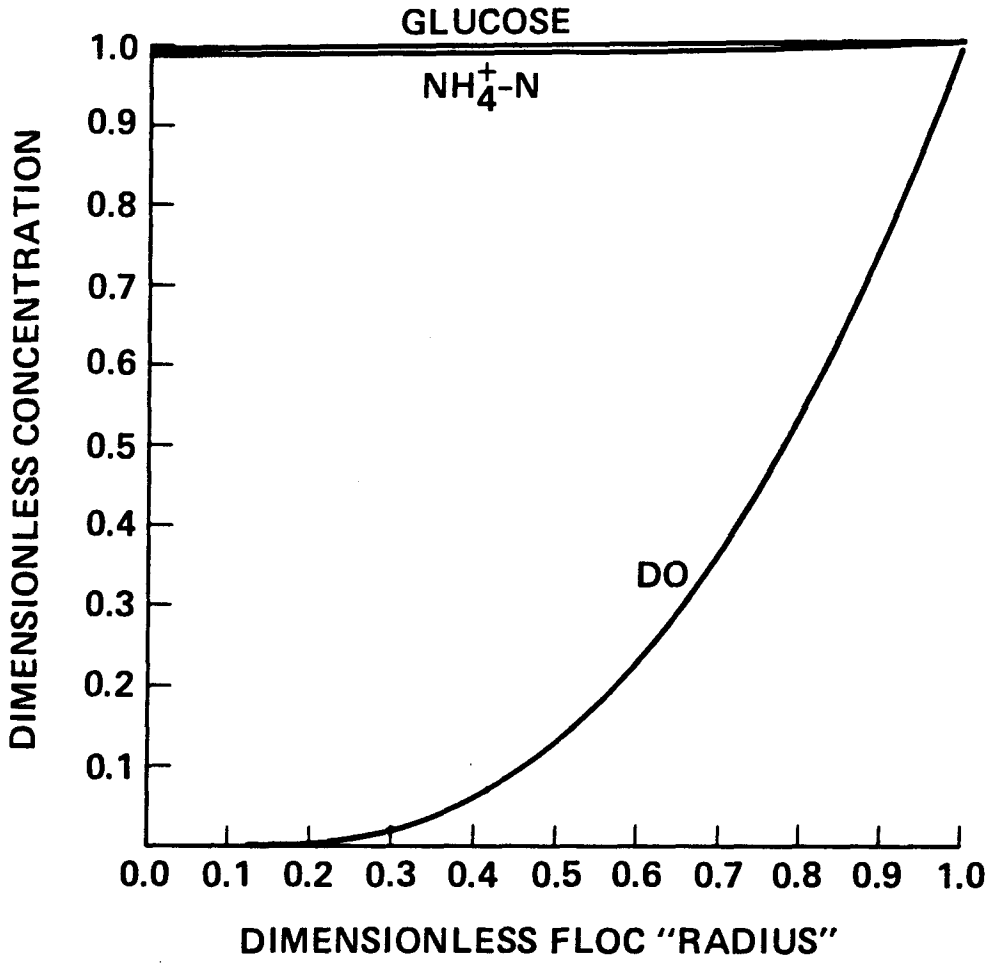

Fig. 6.8 Concentration Distributions

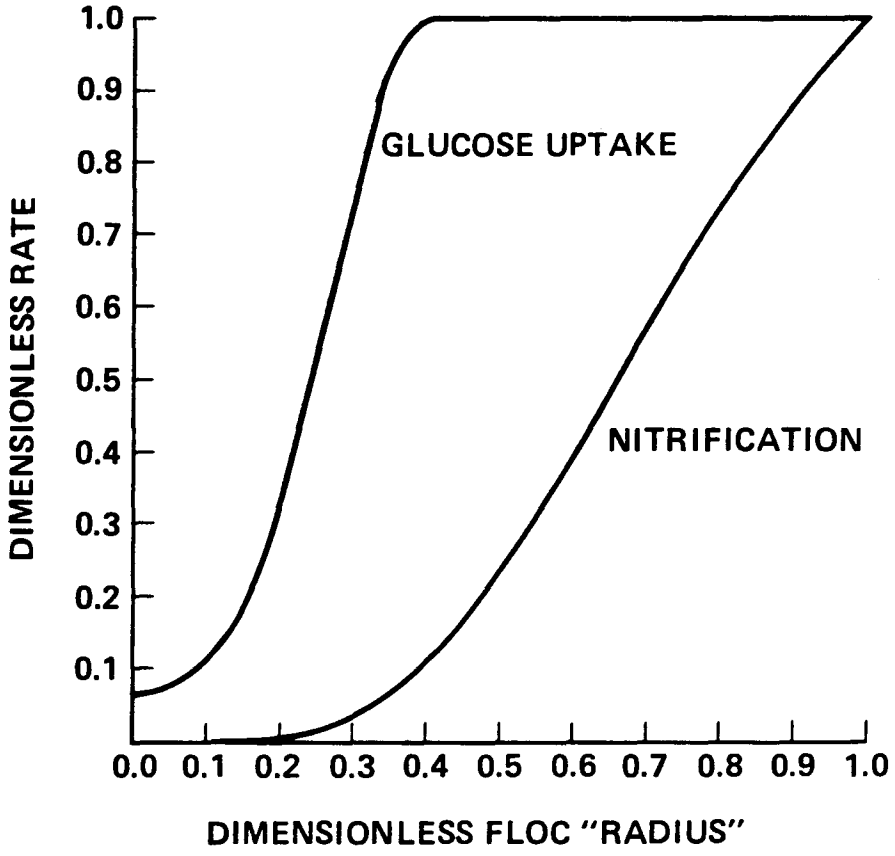

Fig. 6.9 Rate Distribution for Heterotrophs and Nitrifiers with $L^2\rho\tau/\varepsilon = 2 \times 10^{-3}$ cm^2-g/L at Time = 1 hr.
Intrinsic Rates:
Glucose Uptake = 70 mg/g-hr,
Nitrification = 5.42 mg/g-hr

rate of nitrification has increased from 4.8 mg/g-hr to 5.42 mg/g-hr because of the increase in NH_4^+-N concentration, but the effective rate has decreased from 4.1 mg/g-hr to 3.4 mg/g-hr because of the steep DO concentration gradient.

VII. CONCLUSION

From the previously described investigations and computer simulations, the following is concluded.

1. Mass transport limitation can significantly affect the apparent relationship between DO concentration and nitrification under both steady state and transient conditions.

2. Under the steady state conditions investigated here, the apparent limiting DO concentration ranges from 0.5 mg/L to 2.5 mg/L depending on the MCRT and the degree of mass transport resistance.

3. The wash-out MCRT can be expected to be dependent on both DO concentration and the degree of mass transport resistance; a high MCRT may be required to insure nitrification at lower DO concentrations and for higher mass transport resistance.

4. The apparent relationship between DO concentration and nitrification under transient conditions may differ drastically from that under steady state conditions. Because of mass transport resistance and heterotrophic/nitrifier competition for DO, the apparent limiting DO concentration for nitrification can be as high as 4.0 mg/L during an organic shock load.

5. Nitrification can occur under multiple-substrate limiting conditions within activated sludge flocs while single-substrate limiting conditions prevail in the bulk liquid.

6. The exponential kinetic formulation more accurately describes the intrinsic relationship between DO concentration and the rate of oxidation of NH_4^+-N by *Nitrosomonas* than does the Monod model. The value of the half-saturation coefficient for the exponential model is between 0.45 mg/L and 0.56 mg/L.

7. The deficiency of the Monod kinetic formulation is compounded when it is used as a component of an interactive-type multiple-substrate limiting kinetic model for nitrification; the use of exponential components produces much more realistic results.

8. The rate of NH_4^+-N oxidation by *Nitrosomonas* is typically the rate limiting step under steady state conditions, but the rate of NO_2^--N oxidation can become the rate limiting step under transient conditions. The accumulation of NO_2^--N under transient conditions appears to be correlated with transient increases in the rate of NO_2^--N production rather than with low DO concentrations.

VIII. REFERENCES

1. Atkinson B., and Rahman F.-UR. (1979), "Effect of diffusion limitation and floc size distribution on fermenter performance and the interpretation of experimental data," *Biotechnol. Bioengr.*, 21, p. 221.

2. Bader F. G. (1984) in *Microbial Population Dynamics*. M. J. Bazin, Ed., CRC Press, Boca Raton, FL, p. 1.

3. Bader F. G. (1978), "Analysis of double-substrate limited growth," *Biotechnol. Bioengr.*, 20, p. 183.

4. Bader F. G., Meyer J. S., Fredickson A. G., Tsuchiya H. M. (1975), "Comments on microbial growth rate," *Biotechnol. Bioengr.*, 17, p. 79.

5. Baillod C. R., and Boyle W. C. (1970), "Mass transfer limitations in substrate removal," *J. Sanitary Engr. Div. ASCE*, 96, SA2, p. 525.

6. Bard Y. (1974), *Nonlinear Parameter Estimation*, Academic Press, New York.

7. Box G. E. P. and Draper N. R. (1965), "The Bayesian estimation of common parameters from several responses," *Biometrika*, 52, p. 355.

8. Charley R. C., Hooper D. G., and McLee A. G. (1980), "Nitrification kinetics in activated sludge at various temperatures and dissolved oxygen concentrations," *Water Research*, 14, p. 1387.

9. Dabes, J.N., Finn, R.K., Wilke, C.R. (1973) "Equations of Substrate-Limited Growth: The Case for Blackman Kinetics," *Biotech & Bioengr.*, Vol. XV, p. 1159-1177.

10. Fiacco A. V., and McCormick G. P. (1968), *Nonlinear Programming: Sequential Unconstrained Minimization Techniques*, John Wiley and Sons, Inc., New York.

11. Focht D. D., and Chang A. C. (1975) Nitrification and denitrification processes related to wastewater treatment. *Adv. Appl. Microbiol.*, 19, p. 153.

12. Froment G. F. (1972), "Analysis and Design of Fixed Bed Catalytic Fixed Bed Reactors," *Chemical Reaction Engr., Adv. Chem. Series 109 (1) American Chemical Society*, Washington D.C.

13. Gondo S., Isayama S., and Kusunoki K. (1975), "Effect of internal diffusion on the Lineweaver-Burke plots for immobilized enzymes," *Biotechnol. Bioengr.*, 17, p. 423.

14. Grady C. P. L., and Lim H. C. (1980), *Biological Wastewater Treatment: Theory and Application.* Marcel Dekker, New York.

15. Haas C. N. (1981), "Biological process diffusion limitations," *J. Environ. Engr. Div. ASCE,* 107, p. 269.

16. Hao O. J., Richard M. G., Jenkins D., and Blanch H. W. (1983), "The half-saturation coefficient for dissolved oxygen: a dynamic method for its determination and its effect on dual species competition," *Biotechnol. Bioengr.*, 25, p. 403.

17. Hill C. G. (1977), *An Introduction to Chemical Engineering Kinetics and Reactor Design.* John Wiley and Sons, Inc., NY.

18. Knowles G., Downing A. L., and Barrett M. J. (1965), "Determination of kinetic constants for nitrifying bacteria in mixed culture, with the aid of an electronic computer," *J. Gen. Microbiol.*, 38, p. 263-278.

19. Kossen N. W. F. (1979), "Oxygen transport into bacterial flocs and biochemical oxygen consumption," *Prog. Wat. Tech.*, 11, No. 3, p. 9.

20. Kuester J. L., and Mize J. H. (1973), *Optimization Techniques with Fortran.* McGraw Hill Book Company, New York.

21. La Motta E. J., and Shieh W. K. (1979), "Diffusion and reaction in biological nitrification," *J. Environ. Engr. Div. ASCE,* 105, EE4, p. 655.

22. Lau A. O., Strom P. F., Jenkins D. (1984), "The competitive growth of floc-forming and filamentous bacteria: a model for activated sludge bulking," *J. WPCF,* 56, p. 52.

23. Lawrence A. W., and McCarty P. L. (1970), "Unified basis for biological treatment design and operation," *J. Sanitary Engr. Div. ASCE,* 96, SA3, p. 757.

24. Matson J. V., and Characklis W. G. (1976), "Diffusion into microbial aggregates," *Water Research,* 10, p. 877-885.

25. Megee R. D., Drake J. F., Fredrickson A. G., and Tsuchiya H. M. (1972), "Studies in intermicrobial symbiosis," *Saccharomyces cerevisias*

and *Lactobacillus casei. Canadian J. Microbiol.*, 18, p. 1733-1742.

26. Metcalf and Eddy (1977), *Wastewater Engineering Treatment/Disposal/Reuse.* McGraw Hill, NY.

27. Mueller J. A., Boyle W. C., and Lightfoot E. N. (1968), "Oxygen diffusion through zoogloeal flocs," *Biotechnol. Bioengr.*, 10, p. 331.

28. Painter H. A. (1977), "Microbial transformations of inorganic nitrogen. *Prog. Wat. Tech.*, 8, No. 4/5, p. 3.

29. Parker D. S., Kaufman W. J., and Jenkins D. (1970), "Characteristics of biological flocs in turbulent regimes," *SERL Report No. 70-5.*

30. Petersen E. E. (1965), *Chemical Reaction Analysis,"* Prentice-Hall, Englewood Cliffs, NJ.

31. Poduska R. A. (1973), "A dynamic model of nitrification for the activated sludge process, Ph.D. Dissertation, Clemson University, Clemson, SC.

32. Regan D. L., Lilly M. D., and Dunnill P. (1974), "Influence of intraparticle diffusional limitation on the observed kinetics of immobilized enzymes and on catalyst design," *Biotechnol. Bioengr.*, 16, p. 1081.

33. Ryder D. N. and Sinclair C. G. (1972) Model for the growth of aerobic microorganisms under oxygen limiting conditions. *Biotechnol. Bioengr.*, 14, p. 787-798.

34. Sadeghipour J. and Yeh W. G. (1984), "Parameter identification of groundwater aquifer models: a generalized least square approach," *Water Resources Research,* 20, No. 7, p. 971-979.

35. Sharma B., and Alhert R. C. (1977), "Nitrification and nitrogen removal," *Water Research,* 11, p. 897.

36. Stenstrom M. K., and Poduska R. A. (1980), "The effect of dissolved oxygen concentration on nitrification. *Water Research,* 14, No. 6, p. 643.

37. Weisz P. B. (1973), "Diffusion and chemical transformation," *Science,* 179, No. 4072, p. 433-440.

APPENDIX A - EXPERIMENTAL RESULTS

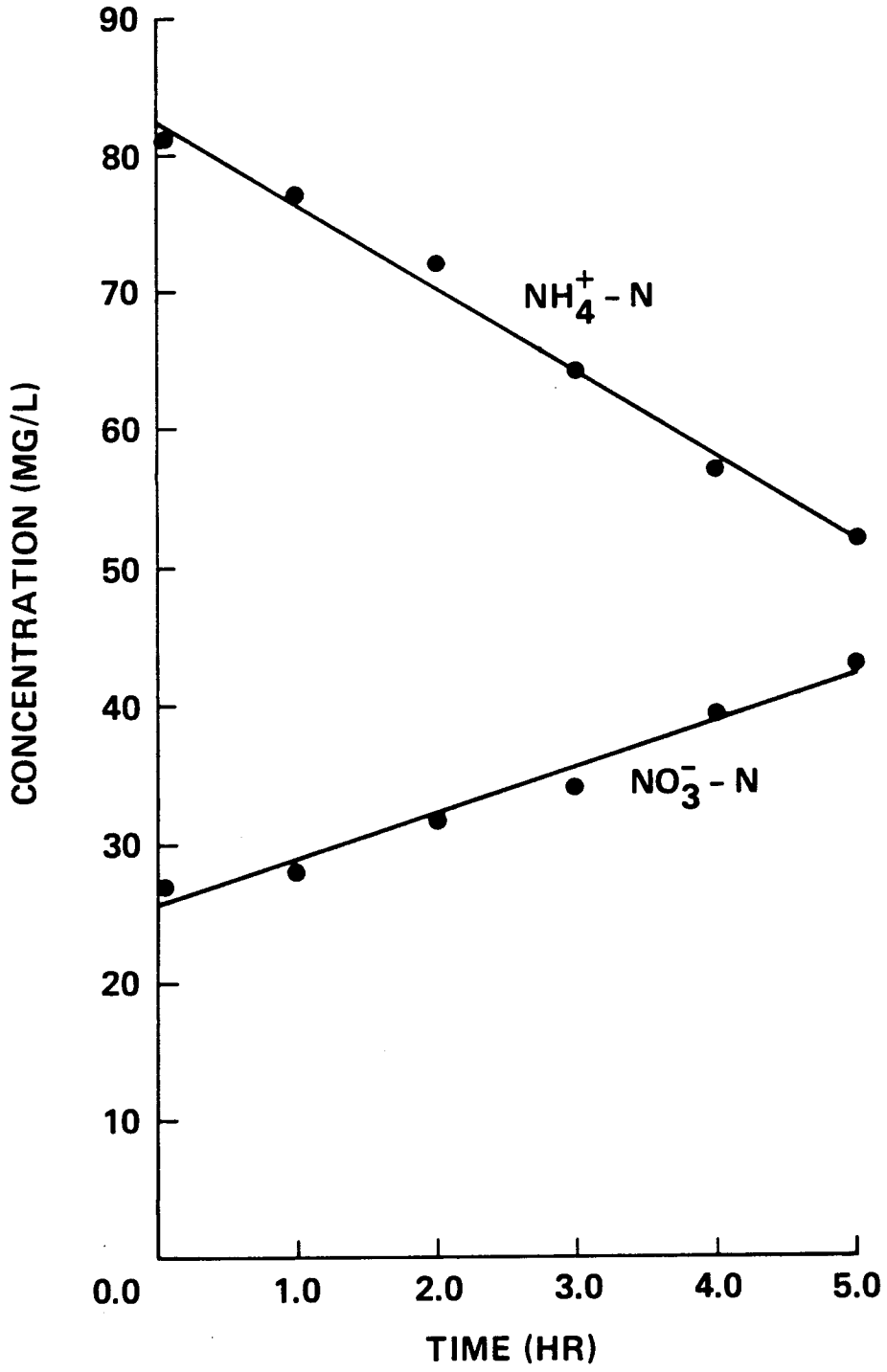

Fig. A.1 Set I: NH_4^+–N and NO_3^-–N Concentration vs. Time at 100 RPM and DO = 0.7 mg/L.

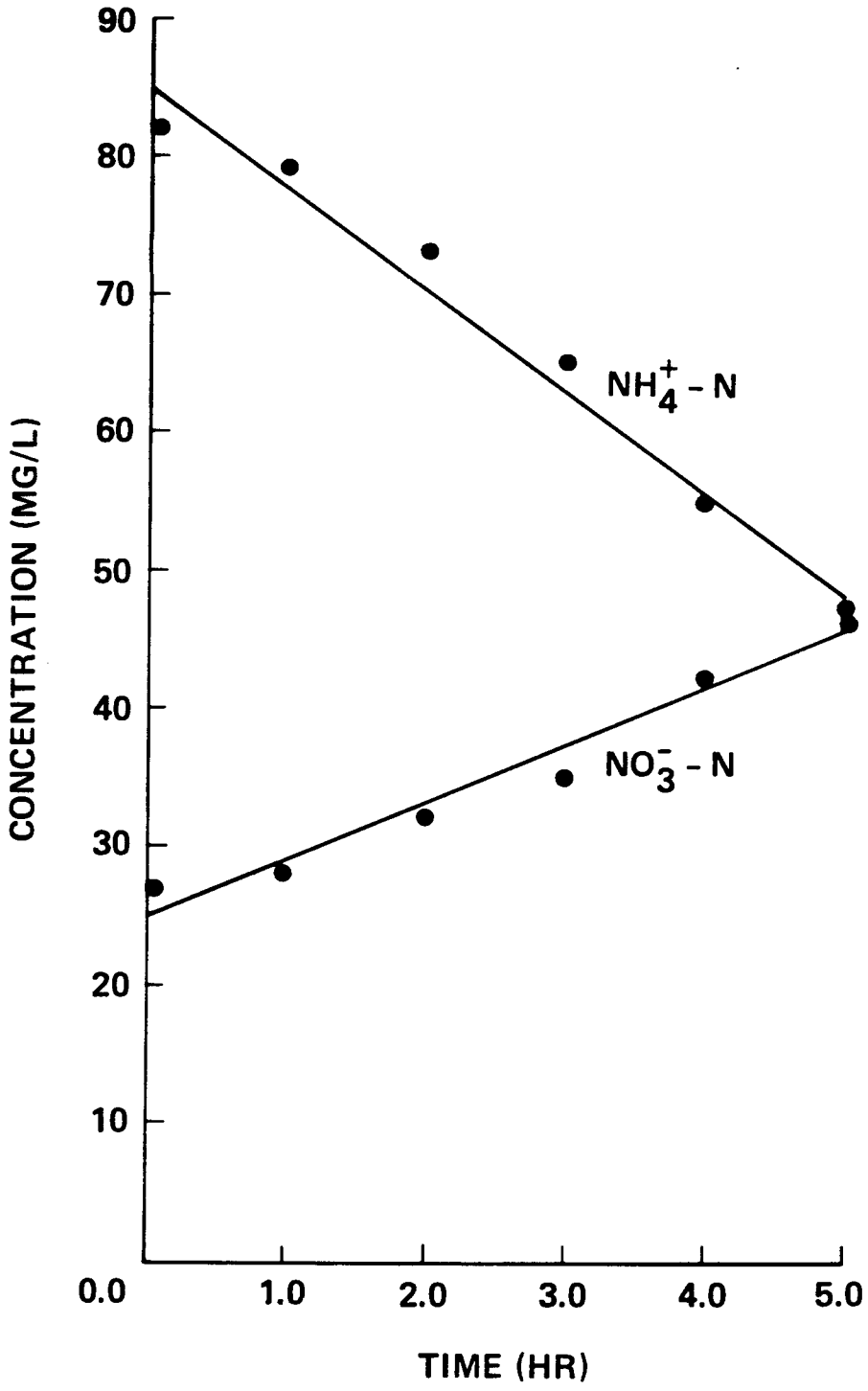

Fig. A.2 Set I: NH_4^+–N and NO_3^-–N Concentration vs. Time at 170 RPM and DO = 0.7 mg/L.

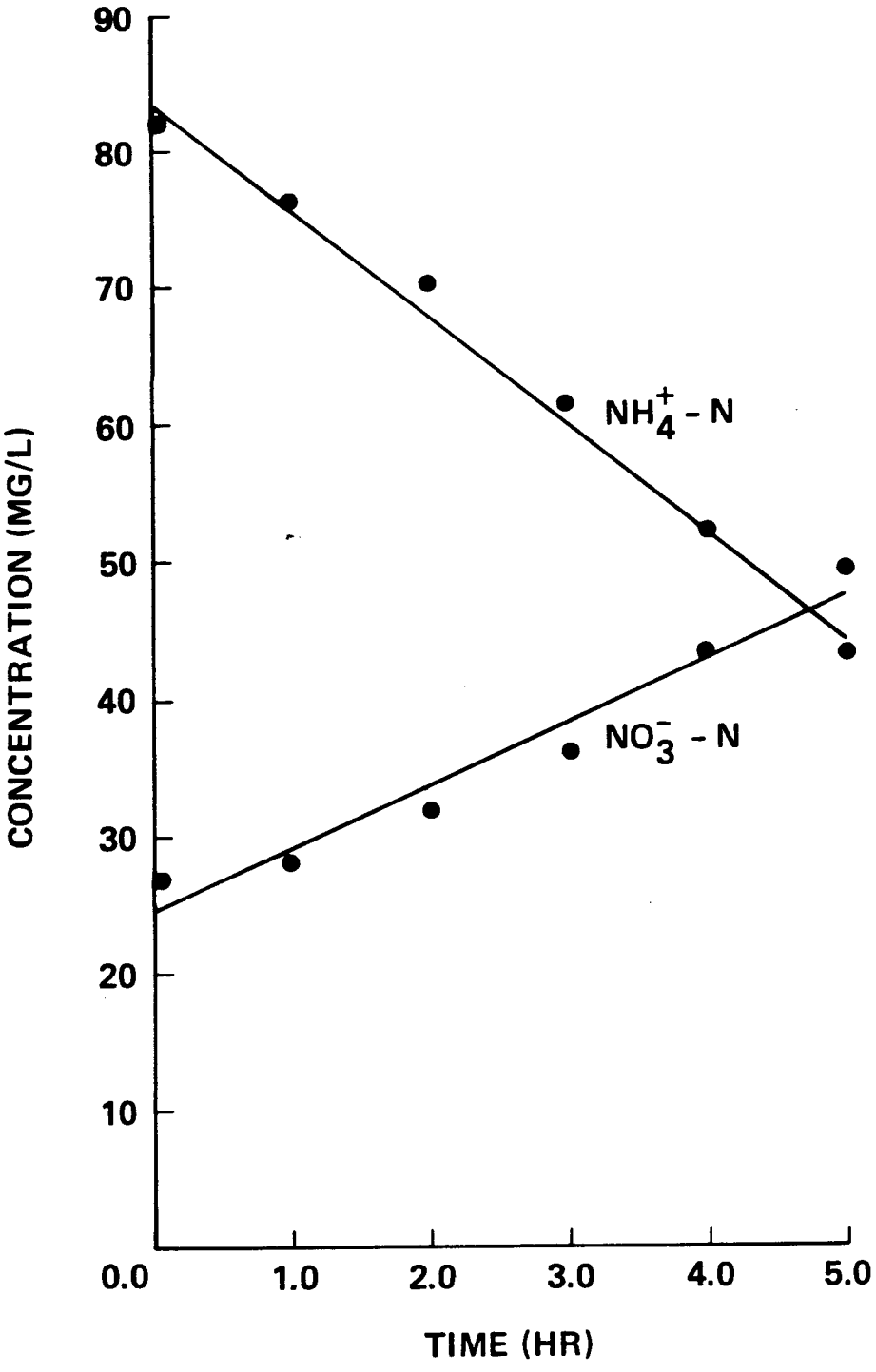

Fig. A.3 Set I: NH_4^+–N and NO_3^-–N Concentration vs. Time at 400 RPM and DO = 0.7 mg/L.

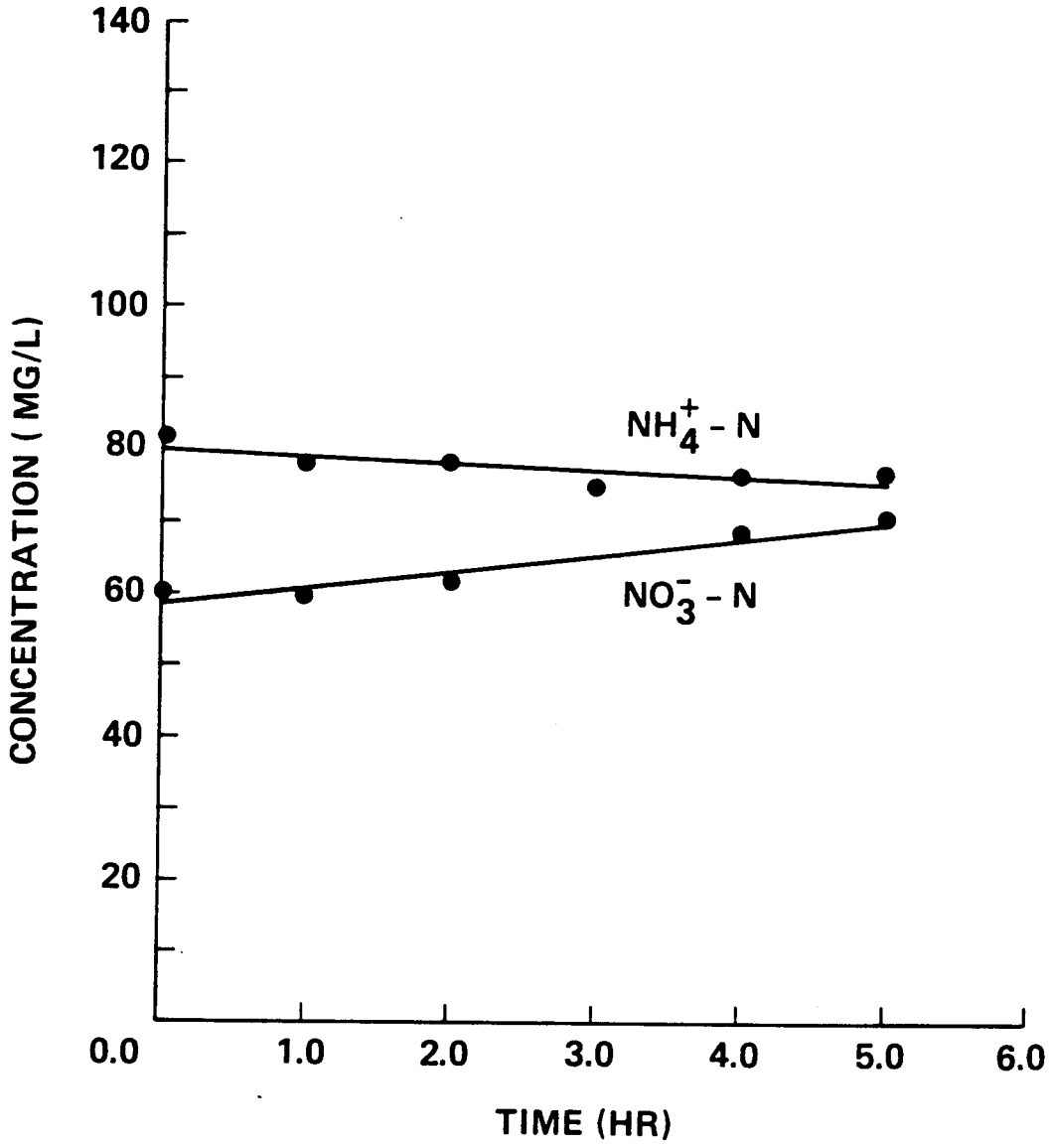

Fig. A.4 Set II: NH_4^+–N and NO_3^-–N Concentration vs. Time at 170 RPM and DO = 0.25 mg/L.

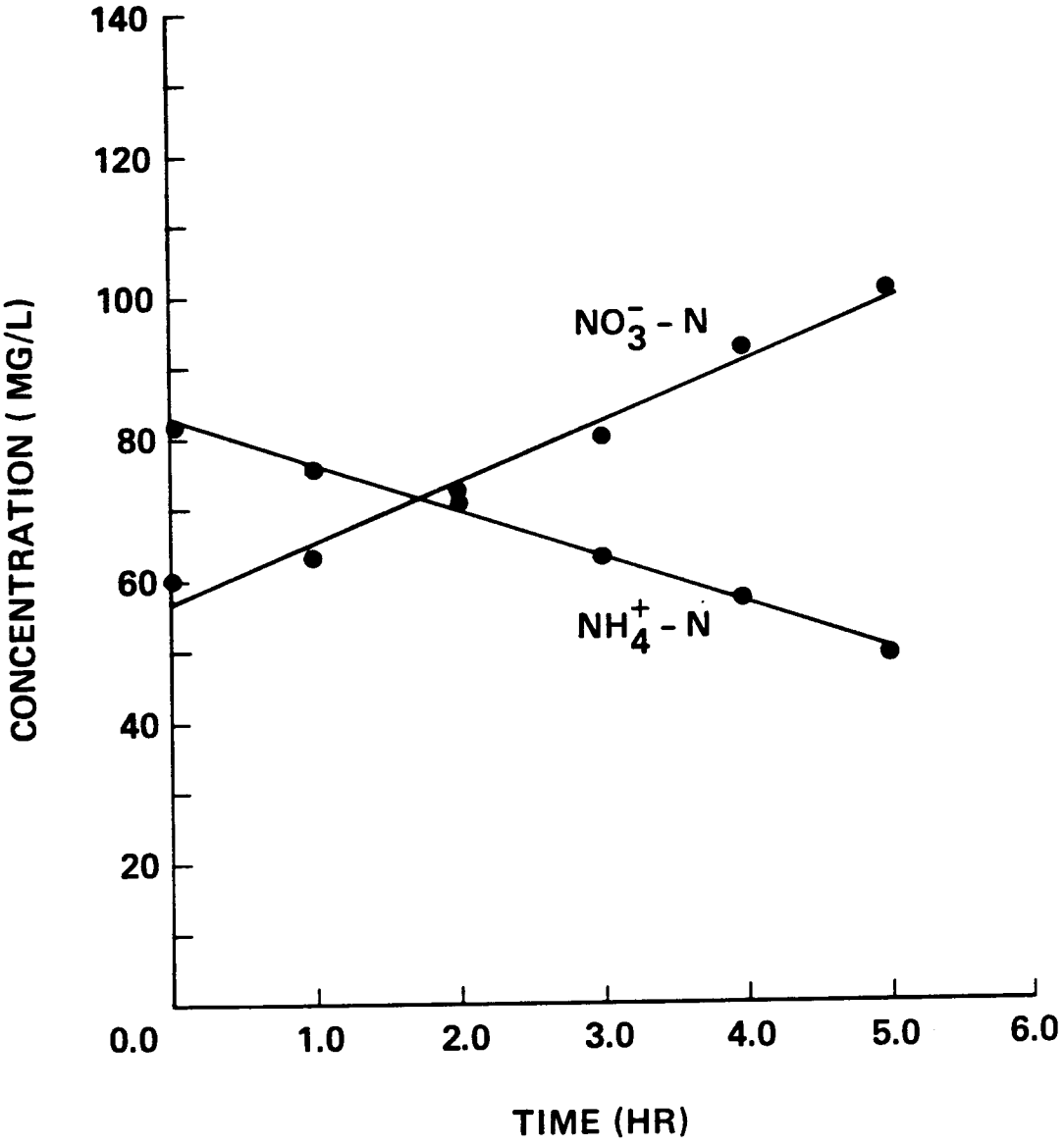

Fig. A.5 Set II: NH_4^+–N and NO_3^-–N Concentration vs. Time at 170 RPM and DO = 1.0 mg/L.

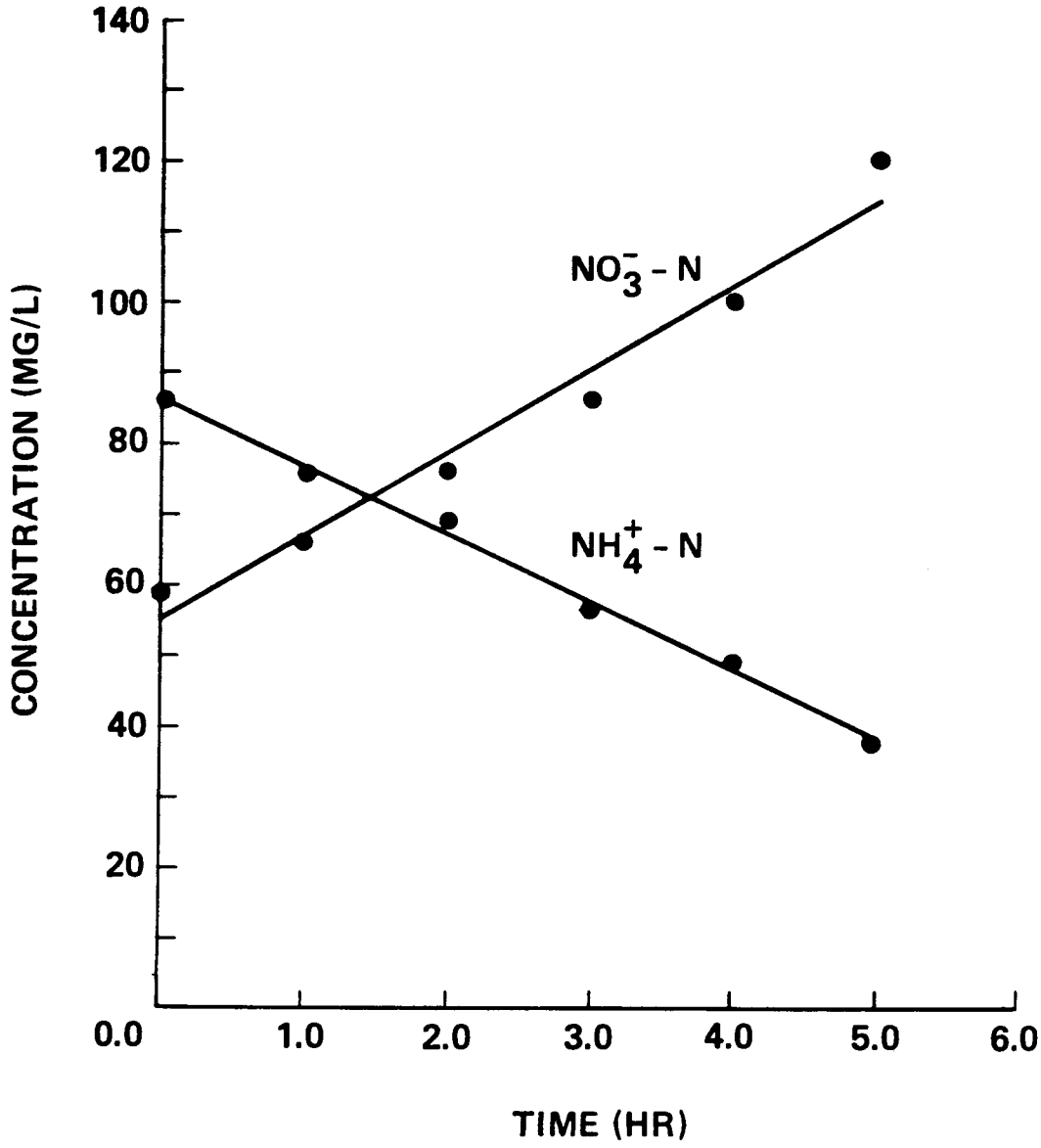

Fig. A.6 Set II: NH_4^+–N and NO_3^-–N Concentration vs. Time at 170 RPM and DO = 4.0 mg/L.

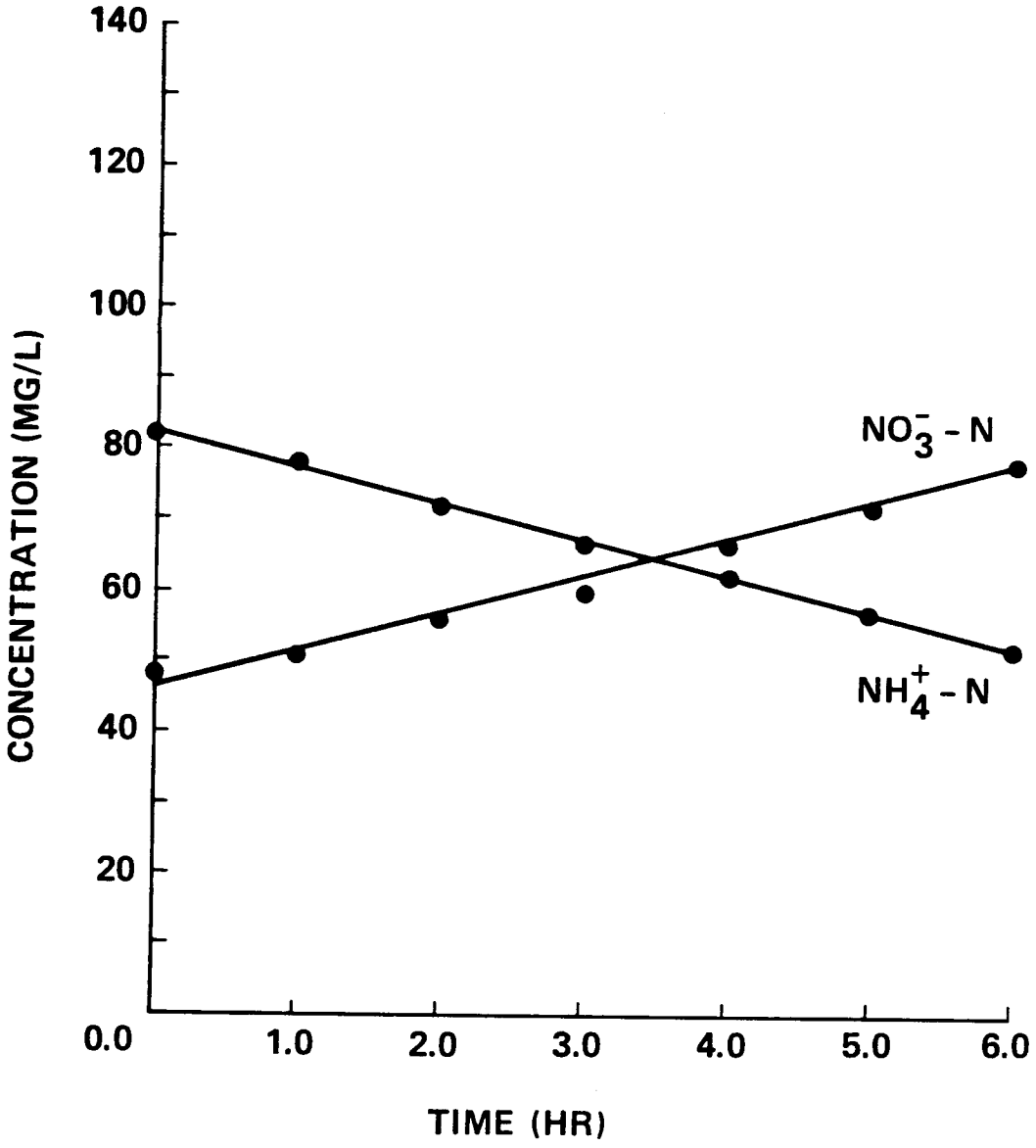

Fig. A.7 Set II: NH_4^+–N and NO_3^-–N Concentration vs. Time at 170 RPM and DO = 0.5 mg/L.

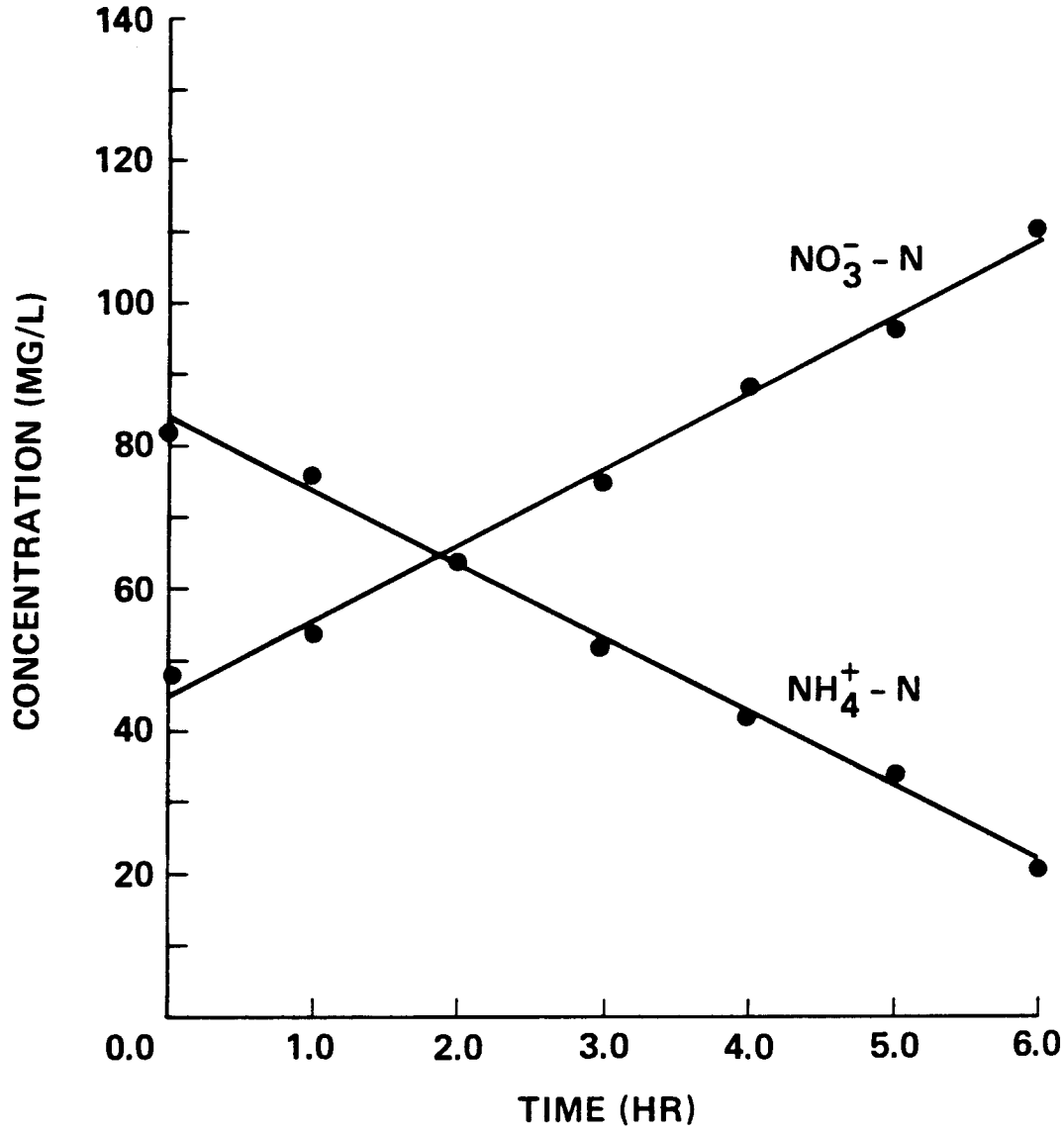

Fig. A.8 Set III: NH_4^+–N and NO_3^-–N Concentration vs. Time at 170 RPM and DO = 2.0 mg/L.

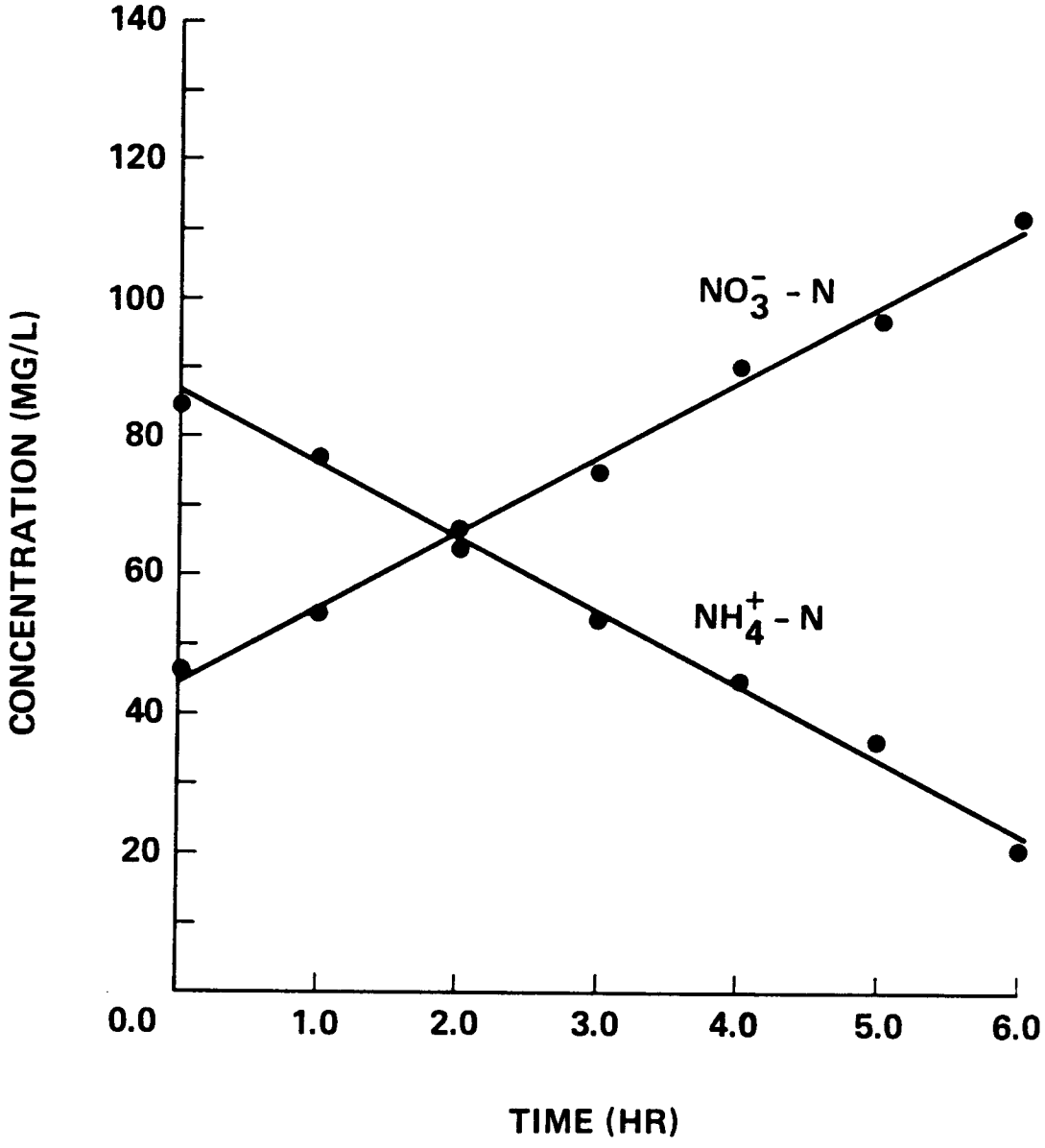

Fig. A.9 Set III: NH_4^+–N and NO_3^-–N Concentration vs. Time at 170 RPM and DO = 4.0 mg/L.

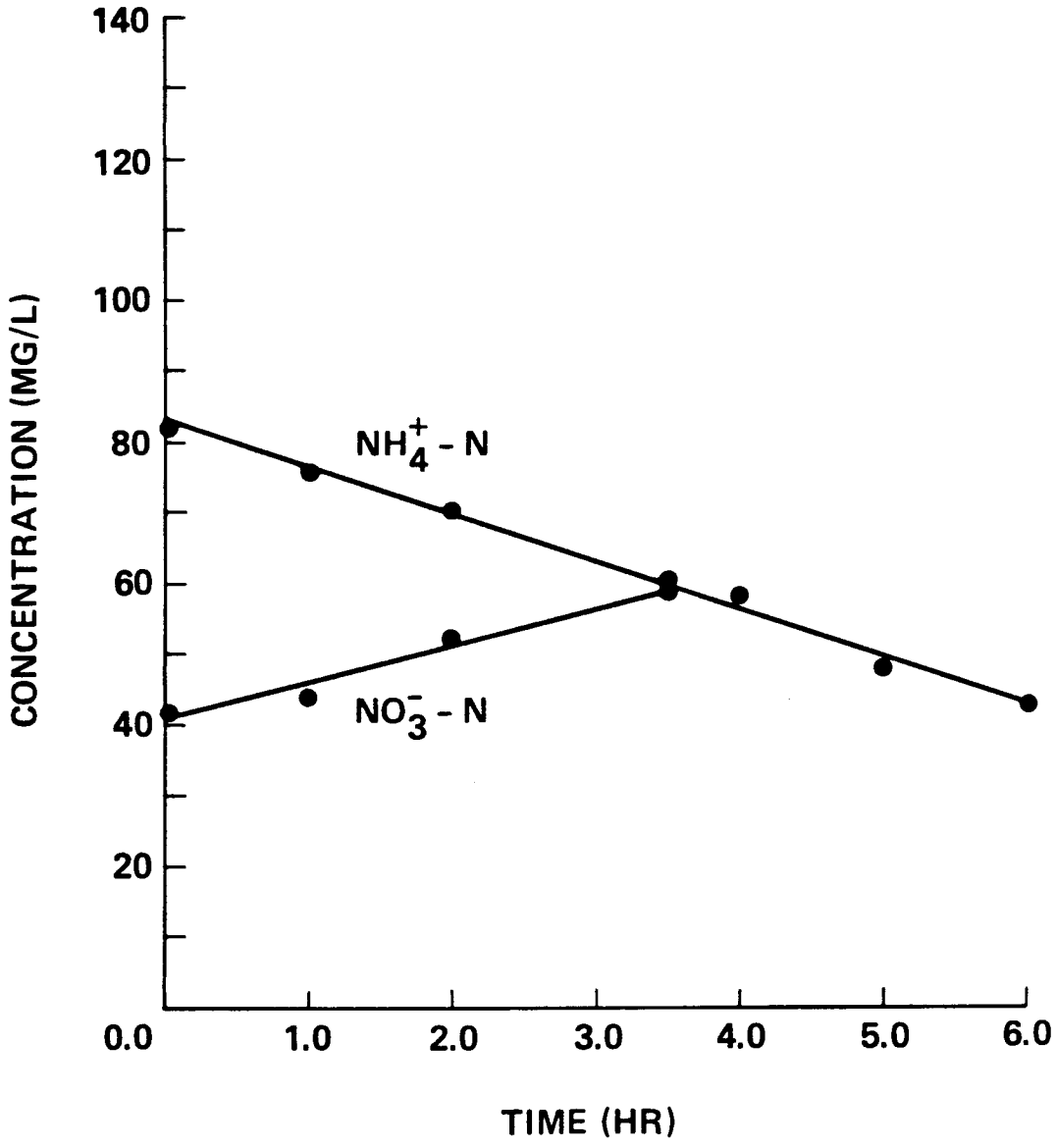

Fig. A.10 Set IV: NH_4^+–N and NO_3^-–N Concentration vs. Time at 170 RPM and DO = 0.7 mg/L.

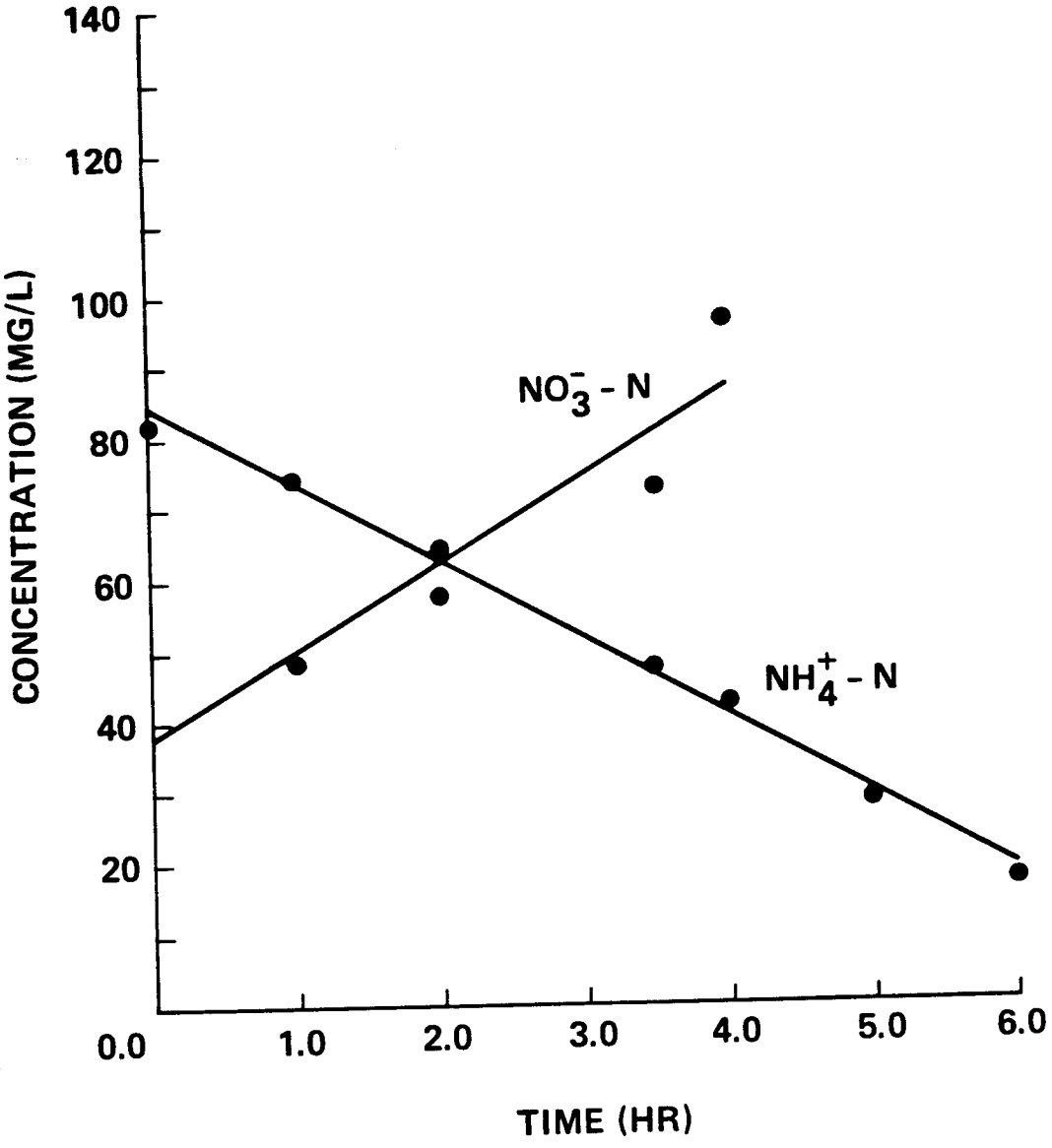

Fig. A.11 Set IV: NH_4^+–N and NO_3^-–N Concentration vs. Time at 170 RPM and DO = 2.0 mg/L.

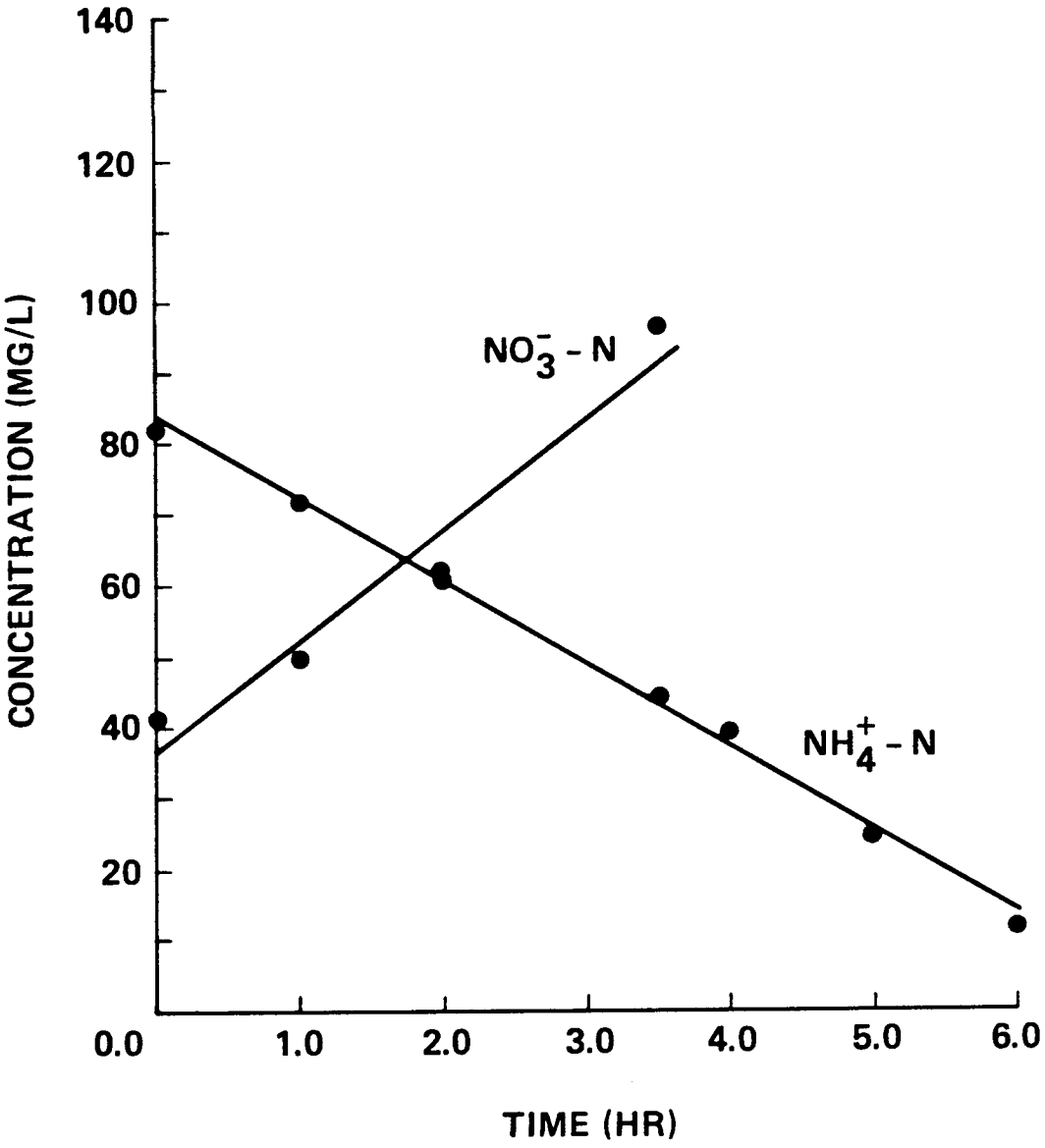

Fig. A.12 Set IV: NH_4^+–N and NO_3^+–N Concentration vs. Time at 170 RPM and DO = 4.0 mg/L.

Table A.1 Results for SET I, Subproblem 1.

RUN 1: RPM = 100 MLSS = 1750 mg/L			RUN 2: RPM = 170 MLSS = 1690 mg/L			RUN 3: RPM = 400 MLSS = 1730 mg/L		
t *	NH_4^+–N**	NO_3^-–N**	t	NH_4^+–N	NO_3^-–N	t	NH_4^+–N	NO_3^-–N
0	81	27	0	82	27	0	82	27
1	77	28	1	79	28	1	76	28
2	72	32	2	73	32	2	70	32
3	64	34	3	65	35	3	61	36
4	57	39	4	55	42	4	52	43
5	52	43	5	46	47	5	43	49
$[NH_4^+–N]$ = 82.38-6.09(t) r = -0.995			$[NH_4^+–N]$ = 85.24-7.43(t) r = -0.986			$[NH_4^+–N]$ = 83.71-7.89(t) r = -0.996		
$[NO_3^-–N]$ = 25.62+3.29(t) r = 0.985			$[NO_3^-–N]$ = 24.81+4.14(t) r = 0.977			$[NO_3^-–N]$ = 24.48+4.54(t) r = 0.976		

* time in (hours)
** concentration in (mg/L)

Table A.2 Results for SET II, Subproblem 1.

RUN 1: DO = 0.25 mg/L MLSS = 1770 mg/L			RUN 2: DO = 1.0 mg/L MLSS = 1820 mg/L			RUN 3: DO = 4.0-7.0 mg/L MLSS = 1800 mg/L		
t*	NH_4^+–N**	NO_3^-–N**	t	NH_4^+–N	NO_3^-–N	t	NH_4^+–N	NO_3^-–N
0	81	60	0	82	60	0	86	59
1	78	60	1	76	63	1	76	66
2	78	62	2	71	72	2	69	76
3	75	65	3	63	80	3	57	86
4	76	68	4	57	92	4	49	100
5	76	70	5	49	100	5	38	120
$[NH_4^+–N]$ = 79.76-0.971(t) r = -0.840			$[NH_4^+–N]$ = 82.76-6.57(t) r = -0.998			$[NH_4^+–N]$ = 86.29-9.51(t) r = -0.998		
$[NO_3^-–N]$ = 58.67+2.20(t) r = 0.977			$[NO_3^-–N]$ = 56.76+8.43(t) r = 0.990			$[NO_3^-–N]$ = 54.71+11.9(t) r = 0.984		

* time in (hours)
** concentrations in (mg/L)

Table A.3 Results for SET III, Subproblem 1.

RUN 1: DO = 0.5 mg/L MLSS = 1630 mg/L			RUN 2: DO = 2.0 mg/L MLSS = 1660 mg/L			RUN 3: DO = 4.0-7.0 mg/L MLSS = 1490 mg/L		
t*	NH_4^+–N**	NO_3^-–N**	t	NH_4^+–N	NO_3^-–N	t	NH_4^+–N	NO_3^-–N
0	82	48	0	82	48	0	85	47
1	78	51	1	76	54	1	77	55
2	72	56	2	64	64	2	67	64
3	67	60	3	52	75	3	54	75
4	62	67	4	42	88	4	45	90
5	57	72	5	34	96	5	36	97
6	52	78	6	21	110	6	21	112
$[NH_4^+–N]$ = 82.36-5.07(t) r = -1.0			$[NH_4^+–N]$ = 83.96-10.3(t) r = -0.998			$[NH_4^+–N]$ = 86.7-10.6(t) r = -0.997		
$[NO_3^-–N]$ = 46.39+5.11(t) r = 0.995			$[NO_3^-–N]$ = 44.93+10.5(t) r = 0.9960			$[NO_3^-–N]$ = 44.46+10/9(t) r = 0.996		

* time in (hours)
** concentrations in (mg/L)

Table A.4 Results for SET IV, Subproblem 1

RUN 1: DO = 0.7 mg/L MLSS = 1750 mg/L			RUN 2: DO = 2.0 mg/L MLSS = 1740 mg/L			RUN 3: DO = 4.0-7.0 mg/L MLSS = 1770 mg/L		
t*	NH_4^+–N**	NO_3^-–N**	t	NH_4^+–N	NO_3^-–N	t	NH_4^+–N	NO_3^-–N
0	82	42	0	82	42	0	82	41
1	76	44	1	74	49	1	72	50
2	70	52	2	64	58	2	62	61
3.5	60	59	3.5	47	73	3.5	44	96
4	58	-	4	42	96	4	39	-
5	48	-	5	29	-	5	25	-
6	43	-	6	17	-	6	12	-
$[NH_4^+–N]$ = 82.70-6.60(t) r = -0.997			$[NH_4^+–N]$ = 84.34-11.0(t) r = -0.998			$[NH_4^+–N]$ = 83.82-11.7(t) r = -0.998		
$[NO_3^-–N]$ = 40.90+5.14(t) r = 0.983			$[NO_3^-–N]$ = 37.97+12.2(t) r = 0.950			$[NO_3^-–N]$ = 36.49+15.7(t) r = 0.973		

* time in hours
** conc. in mg/L

Table A.5 SET I - RUN 1 (Nitrifiers)

t*	NH_4^+–N**	NO_2^-–N	NO_3^-–N	Total Inorganic N	OUR^+
0.0	53	1.1	56	110.1	-
0.5	41	4.7	65	110.7	98
1.0	29	8.0	75	112.0	116
1.5	20	11.2	84	115.2	95
2.0	11	13.8	90	114.8	-
3.0	0.14	13.2	104	117.3	-
5.0	0.27	0.02	125	125.3	17
6.3	0.07	0.03	140	140.1	16

* time in (hours)
** concentrations in (mg/L)
+ oxygen uptake rates in (mg/L-hr)

MLSS = 5 g/L

Table A.6 Set I - RUN 2 (Nitrifiers)

t*	NH_4^+–N**	NO_2^-–N	NO_3^-–N	Total Inorganic N	OUR^+
0.0	38	0.13	50	88.13	43
0.5	29	0.10	58	87.1	102
1.0	21	0.59	67	88.9	95
1.5	11	1.3	77	89.3	79
2.0	3.8	1.3	86	91.1	88
2.5	0.14	0.07	93	93.21	26
3.0	0.20	0.01	94	94.21	25
3.5	0.15	0.02	95	95.17	19
5.25	0.13	0.01	100	100.14	14

* time in (hours)
** concentrations in (mg/L)
\+ oxygen uptake rates in (mg/L-hr)

MLSS = 4.2 g/L

Table A.7 SET II - RUN 1 (Heterotrophs and Nitrifiers)

t*	NH_4^+–N**	NO_2^-–N	NO_3^-–N	Total Inorganic N	TOC	OUR^+
0.0	100	0.78	45	145.8	190	195
0.5	85	6.2	46	137.2	87	50
1.0	73	10.4	52	135.4	20	-
1.5	60	5.5	58	123.5	17	-
2.0	52	8.3	65	125.3	17	66

* time in (hours)
** concentrations in (mg/L)
\+ oxygen uptake rates in (mg/L-hr)

MLSS = 4.2 g/L

Table A.8: SET II - RUN 2 (Heterotrophs and Nitrifiers)

t*	NH_4^+–N**	NO_2^-–N	NO_3^-–N	Total Inorganic N	TOC	OUR+
0.0	76	0.5	50	126.5	175	-
0.5	69	4.6	53	126.6	95	150
1.0	64	11.7	53	128.7	45	83
1.5	58	14.3	52	124.3	25	63
2.0	51	17.9	53	122.0	22	61
2.5	45	19.0	56	120.0	17	68
3.0	39	22.0	60	121.0	17	67
4.0	26	21.6	71	118.6	25	66
5.0	16	20.8	88	124.8	27	62.5
6.5	2.3	19.0	109	130.3	27	20
9.0	0.2	0.0	138	138.2	27	27

* time in (hours)

** concentrations in (mg/L)

***oxygen uptake rates in (mg/L-hr)

MLSS = 4.1 g/L

Table A.9 Steady-State Simulation Results I

$L^2\rho$	MCRT	DO	NH_4-N	NO_3-N	Glucose	SOUR	Q_{H3}	Q_{H2}	X_H	X_N	X_T	f_N
$1x10^{-3}$	3	4.0	0.426	45.7	4.26	40.6	-69.5	6.39	1240	38.4	1278	3.0%
		3.0	0.469	45.0	4.38	41.1	69.5	6.41	1210	37.8	1248	3.0%
		2.0	2.72	40.3	4.67	40.3	69.6	6.00	1160	33.7	1194	2.8%
		1.5	19.2	23.9	4.71	32.0	70.3	4.06	1150	22.5	1173	1.9%
		1.0	35.3	8.04	4.73	23.6	71.0	1.73	1150	9.50	1160	0.82%
		0.5	42.5	0.070	4.80	19.5	71.5	0.33	1160	1.79	1162	0.15%
		0.25	42.1	0.03	6.48	17.8	71.6	0.04	1190	0.237	1190	0.02%
$7.5x10^{-5}$	3	4.0	0.325	46.0	2.93	40.8	69.5	6.40	1240	38.6	1279	3.0%
		3.0	0.343	45.6	2.99	40.9	69.5	6.43	1230	38.3	1268	3.0%
		2.0	0.434	44.3	3.12	41.5	69.5	6.40	1190	36.9	1227	3.0%
		1.5	1.09	41.9	3.23	41.3	69.6	6.10	1160	34.3	1194	2.9%
		1.0	19.6	23.5	3.24	31.5	70.3	4.05	1160	22.5	1183	1.9%
		0.5	38.2	5.02	3.24	21.9	71.2	1.33	1160	7.29	1167	0.62%
		0.25	42.8	0.530	3.24	19.6	71.5	0.248	1160	1.35	1161	0.12%

Table A.10 Steady-State Simulation Results II

$L^2\rho$	MCRT	DO	NH_4-N	NO_3-N	Glucose	SOUR	Q_{H3}	Q_{H2}	X_H	X_N	X_T	f_N
$1x10^{-3}$	6	4.0	0.210	52.9	2.32	28.2	69.4	6.60	2040	65.5	2106	3.1%
		3.0	0.212	52.8	2.32	28.1	69.4	6.71	2040	66.6	2107	3.2%
		2.0	0.233	52.2	2.32	27.9	69.3	6.80	2040	67.5	2108	3.2%
		1.5	0.271	51.1	2.32	27.6	69.3	6.85	2040	68.0	2108	3.2%
		1.0	0.461	47.9	2.32	26.6	69.3	6.84	2040	67.9	2108	3.2%
		0.75	16.4	30.1	2.34	21.4	70.0	4.84	2040	47.5	2088	2.3%
		0.50	39.0	7.65	2.35	14.7	71.0	1.71	2040	16.6	2057	0.81%
		0.25	45.5	0.433	2.38	12.0	71.5	0.237	2090	2.35	2092	0.11%
$7.5x10^{-5}$	6	4.0	0.151	53.6	1.56	28.4	69.3	6.84	2040	68.1	2108	3.2%
		3.0	0.151	53.5	1.57	28.4	69.3	6.93	2040	69.0	2109	3.3%
		2.0	0.163	53.2	1.57	28.2	69.3	7.01	2040	69.7	2110	3.3%
		1.5	0.180	52.6	1.57	28.0	69.2	7.05	2040	70.3	2110	3.3%
		1.0	0.233	51.1	1.57	27.5	69.2	7.08	2040	70.5	2111	3.3%
		0.75	0.314	49.4	1.57	27.0	69.2	7.07	2040	70.3	2110	3.3%
		0.50	9.59	36.8	1.57	23.4	69.7	5.70	2040	56.3	2096	2.7%
		0.25	40.8	5.82	1.57	14.2	71.1	1.58	2040	15.3	2055	0.74%

Table A.11 Steady-State Simulation Results III

$L^2\rho$	MCRT	DO	NH_4-N	NO_3-N	Glucose	SOUR	Q_{H3}	Q_{H2}	X_H	X_N	X_T	f_N
$1x10^{-3}$	12	4.0	0.126	59.5	1.53	21.7	69.1	7.53	2960	109	3069	3.6%
		3.0	0.126	59.6	1.51	21.5	69.1	7.60	2990	111	3101	3.6%
		2.0	0.134	59.3	1.50	21.4	69.0	7.67	3010	113	3123	3.6%
		1.5	0.148	58.8	1.49	21.1	69.0	7.72	3030	114	3144	3.6%
		1.0	0.193	57.1	1.48	20.6	69.0	7.75	3050	115	3165	3.6%
		0.75	0.269	54.9	1.47	20.1	69.0	7.75	3070	116	3186	3.6%
		0.50	6.46	44.7	1.39	17.4	69.3	6.74	3230	106	3336	3.2%
		0.25	47.2	3.98	1.37	9.50	71.2	1.17	3330	18.5	3349	0.55%
$7.5x10^{-5}$	12	4.0	0.090	60.1	1.01	21.7	69.0	7.64	2990	112	3102	3.6%
		3.0	0.090	60.2	1.00	21.5	69.0	7.71	3010	114	3124	3.6%
		2.0	0.095	60.0	0.997	21.4	69.0	7.77	3030	115	3145	3.7%
		1.5	0.104	59.7	0.990	21.2	69.0	7.82	3050	117	3167	3.7%
		1.0	0.127	58.8	0.984	20.9	69.0	7.86	3070	118	3188	3.7%
		0.75	0.155	57.7	0.987	20.5	69.0	7.88	3090	119	3209	3.7%
		0.50	0.231	55.3	0.970	19.9	69.0	7.87	3110	120	3230	3.7%
		0.25	20.5	30.8	0.921	14.7	69.8	5.27	3260	83.1	3343	2.5%

APPENDIX B - STOICHIOMETRY

Heterotrophic Respiration:

$$C_6H_{12}O_6 + 6O_2 \longrightarrow 6CO_2 + 6H_2O \tag{B.1}$$

Heterotrophic Synthesis:

$$5C_6H_{12}O_6 + 6NH_4^+ \longrightarrow 6C_5H_7NO_2 + 18H_2O + 6H^+ \tag{B.2}$$

Net Equation:

The molar yield is related to the mass yield by

$$Y_{H3} \cdot \frac{(moles\ of\ cells/113g\ cells)}{(moles\ of\ glucose/180g\ glucose)} = 1.59\ Y_{H3}$$

The sum of 6.637 Y_{H3} times equation (B.2) and (1-1.327 Y_{N3}) times equation (B.1) gives equation (3.10).

Nitrifier Respiration:

$$NH_4^+ + 2O_2 \longrightarrow NO_3^- + 2H^+ + H_2O \tag{B.3}$$

Nitrifier Synthesis:

$$5CO_2 + NH_4^+ + 19H^+ + 20e^- \longrightarrow C_5H_7NO_2 + 8H_2O \tag{B.4}$$

$$NH_4^+ + 13H_2O \longrightarrow NO_3^- + 10H^+ + 8e^- \tag{B.5}$$

The sum of 2 times equation (B.4) and 5 times equation (B.5) gives:

$$10CO_2 + 7NH_4^+ \longrightarrow 2C_5H_7NO_2 + 5NO_3^- + 12H^+ + H_2O \tag{B.6}$$

Net Equation:

The molar yield is related to the mass yield by

$$Y_{N2} \cdot \frac{(moles\ of\ nitrif/113\ g)}{(moles\ of\ NH_4^+\text{–}N/14g)} = 0.124\ Y_{N2}$$

The sum of (1-0.434 Y_{N2}) times equation (B.3) and 0.0619 Y_{N2} times equation (B.6) gives

$$\begin{aligned} NH_4^+ + (2\text{–}0.867\ Y_{N2})O_2 + (0.619\ Y_{N2})CO_2 \longrightarrow\ & (0.124\ Y_{N2})C_5H_7NO_2 \\ & + (1\text{–}0.124\ Y_{N2})NO_3^- \\ & + (2\text{–}0.124\ Y_{N2})H^+ \\ & + (1\text{–}0.372\ Y_{N2})H_2O \end{aligned} \quad \text{(B.7)}$$

The bicarbonate equilibrium is

$$CO_2 + H_2O \longleftrightarrow H_2CO_3 \longleftrightarrow H^+ + HCO_3^-$$

Addition of the following equations to equation (B.7) gives equation (3.11).

$$(0.619\ Y_{N2})[H_2CO_3 \longrightarrow CO_2 + H_2O]\ \ \&$$

$$(2\text{–}0.124\ Y_{N2})[H^+ + HCO_3^- \longrightarrow H_2CO_3]$$

APPENDIX C - MODEL SOURCE CODE LISTING

```
C*JOB CHECK
C.....................................................................
C 10/16
C SIMULATION OF CFSTR BEHAVIOR WITH GLOBAL REACTIONS - STEADY STATE
C INTEGRATION PERFORMED BY THE IMSL SUBROUTINE DGEAR
C
C.....................................................................
      IMPLICIT REAL*8 (A-H,O-Z)
      DIMENSION SB(6), SBLAST(6), SBDOT(6), WK(103), IWK(6)
      EXTERNAL CFSTR, FCNJ
C
      REAL*8 K1H, K1N, K2N, K3H, KK1H, KK1N, KK2N, KK3H, KLA, MCRT
      REAL SDUMMY
C
      COMMON/GEAR/DUMMY(48), SDUMMY(4), IDUMMY(38)
      COMMON/REACTR/SDOT(6), SBIN(4), D, MCRT, KLA, S1SAT,
     $              FN0, FH0, IAIR, NFITER
      COMMON/RXN/REAC(7,130),RRHS(3,130),ALPHA(4),YH3,YN2,
     $           QH3,QN2,QD1,QH2,QH1,QN1,QN4,QD2,K1H,K1N,K2N,
     $           K3H,IGEOM,NP1,NP2,NM1,MOD
C
C..DGEAR PARAMETERS
      NEQ=6
      T=0.0
      TOL=1.0D-03
      H=1.0D-03
      METH=1
      MITER=0
      INDEX=1
C
      READ(5,1) SB,SBIN,D,MCRT,KLA,S1SAT
1     FORMAT(G10.0)
C
      IPRTF=1
      MOD=0
      CALL FLOC(IPRTF,&9999)
C
      WRITE(6,2000) D, MCRT, SBIN
2000  FORMAT(///,T2,'SIMULATION: CFSTR WITH GLOBAL REACTIONS',//,
     $      T2,'D=',G10.3,'1/HR',2X,'MCRT=',G10.3,'DAYS',//,
     $      T2,'SBIN(1)=',G10.3,'MG/L',2X,'SBIN(2)=',G10.3,'MG/L',2X,
     $      'SBIN(3)=',G10.3,'MG/L',2X,'SBIN(4)=',G10.3,'MG/L')
      IF(MOD.EQ.0) GO TO 3
      IF(MOD.EQ.1) WRITE(6,2001)
2001  FORMAT(/,T2,'*** USING MULTIPLE-MONOD KINETICS ***')
      GO TO 4
3     WRITE(6,2002)
2002  FORMAT(/,T2,'*** USING MULTIPLE-EXPONENTIAL KINETICS ***')
C
4     DO 5 I=1,NEQ
        SBLAST(I)=SB(I)
5     CONTINUE
      MCRT=MCRT*24.0
      FN0=SB(6)/(SB(5)+SB(6))
      FH0=1.-FN0
      IAIR=0
      NFITER=0
C
      CALL CFSTR(NEQ,T,SB,SBDOT)
      WRITE(6,2010)
2010  FORMAT(//,T5,'TIME',T15,'OXYGEN',T28,'NH4-N',T39,'GLUCOSE',
     $       T52,'NO3-N',T66,'XH',T77,'XN',T89,'RERR',T105,'NFE',T115,
     $       'NFITER')
      WRITE(6,2020) T,SB,ERR,IDUMMY(8),NFITER
2020  FORMAT(/,T2,10(G10.3,2X))
      WRITE(6,2021) SDOT, QH3, QN2
```

```
2021  FORMAT(T12,8(G10.3,2X))
C
C..FIND STEADY STATE EFFLUENT CONCENTRATIONS
      TEND=1./D
      TMAX=2.0*MCRT
10    ERR=0.0
      CALL DGEAR(NEQ,CFSTR,FCNJ,T,H,SB,TEND,TOL,METH,MITER,INDEX,IWK,
     $           WK,IER)
      IF(IER.GT.128) GO TO 90
C..CHECK FOR STEADY STATE
      DO 12 I=2,NEQ
        RERR=DABS((SB(I)-SBLAST(I))/SB(I))
        ERR=DMAX1(ERR,RERR)
        SBLAST(I)=SB(I)
12    CONTINUE
      WRITE(6,2020) T,SB,ERR,IDUMMY(8),NFITER
      WRITE(6,2021) SDOT, QH3, QN2
      IF(ERR.LT.1.0E-02 .OR. TEND.GE.TMAX) GO TO 16
      TEND=TEND+1./D
C..CHECK FOR STIFFNESS
      IF(ERR.LT.0.00 .AND. METH.EQ.1) GO TO 14
      GO TO 10
14    METH=2
      MITER=2
      INDEX=1
      H=1.0D-03
      WRITE(6,2030)
2030  FORMAT(T2,'*** SWITCH TO STIFF METHOD ***')
      GO TO 10
16    IF(TEND.GE.TMAX) GO TO 9997
      WRITE(6,2040)
2040  FORMAT(/,T2,'*** STEADY STATE ***',/)
      GO TO 9998
C
9997  WRITE(6,2100)
2100  FORMAT(/,T2,'*** NOT STEADY STATE: STOPPED AFTER 2 MCRTS ***')
C
9998  T=0.0
      TEND=1./D
      H=1.0E-03
      INDEX=1
      WRITE(6,2010)
      IF(SB(1) .LT. 0.3) GO TO 9999
      IF(SB(1) .LT. 0.6) GO TO 29
      IF(SB(1) .LT. 0.8) GO TO 30
      IF(SB(1) .LT. 1.2) GO TO 31
      IF(SB(1) .LT. 1.7) GO TO 32
      IF(SB(1) .LT. 2.5) GO TO 33
      IF(SB(1) .LT. 3.5) GO TO 34
      SB(1)=3.0
      GO TO 10
29    SB(1)=0.25
      GO TO 10
30    SB(1)=0.50
      GO TO 10
31    SB(1)=0.75
      GO TO 10
32    SB(1)=1.0
      GO TO 10
33    SB(1)=1.5
      GO TO 10
34    SB(1)=2.0
      GO TO 10
9999  STOP
C
90    CONTINUE
```

```
      WRITE(6,2200) IER, H
 2200 FORMAT(T2,'IER=',I3,10X,'H=',G10.3)
      STOP
      END
C*********************************************************************
      SUBROUTINE CFSTR(NEQ,T,SB,SBDOT)
C.....................................................................
C THIS IS THE REACTOR MODEL
C
C  SB(I)   = CONCENTRATION OF SPECIES I (MG/L)
C              1 FOR OXYGEN, 2 FOR NH4-N, 3 FOR GLUCOSE, 4 FOR NO3-N,
C              5 FOR HETEROTROPHS, 6 FOR NITRIFIERS
C  SBIN(I) = INFLUENT CONCENTRATION OF SPECIES I (MG/L)
C  D       = DILUTION RATE (1/HR)
C  MCRT    = MEAN CELL RETENTION TIME (HR)
C  KLA     = OXYGEN TRANSFER COEFFICIENT (1/HR)
C  S1SAT   = SATURATION DO CONCENTRATION (MG/L)
C  XH      = CONCENTRATION OF HETEROTROPHS (MG/L)
C  XN      = CONCENTRATION OF NITRIFIERS (MG/L)
C  FN      = NITRIFIERS FRACTION (MG NITRIFIERS/MG TOTAL CELLS)
C  XT      = MLSS CONCENTRATION OF TOTAL SOLIDS (G/L)
C.....................................................................
      IMPLICIT REAL*8(A-H,O-Z)
      DIMENSION SB(NEQ), SBDOT(NEQ), RAVG(7), ETA(4)
      COMMON/REACTR/SDOT(6), SBIN(4), D, MCRT, KLA, S1SAT,
     $              FN0, FH0, IAIR, NFITER
      COMMON/RXN/REAC(7,130),RRHS(3,130),ALPHA(4),YH3,YN2,
     $           QH3,QN2,QD1,QH2,QH1,QN1,QN4,QD2,K1H,K1N,K2N,
     $           K3H,IGEOM,NP1,NP2,NM1,MOD
C
      REAL*8 K1H, K1N, K2N, K3H, KK1H, KK1N, KK2N, KK3H, KLA, MCRT
C
      XH=SB(5)
      XN=SB(6)
      XT=(XH+XN)/1000.
      FN=XN/(XN+XH)
      FH=1.-FN
      QH3=QH3*FH/FH0
      QN2=QN2*FN/FN0
C
      CALL RATES(SB,RAVG,ETA,ITER)
      SBDOT(1)=IAIR*(KLA*(S1SAT-SB(1))+RAVG(1)*XT)
C..OXYGEN UPTAKE RATE
      SDOT(1)=RAVG(1)*XT
      DO 10 I=2,4
        SBDOT(I)=D*(SBIN(I)-SB(I))+RAVG(I)*XT
        SDOT(I)=SBDOT(I)
10    CONTINUE
      SBDOT(5)=XT*(RAVG(6)+FH*RAVG(5))-XH/MCRT
      SBDOT(6)=XT*(RAVG(7)+FN*RAVG(5))-XN/MCRT
      SDOT(5)=SBDOT(5)
      SDOT(6)=SBDOT(6)
      FN0=FN
      FH0=FH
      NFITER=NFITER+ITER
      RETURN
      END
C*********************************************************************
      SUBROUTINE FCNJ(NEQ,T,SB,PD)
      IMPLICIT REAL*8(A-H,O-Z)
      DIMENSION SB(NEQ), PD(NEQ,NEQ)
      RETURN
      END
C*********************************************************************
      SUBROUTINE FLOC(IPRTF,*)
C.....................................................................
```

```
C THIS SUBROUTINE SOLVES THE STEADY STATE FLOC MODEL FOR THE VOLUME
C AVERAGED REACTION RATES FOR A SET OF GIVEN BOUNDARY CONDITIONS.
C
C  C(I,K)      = DIMENSIONLESS CONCENTRATION OF SPECIES I AT POINT K
C                I = 1 FOR OXYGEN, I = 2 FOR NH4-N, I = 3 FOR GLUCOSE,
C                I = 4 FOR NO3-N
C  X(K)        = DIMENSIONLESS DISTANT FROM FLOC CENTER AT POINT K
C  SB(I)       = BULK CONCENTRATION OF SPECIES I (MG/L)
C  RAVG(I)     = VOLUME AVERAGED RATES:  (MG/G-HR)
C                  SPECIFIC REACTION RATES I = 1, 2, 3, 4
C                  SPECIFIC GROWTH RATES I = 5 FOR ENDOGENEOUS DECAY
C                                           6 FOR HETEROTROPHS
C                                           7 FOR NITRIFIERS
C  ETA(I)      = EFFECTIVENESS FACTORS
C  QH3,QN2,QD1= MAXIMUM SPECIFIC RATES (MG/G-HR)
C  YH3,YN2     = YIELDS
C  KK1H,KK1N,
C  KK2N,KK3H   = HALF-SATURATION CONSTANTS (MG/L)
C  RE          = REYNOLDS NUMBER
C  RHOL2       = (L**2)*RHO  (CM**2-G/L)
C  DEDL        = RATIO OF EFFECTIVE TO LIQUID DIFFUSIVITY
C  RELERR      = RELATIVE ERROR CONVERGENCE CRITERION
C  IGEOM       = GEOMETRIC FACTOR (PLANAR=1, CYLINDRICAL=2, SPHERICAL=3)
C  NGRID       = 2**NGRID GIVES N FINITE DIFFERENCE GRID POINTS
C  ITMAX       = MAXIMUM NUMBER OF ITERATIONS
C  MOD         = 0 TO USE EXPONENTIAL KINETICS
C                1 TO USE MONOD KINETICS
C  IPRTF       = 0 PRINTS ONLY ERROR MESSAGES
C                1 ALSO PRINTS FLOC PARAMETERS
C                2 ALSO PRINTS FINAL PROFILES, RAVG AND ETA
C                3 ALSO PRINTS ALL ITERATIONS IF NGRID<=3
C
C.....................................................................
      IMPLICIT REAL*8 (A-H,O-Z)
      DIMENSION C(4,130), X(130), SB(6), RAVG(7), ETA(4), AL2ROD(4),
     $          THIELE(4)
      DIMENSION AA(130), AB(130), AC(130), RHS(130), ETA0(7), BI(4),
     $          DL(4), IPERM(3)
C
      COMMON/RXN/REAC(7,130),RRHS(3,130),ALPHA(4),YH3,YN2,
     $           QH3,QN2,QD1,QH2,QH1,QN1,QN4,QD2,K1H,K1N,K2N,
     $           K3H,IGEOM,NP1,NP2,NM1,MOD
C
      DATA IPERM/1,3,2/
C
      REAL*8 K1H, K1N, K2N, K3H, KK1H, KK1N, KK2N, KK3H
C
      READ(5,1000) QH3,QN2,QD1,YH3,YN2,KK1H,KK1N,KK2N,KK3H,RE,RHOL2,
     $             DEDL,RELERR,IGEOM,NGRID,ITMAX,MOD
1000  FORMAT(G10.0)
C
      IF(IPRTF.LT.3 .OR. NGRID.LE.3) GO TO 1
      IPRTF=1
      WRITE(6,1990)
1990  FORMAT(T1,'1',T2,'IPRTF WAS RESET FROM 3 TO 1 BECAUSE NGRID > 3')
C
C..LIQUID DIFFUSIVITIES (CM**2/HR)
1     DL(1)=7.9D-2
      DL(2)=7.2D-2
      DL(3)=2.5D-2
      DL(4)=1.1D-1
C
C..BIOT NUMBERS
      BI(1)=(2.+0.6*DSQRT(RE)*7.438)/DEDL
      BI(2)=(2.+0.6*DSQRT(RE)*7.676)/DEDL
      BI(3)=(2.+0.6*DSQRT(RE)*10.94)/DEDL
```

```
      BI(4)=(2.+0.6*DSQRT(RE)*6.599)/DEDL
C
      GEOM2=IGEOM*IGEOM
C..SET UP FINITE DIFFERENCE GRID
      IF (NGRID.GT.0 .AND. NGRID.LT.8) GO TO 2
        WRITE(6,2000)
2000    FORMAT(T2,'NGRID MUST BE > 0 AND <= 7',/)
        RETURN 1
2     N=2**NGRID
      NP1=N+1
      NP2=N+2
      NM1=N-1
      DELX=1./N
      DXX=DELX*DELX
      DO 4 K=1,NP1
        X(K)=DELX*(K-1)
4     CONTINUE
C
      DO 6 I=1,4
        AL2ROD(I)=GEOM2*RHOL2/(DL(I)*DEDL)
        C(I,1)=X(2)
        C(I,N+2)=1.0
        DO 6 K=2,NP1
          C(I,K)=X(K)
6     CONTINUE
C
      IF(IPRTF .LT. 1) RETURN
      WRITE(6,2010) QH3,QN2,QD1,YH3,YN2,KK1H,KK1N,KK2N,KK3H,BI,RHOL2,
     $              DEDL,RELERR,IGEOM,N
2010  FORMAT(T1,'1',T2,'INPUT PARAMETERS:',//,T2,'QH3=',G10.3,T30,
     $'QN2=',G10.3,T60,'QD1=',G10.3,/,T2,'YH3=',G10.3,T30,'YN2=',G10.3,
     $/,T2,'KK1H=',G10.3,T30,'KK1N=',G10.3,T60,'KK2N=',G10.3,T90,
     $'KK3H=',G10.3,/,T2,'BI(1)=',G10.3,T30,'BI(2)=',G10.3,T60,
     $'BI(3)=',G10.3,T90,'BI(4)=',G10.3,/,T2,'RHOL2=',G10.3,T30,
     $'DEDL=',G10.3,
     $//,T2,'RELERR=',G10.3,/,T2,'IGEOM=',I1,/,T2,'N=',I3,///)
      IF(MOD.EQ.1) GO TO 7
      IF(MOD.EQ.0) WRITE(6,2011)
2011  FORMAT(/,T2,'*** USING MULTIPLE-EXPONENTIAL KINETICS ***')
      GO TO 8
7     WRITE(6,2012)
2012  FORMAT(/,T2,'*** USING MULTIPLE-MONOD KINETICS ***')
8     RETURN
C
C.....................................................................
C
      ENTRY RATES(SB,RAVG,ETA,ITER)
C
      QH1=0.178*(6.-7.97*YH3)*QH3
      QH2=0.124*YH3*QH3
      QN1=2.29*(2.-0.868*YN2)*QN2
      QN4=-(1.-0.124*YN2)*QN2
      QD2=-0.173*QD1
C
      DO 9 I=1,3
        IF(SB(I) .GT. 1.0D-60) GO TO 9
          WRITE(6,2013) I, SB(I)
2013      FORMAT(T2,'*** WARNING:  SB(',I1,')=',G10.3,2X,
     $          'RESET TO BE 1.0D-05 ***')
          SB(I)=1.0D-05
9     CONTINUE
C..DIMENSIONLESS HALF-SATURATION CONSTANTS
      K1N=KK1N/SB(1)
      K1H=KK1H/SB(1)
      K2N=KK2N/SB(2)
      K3H=KK3H/SB(3)
```

```
C..ALPHA IS (A*L)**2*RHO/DEFF/SB & HAS THE UNITS OF 1/(MG/G-HR)
      DO 10 I=1,4
        ALPHA(I)=AL2ROD(I)/SB(I)
10    CONTINUE
      CALL REACTN(C,X,130,N,2,RAVG,ETA0)
C
      IF(IPRTF .LT. 3) GO TO 14
      WRITE(6,2020) SB
2020  FORMAT(T2,'BULK SUBSTRATE CONCENTRATIONS:',2X,'SB(1)=',G10.3,2X,
     $'SB(2)=',G10.3,2X,'SB(3)=',G10.3,2X,'SB(4)=',G10.3,//)
      WRITE(6,2030)
2030  FORMAT(T2,'FINITE DIFFERENCE POINTS AT:',/)
      WRITE(6,2040) (X(I), I=1,NP1)
2040  FORMAT(T2,10(G10.3,1X))
      WRITE(6,2050)
2050  FORMAT(/,T2,'INITIAL GUESS OF CONCENTRATION PROFILES:',/)
      DO 12 I=1,4
        WRITE(6,2040) (C(I,K), K=1,NP2)
12    CONTINUE
      DO 13 I=1,4
        WRITE(6,2060) I, RAVG(I), ETA0(I)
2060    FORMAT(T25,'RAVG ',I1,' = ',G10.3,' MG/G-HR',7X,'ETA = ',F6.3)
13    CONTINUE
C
14    ERR=0.0
      ITER=0
15    ITER=ITER+1
      DO 20 I=1,3
        IP=IPERM(I)
        CALL REACTN(C,X,130,N,1,RAVG,ETA)
        AA(1)=0.0
        AB(1)=-2.*IGEOM+REAC(IP,1)*DXX
        AC(1)=2.*IGEOM
        RHS(1)=-RRHS(IP,1)*DXX
        DO 18 K=2,N
          BB=(IGEOM-1)*DELX/2./X(K)
          AA(K)=1.-BB
          AB(K)=-2.+REAC(IP,K)*DXX
          AC(K)=1.+BB
          RHS(K)=-RRHS(IP,K)*DXX
18      CONTINUE
        AA(NP1)=2.
        AB(NP1)=-2.-BI(IP)*IGEOM*DELX*(2.+DELX*(IGEOM-1))
     $           +REAC(IP,NP1)*DXX
        AC(NP1)=0.0
        RHS(NP1)=-BI(IP)*IGEOM*DELX*C(IP,NP2)*(2.+DELX*(IGEOM-1))
     $           -RRHS(IP,NP1)*DXX
        CALL TRIDIA(AA,AB,AC,RHS,130,NP1)
        DO 19 K=1,NP1
          C(IP,K)=RHS(K)
19      CONTINUE
20    CONTINUE
C
C..CHECK FOR CONVERGENCE
      CALL REACTN(C,X,130,N,2,RAVG,ETA)
      ERR=0.0
      DO 30 I=1,3
        ERR1=DABS((ETA0(I)-ETA(I))/ETA(I))
        ERR=DMAX1(ERR,ERR1)
        ETA0(I)=ETA(I)
30    CONTINUE
C
      IF(IPRTF .LT. 3) GO TO 34
      WRITE(6,2070) ITER, ERR
2070  FORMAT(//,T2,'ITER=',I2,3X,'MAXIMUM RELATIVE ERROR = ',G10.3,/)
      DO 32 I=1,3
```

```
        WRITE(6,2040) (C(I,K), K=1,NP2)
32    CONTINUE
      DO 33 I=1,4
        WRITE(6,2060) I, RAVG(I), ETA(I)
33    CONTINUE
C
34    IF(ERR.GT.RELERR .AND. ITER.LT.ITMAX) GO TO 15
      IF(ERR.GT.RELERR) GO TO 55
C
C..CALCULATE NO3-N CONCENTRATION PROFILE
      IF(IPRTF .LT. 2) RETURN
      AB(1)=-2.*IGEOM
      AC(1)=2.*IGEOM
      RHS(1)=-REAC(4,1)*DXX
      DO 40 K=2,N
        BB=(IGEOM-1)*DELX/2./X(K)
        AA(K)=1.-BB
        AB(K)=-2.
        AC(K)=1.+BB
        RHS(K)=-REAC(4,K)*DXX
40    CONTINUE
      AA(NP1)=2.
      AB(NP1)=-2.-BI(4)*IGEOM*DELX*(2.+(IGEOM-1)*DELX)
      RHS(NP1)=-REAC(4,NP1)*DXX-BI(4)*IGEOM*DELX*C(4,NP2)*
     $         (2.+(IGEOM-1)*DELX)
      CALL TRIDIA(AA,AB,AC,RHS,130,NP1)
      DO 41 K=1,NP1
        C(4,K)=RHS(K)
41    CONTINUE
      WRITE(6,2071)
2071  FORMAT(//,T2,'FINAL CONCENTRATION PROFILES:',/)
      DO 42 I=1,4
        WRITE(6,2040) (C(I,K), K=1,NP2)
42    CONTINUE
      THIELE(1)=DABS(REAC(1,NP2)/GEOM2)
      THIELE(2)=DABS(REAC(2,NP2)/GEOM2)
      THIELE(3)=DABS(REAC(3,NP2)/GEOM2)
      WRITE(6,2072)
2072  FORMAT(//,T2,'FINAL RATE PROFILES:',/)
      DO 44 I=1,4
        DO 43 K=1,NP2
          REAC(I,K)=REAC(I,K)/ALPHA(I)
43      CONTINUE
        WRITE(6,2040) (REAC(I,K), K=1,NP2)
44    CONTINUE
      DO 45 I=1,4
        WRITE(6,2060) I, RAVG(I), ETA(I)
45    CONTINUE
C
      DO 46 I=5,7
        WRITE(6,2061) I, RAVG(I)
2061    FORMAT(T25,'SPEC. GROWTH RATE ',I1,' = ',G10.3,
     $         ' MG/G TOTAL CELLS-HR')
46    CONTINUE
      WRITE(6,2080)
2080  FORMAT(//,T2,'SQUARE OF THIELE MODULUS:')
      DO 54 I=1,3
        WRITE(6,2090) I, THIELE(I)
2090    FORMAT(T2,'THIELE ',I1,' = ',G10.3)
54    CONTINUE
      RETURN
C
55    WRITE(6,2100)
2100  FORMAT(T2,'FLOC DID NOT CONVERGE')
      RETURN
      END
```

```
C*********************************************************************
      SUBROUTINE REACTN(C,X,ND,N,IOPTN,RAVG,ETA)
C.....................................................................
C THIS SUBROUTINE CALCULATES THE PROFILES OF THE REACTION RATE TERMS AND
C THE PROFILES OF THE REACTION RATES.
C
C  ND         = DIMENSION OF ARRAYS IN CALLING SEGMENT
C  IOPTN      = 1 CALCULATES THE "FACTORED" REACTION RATE TERMS FOR
C                 FOR FINITE DIFFERENCE
C             = 2 CALCULATES REACTION RATE PROFILES FOR EACH SPECIES,
C                 VOLUME AVERAGED RATES, AND THE EFFECTIVENESS FACTORS
C  REAC(I,K) = DIMENSION LESS REACTION RATE FOR SPECIES I AT POINT K
C  MOD        = 0 TO USE MULTIPLE-EXPONENTIAL KINETICS
C               1 TO USE MULTIPLE-MONOD KINETICS
C.....................................................................
      IMPLICIT REAL*8 (A-H,O-Z)
      DIMENSION C(4,ND), X(ND), RAVG(7), ETA(4)
C
      COMMON/RXN/REAC(7,130),RRHS(3,130),ALPHA(4),YH3,YN2,
     $           QH3,QN2,QD1,QH2,QH1,QN1,QN4,QD2,K1H,K1N,K2N,
     $           K3H,IGEOM,NP1,NP2,NM1,MOD
C
      REAL*8 K1H, K1N, K2N, K3H, KK1H, KK1N, KK2N, KK3H
C
      A=-DLOG(2.0D00)
      AA=-170.
      DO 10 K=1,NP2
        IF(MOD.EQ.1) GO TO 2
C..EXPONENTIAL KINETICS
        R1H=1.-DEXP(DMAX1(AA,A*C(1,K)/K1H))
        R1N=1.-DEXP(DMAX1(AA,A*C(1,K)/K1N))
        R2N=1.-DEXP(DMAX1(AA,A*C(2,K)/K2N))
        R3H=1.-DEXP(DMAX1(AA,A*C(3,K)/K3H))
        GO TO 3
C..MONOD KINETICS
2       R1H=C(1,K)/(K1H+C(1,K))
        R1N=C(1,K)/(K1N+C(1,K))
        R2N=C(2,K)/(K2N+C(2,K))
        R3H=C(3,K)/(K3H+C(3,K))
C
3       RH13=R1H*R3H
        RH123=RH13*R2N
        RN12=R1N*R2N
C..SPECIFIC DECAY RATE IN (MG/G-HR)
        REAC(5,K)=QD1*R1H*0.706
C..REACTION RATE TERMS FOR FINITE DIFFERENCE
        REAC(1,K)=ALPHA(1)*(QH1*RH13+QN1*RN12+QD1*R1H)/C(1,K)
        REAC(2,K)=ALPHA(2)*(QH2*RH123+QN2*RN12)/C(2,K)
        REAC(3,K)=ALPHA(3)*QH3*RH13/C(3,K)
        REAC(4,K)=ALPHA(4)*QN4*RN12
        RRHS(1,K)=0.0
        RRHS(3,K)=0.0
        RRHS(2,K)=ALPHA(2)*(QD2*R1H)
        IF(IOPTN .EQ. 1) GO TO 10
        DO 9 I=1,3
C..REACTION RATES
          REAC(I,K)=REAC(I,K)*C(I,K)+RRHS(I,K)
9       CONTINUE
10    CONTINUE
C
C..VOLUME AVERAGED RATES INTEGRATED WITH SIMPSON'S 1/3 RULE
      IF(IOPTN .EQ. 1) RETURN
      DO 20 I=1,5
        SUM=0.0
        SUM=SUM+4.*REAC(I,2)*X(2)**(IGEOM-1)
        IF(N.EQ.2) GO TO 16
```

```
        DO 15 K=3,NM1,2
          SUM=SUM+2.*REAC(I,K)*X(K)**(IGEOM-1)
     $         +4.*REAC(I,K+1)*X(K+1)**(IGEOM-1)
15      CONTINUE
16      SUM=(SUM+REAC(I,N+1))*IGEOM/3./N
        IF(I.LE.4) GO TO 17
C..VOLUME AVERAGED SPECIFIC DECAY RATE (MG/G-HR)
          RAVG(I)=SUM
          GO TO 20
C..VOLUME AVERAGED REACTION RATES IN (MG/G-HR)
17      RAVG(I)=SUM/ALPHA(I)
C..EFFECTIVENESS FACTORS
        ETA(I)=SUM/REAC(I,N+2)
20    CONTINUE
C..VOLUME AVERAGED SPECIFIC GROWTH RATES IN (MG/G-HR)
      RAVG(6)=-RAVG(3)*YH3
      RAVG(7)=RAVG(4)*YN2/(1.-.124*YN2)
      RETURN
      END
C*********************************************************************
      SUBROUTINE TRIDIA(A,B,C,RHS,ND,N)
C.....................................................................
C THIS SUBROUTINE SOLVES TRIDIAGONAL MATRICES BY USING THE THOMAS
C ALGORITHM.
C
C   A,B,C = VECTORS CONTAINING THE LEFT DIAGONAL, MAIN DIAGONAL, AND
C           RIGHT DIAGONAL, RESPECTIVELY
C   RHS   = RIGHT HAND SIDE VECTOR OF CONSTANTS AND RETURNS THE
C           SOLUTION VECTOR
C   ND    = DIMENSION OF ARRAYS IN CALLING SEGMENT
C   N     = NUMBER OF ROWS IN THE MATRIX
C.....................................................................
      IMPLICIT REAL*8 (A-H,O-Z)
      DIMENSION A(ND), B(ND), C(ND), RHS(ND)
      DIMENSION BETA(130), GAMMA(130)
C
      BETA(1)=B(1)
      GAMMA(1)=RHS(1)/B(1)
      DO 10 I=2,N
        BETA(I)=B(I)-A(I)*C(I-1)/BETA(I-1)
        GAMMA(I)=(RHS(I)-A(I)*GAMMA(I-1))/BETA(I)
10    CONTINUE
      RHS(N)=GAMMA(N)
      NM1=N-1
      DO 20 I=1,NM1
        J=N-I
        RHS(J)=GAMMA(J)-C(J)*RHS(J+1)/BETA(J)
20    CONTINUE
      RETURN
      END
```

```
  4.0D 00       SB(1) OXYGEN (MG/L)
 .284D 00         (2) NH4-N
 2.23D 00         (3) GLUCOSE
 48.0D 00         (4) NO3-N
2053.D 00         (5) IS XH
 47.5D 00         (6) IS XN
  0.0D 00       SBIN(1) (MG/L)
  5.5D 01           (2)
  3.0D 02           (3)
  0.0D 00           (4)
 .143D 00       DILUTION RATE (1/HR)
 12.0D 00       MCRT (DAYS)
```

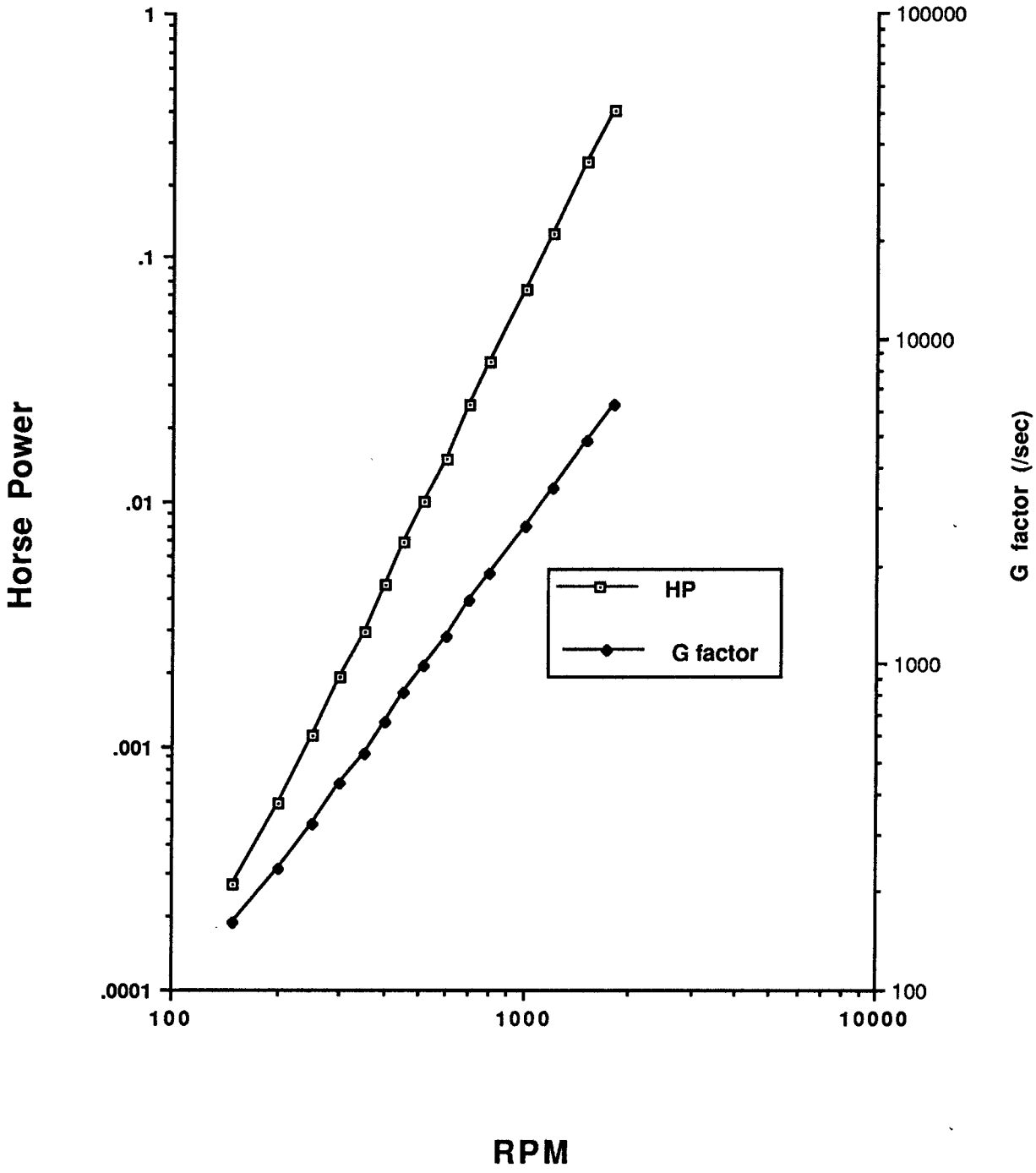
Horse Power
1
.1
.01
.001
.0001
100000
10000
1000
100
G factor (/sec)
HP
G factor
100
1000
10000
RPM

N/P/G DATA"

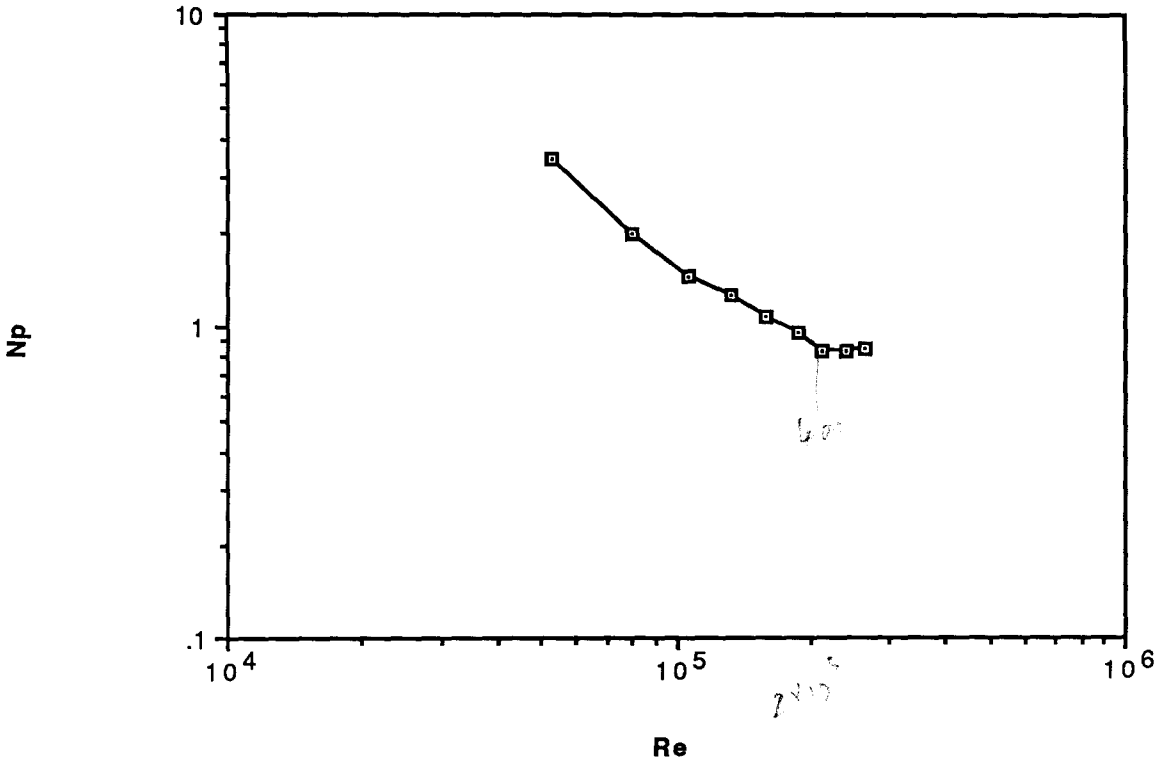

"N/P/G DATA"